European Commission

Horizon 2020
European Union funding
for Research & Innovation

REDUCTION OF RADIOLOGICAL ACCIDENT CONSEQUENCES

Action	Research and Innovation Action NFRP-2018-1
Grant Agreement #	847656
Project name	**R**eduction of **R**adiological **C**onsequences of design basis and design extension **A**ccidents
Project Acronym	R2CA
Project start date	01.09.2019
Deliverable #	D4.2
Title	Final Report on experimental database reassessment and on model/code improvements for fission product releases during a SGTR transient.
Author(s)	Luis E. Herranz, Rafael Iglesias (CIEMAT), Raphael Zimmerl (BOKU), Jeremy Bittan (EDF), Francois Kremer (IRSN), Adam Kecek (UJV), Gumenyuk Dmytro (SSTC)
Version	01
Related WP	WP4 SGTR
Related Task	T4.1. Fission product transport and release from the primary circuit to the environment (CIEMAT)
Lead organization	CIEMAT
Submission date	31.07.2023
Dissemination level	PU

This project has received funding from the Euratom research and training programme 2014-2018 under the grant agreement n° 847656

History

Date	Submitted by	Reviewed by	Version (Notes)
31.07.2023	Luis E. Herranz (CIEMAT)	Z. Hózer (EK) N. Girault (IRSN)	01

Contents

Abbreviations

DBA	Design Basis Accident
DEC	Design Extension Conditions
FP	Fission Product
IS	Iodine Spiking
LOCA	Loss Of Coolant Accident
LWR	Light Water Reactor
NPP	Nuclear Power Plant
PC	Partition Coefficient
PV	Pressure Vessel
PWR	Pressurized Water Reactor
R2CA	Reduction of Radiological Consequences of design basis and design extension Accidents
SDA	Steam dump to atmosphere
SG	Steam Generator
SGTR	Steam Generator Tube Rupture
WP	Work Package

1. Introduction

According to the Detailed Program of work for WP 4 [1], the main objective of task 4.1 is to improve models and codes for the simulation of fission products behaviour during a SGTR transient, with special attention to:

- Fission product (FP) transport and behaviour (especially for iodine) in the primary circuit and
- FP behaviour in failed SG; release to the secondary side and environment.

In order to meet this objective, an evaluation of the available open literature and of the experimental database gathered in [2] has been carried out and new models have been developed for application in the different simulation tools used by the partners.

This document presents the final report of the task. It includes the descriptions of the models developed by each partner as well as their assessments. The structure of the report is straightforward. Chapter 2 outlines the main achievements of each individual partner. Each of the section does have a specific, more comprehensive description of the work done in the corresponding appendix at the end of the report. Some final remarks have been gathered as chapter 3.

2. Summary of the work performed

BOKU

BOKU's aimed at enhancing the RELAP5-3D capability to simulate the FP transport and behaviour during SGTR transients in the primary and secondary circuit. Attention has been paid to fission products decay chains as formulated within the code, and a number of shortfalls have been identified. A few ways of enhancement have been explored.

In order to obtain sufficient data to model the fission product behaviour with RELAP5-3D, an extensive literature survey regarding iodine measurements at NPP has been conducted. Very few data publicly available have been found. Most of them were taken more than 3 decades ago, although some additional ones have been found in individual investigations and nuclear power plants reports (hereafter referred to as, second data set (Zoltán Hózer 2001, Smiesko et al. 2005)).

The first study considered was conducted by the NRC and includes 168 data entries of reactor trips which occurred in US PWRs (Adams and Atwood, 1989, Appendix A). Since the power excursion causes the iodine spike, it can be assumed that the probability of an SGTR event leading to an iodine spike of a certain magnitude corresponds to the same probability resulting from a reactor shutdown (i.e., every shutdown involves an iodine spike in the primary system). In the second data set, 15 data entries of reactor trips are considered. A model to estimate the release rates was used and validated against real data. Unfortunately, the data were never published. The mean of the iodine activity during the normal operation was estimated to be about 3.5 times larger than the mean of the NRC PWR study. It has been noted that data might in fact not be fully comparable, as the scenarios might be different in key aspects, like the rates of the events, the NPP power, the degree of defective fuel rods, etc.

The capability of the RELAP5/MOD3 code to model iodine spiking and potential improvement have been also assessed. RELAP5-3D provides a multi-dimensional thermal-hydraulic and kinetic modelling capability and is used primarily for the analysis of potential accidents and transients in water-cooled nuclear power plants, and for the analysis of advanced reactor systems. However, RELAP5-3D is not capable to model radioactive decay adequately. A BOKU's assessment was conducted to analyse whether RELAP5-3D is capable of simulating fission product behaviour in a simple environment.

BOKU has collected as many data as possible regarding IS phenomena and created an empirical model that not only considers the power as explaining variable (like the NRC model) but also the current position (number of days) of the fuel cycle. The current position in the fuel cycle is an important indicator as an IS only can take place if there are small breaks at the fuel rods. Those defects develop over time. Therefore, it can be assumed that if the reactor is further in the fuel cycle it is more likely to have defects at the fuel rods. For this reason, the dataset was expended by including information regarding the fuel cycle of the different reactors of the US nuclear fuel annual reports.

Considering the above, a restricted linear regression model was constructed using two explanatory variables, the "power [MW]" of the reactor and the "time in fuel cycle [days]". The model allows a wider range of analysis as it is now possible to conduct several calculations at different points of time in the fuel cycle, being possible to make a more accurate prediction of the severity of an accident where iodine reaches the environment. However, it must be said that the issue regarding the small dataset still remains as not for all reactors data regarding the fuel cycle was available.

As the fission product transport model of RELAP5-3D is not capable of considering reductive effects on iodine, several retention effects via a postprocessing function were included in the model: primary side coolant purification system, secondary side pool-scrubbing and containment retention effects.

Considering that the clean-up system can process up to 30 kg of coolant per second in the PWR reactor type a clean-up coefficient of 0.01225 was calculated and used in the simulation of the VVER-1000 DEC-A SGTR scenario. It has been shown that the impact of such a system in the first hours of a transient scenario is only moderate (Figure 1).

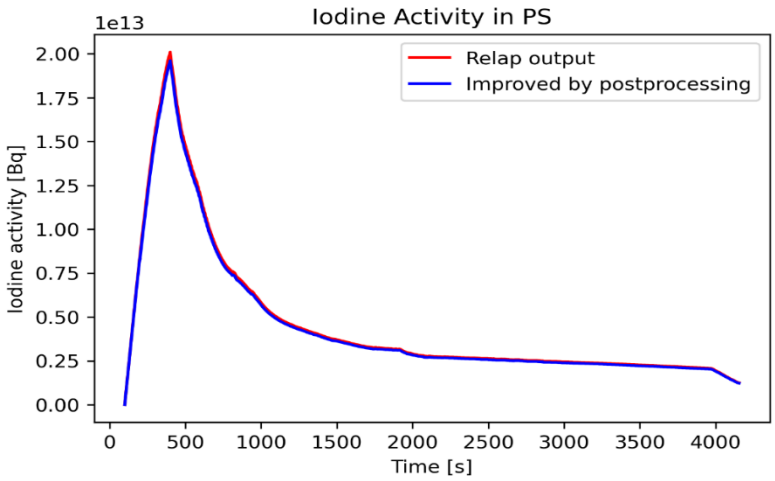

Figure 1. Effect of the cleanup system on iodine activity.

The detailed analysis of this assessment and models is presented the Appendix A to this document.

EDF

EDF enhanced and verified the models implemented in MAAP version 5 code for the FP releases from the primary side to the secondary side and eventually to the environment.

The Modular Accident Analysis Program, Version 5 (MAAP5) is a computer code that simulates the response of light water reactor (LWR) power plants during severe accidents. MAAP5 treats the full spectrum of important

phenomena that could occur during an accident, simultaneously modelling those that relate to the thermal-hydraulic and the fission products. It also simultaneously models the primary system, core, containment, and reactor/auxiliary building. Thus, given a set of initiating events and operator actions, MAAP5 predicts both the thermal-hydraulic and fission product response of the entire plant as the accident progresses.

EPRI MAAP5 allows following the activity released to the environment for 65 radionuclides. The evaluation of the mass of FPs transferred from the RCS to the SGs at each time step is performed by grouping FPs according to their volatility. In the present version of MAAP5, 18 FP groups are considered.

The model developed by EDF to better estimate FP releases during a SGTR transient does embed different correlations depending on the status of the affected SG (whether overflown or not), which notably affects releases to environment. As soon as the affected SG is overflowing, all the FPs transferred from the RCS to the affected SG are assumed to the released to the environment.

Additionally, a simplified model related to the iodine spiking has been added to the EDF MAAP5 code. It contains multiplicative factors for iodine, caesium and the rest of FPs (except for noble gases).

In order to understand and compare the applicability of the new release model for SGTR transients and iodine spiking model in the MAAP EDF version concerning FP modelling, two transients have been run with both EDF MAAP5 and the EDF reference code COSAQUE on 2 different French plant types: a PWR 3-Loop plant (900MWe) and a PWR 4-Loop plant (1450MWe – N4). A transient initiated in hot shutdown state (pre-established iodine spiking), and a transient initiated at full power (for the iodine spiking model).

Figure 62 shows the iodine activity released to the environment versus time for both EDF MAAP5.04 and COSAQUE codes for the case of the transient initiated in hot shutdown state (3 Loop plant). The level of activity released increases rapidly for the 2 codes after around 5 % of the total transient calculation time, when the affected SG starts overflowing. The kinetics of release is quite the same. As can be seen in Figure 2, at around 45% of the calculation time, an increase in the activity of iodine released to the environment appears in the EDF MAAP5.04 calculation with respect to the COSAQUE calculation. At this time, the affected SG stops overflowing and, as a consequence, more steam is produced, and further activity is carried to the environment. The 6% difference at the end of the calculation between both codes is considered acceptable.

In Figure 3 the iodine activity released to the environment for the case of the transient initiated at full power (3 Loop plant) is shown. Both codes show a fast increase after around 4% of the total transient calculation time, when the affected SG starts overflowing. The kinetics of release is close, but slightly slower in COSAQUE. However, COSAQUE predicts a longer release and the integral activity ends up being higher than MAAP5.04 before roughly 27% of the calculation time. Nonetheless, after around 70% of the calculation time MAAP5.04 experiences the effect of producing further steam, as occurred in the hot shutdown case, and the integral activity difference between both codes ends up being about 3%.

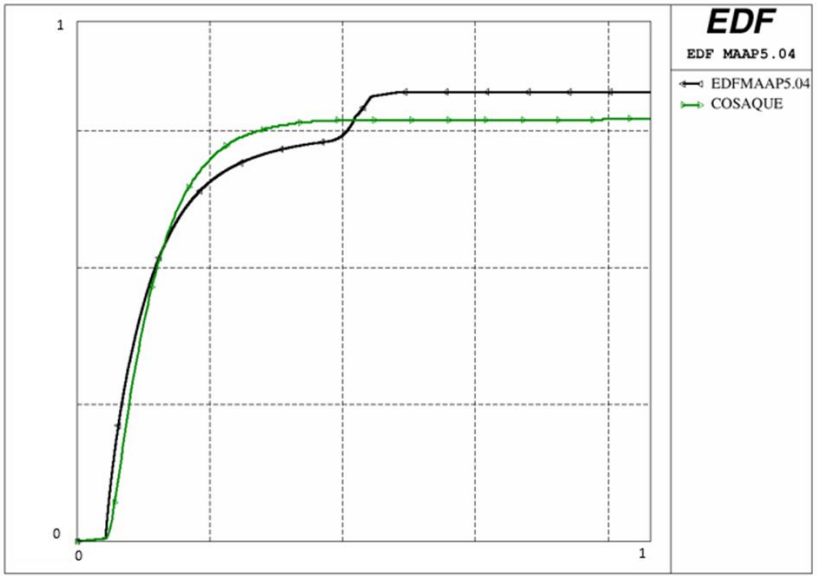

Figure 2. Iodine activity released to the environment vs time in case of transient initiated in hot shutdown state.

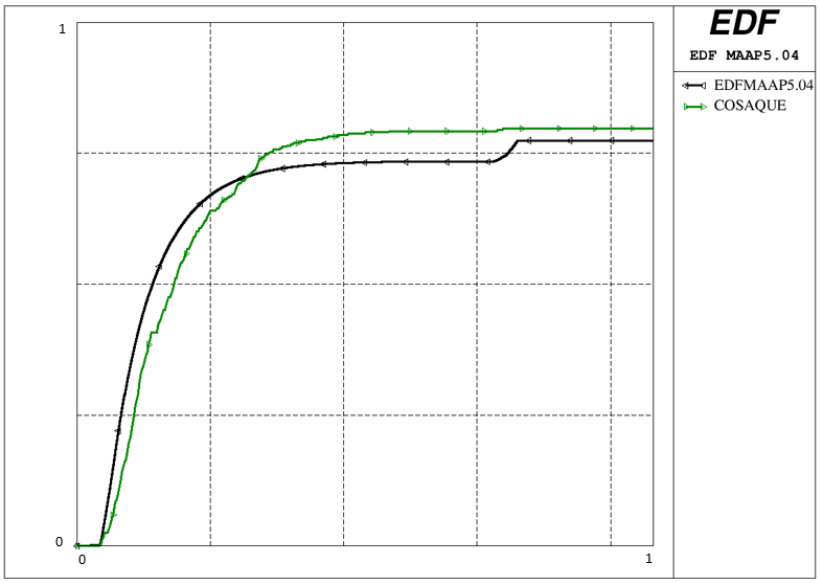

Figure 3. Iodine activity released to the environment vs time in case of transient initiated at full power.

The results of the validation of the models are presented in a detail in the Appendix B to this document.

IRSN

The ASTEC integral code aims at modelling all the phenomena which occur during a severe accident in water cooled reactors, from the initiating event to the releases of FPs into the environment. ASTEC is divided in several modules, each one simulating a specific set of physical phenomena or related to a given reactor zone. Each module can be used in coupled or stand-alone mode. The main modules related to FP transport and release are:

- ISODOP module: simulation of FPs and actinide isotopes decay in different zones of the reactor and the containment.
- ELSA module: simulation of release of FPs from the fuel and of structure materials
- SOPHAEROS module: simulation of FPs and structure materials transport and chemistry in the whole reactor plant (reactor cooling systems and containment).
- DOSE module: computation of the dose rate in the containment (liquid/gas phase and inner walls).
- MDB module: the Material Data Bank shared by all ASTEC modules.

The ASTEC FP modules mentioned above have some limitations regarding the specificities of FP transport and release during a SGTR accident. The first limitation concerns the modelling of phenomenology of iodine flashing at the SG tube breach (As the break flow passes from the high temperature and pressure of the RCS to the lower temperature and pressure of the secondary system, a fraction of the water flashes to steam. The iodine associated with the flashing fraction passes, unmixed with the secondary coolant, to the steam space), which is not taken into account in SOPHAEROS. The second limitation concerns the ISODOP module limitations in estimation of activity in the different components of the RCS, and in the different phases (liquid, gaseous…).

In an effort to address the aforementioned limitations of FP models of ASTEC, two new modules were developed: DROPLET and SAFARI.

- DROPLET module: activated to simulate the flashing phenomenon during a SGTR transient.
- SAFARI module: calculation of the FP transport and activities in a reactor, associated to a simplified modelling of the reactor different zones, in order to improve the computing times.

The DROPLET model was developed and implemented in the ASTEC code system (Figure 3). The pressurized primary water bursting out of the break undergoes a mechanical fragmentation and an adiabatic expansion, thus forming overheated droplets with vapour germs, which reach equilibrium through droplet-atmosphere exchanges and germ growth. Under such conditions the transfer of iodine to the gaseous phase of the SG (so-called ‘iodine flashing rate’) depends on the following parameters:

- The hydraulic flashing rate (splitting of the vapour and liquid phases) at the break, leading to an iodine transfer in gaseous form and in liquid form by the droplets;
- The droplet-size distribution;
- The iodine chemical speciation at the break.

DROPLET calculates an iodine flashing rate until the break is reflooded and models the following mechanisms: mechanical and thermal fragmentation of droplets; depressurization and vapour germ formation; iodine transfers toward vapour germs and at the droplet surface and the germ growth.

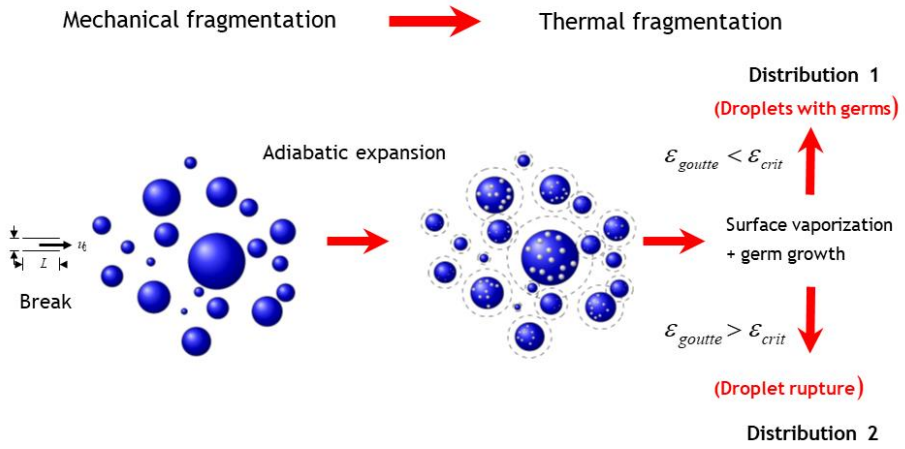

Figure 4. DROPLET main modelling diagram.

SAFARI (SGTR Accident Fission product Activity and Release Inventory) was developed and implemented in the ASTEC code system to calculate the activity transfer from a reactor's primary circuit to its secondary circuit, and the releases to the environment, in case of a SGTR accident. SAFARI calculates the FP transport, the isotopic inventory, and its associated activities in each defined zone – basically the coarse-meshed RCS main zones, plus a zone to simulate the environment. SAFARI has been chosen over the ISODOP module, because of its ability to discriminate each steam generator, and the liquid and gaseous phases in each one, when providing activity calculation results.

The iodine spiking is not yet calculated by SAFARI. The start time and the duration of the peak are input data provided by the user, as well as the initial and peak isotope activities.

A description of the models is presented in details in the Appendix C to this document.

UJV

The UJV's contribution is aimed at complex approach to the computation of radiological consequences during SGTR, emphasizing the DBA events. The previously proposed idea to use ATHLET-CD for fission product transport simulation in the primary and secondary circuit was abandoned due to lack of appropriate validation experiments and NPP models. The newly proposed idea is to create a standalone computational tool using balance equations. Such approach will be code-independent and able to use existing and future thermal hydraulic calculations as initial and boundary conditions. Furthermore, the proposed computational tool can create standardized source terms, which can be used directly by codes for radiological consequences evaluation, such as JRODOS.

UJV conducted a literature review to find a general description of the processes concerning the transport phenomenal during SGTR conditions, recommendations, and specific information on partition coefficients. Most of the information in the literature aim at iodine, which is a dominant contributor to radiological consequences.

The new proposed methodology is based on the literature survey also considering the regulations of the Czech regulatory body in relation on conservative approach for DBA events.

In general, the coolant from the primary can enter the secondary side either as steam (bypass) or as water. Once the water enters the secondary side, fraction of this release is not mixed with the steam generator water content, but thanks to thermal hydraulic conditions it flashes immediately (flashing). The remaining water mixes with the

steam generator water volume. Due to the heating of the steam generator water content, evaporation of the water can occur. The steam from the SG moves forward through the steam line.

Regarding the fission products three main pathways were assumed for activity release from steam generator to the steam line (see Figure 5). Firstly, the fission products entraining the steam generator with steam from primary coolant. Depending on the position of the SGTR, the release can be covered (under water) or uncovered. For the covered case, pool scrubbing may occur. Second path, related to flashing, defines the activity, which is torn off with the flashing content. The remaining activity is assumed to be mixed with bulk water. Finally, due to evaporation, fraction of the activities may enter the steam space (partitioning). Depending on the thermal hydraulic conditions, some of the effects may not have any effect.

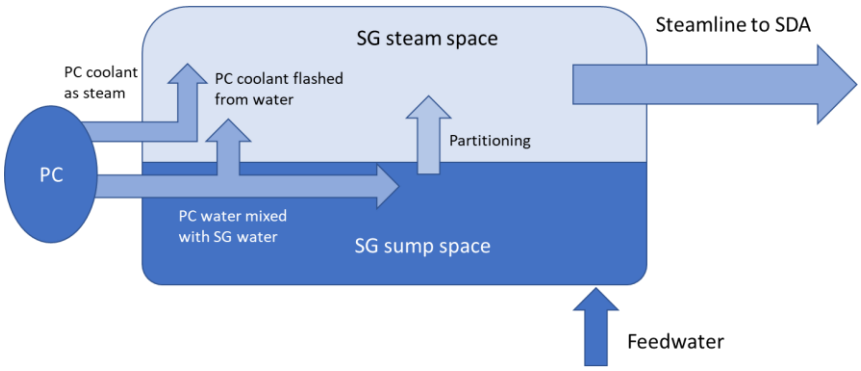

Figure 5. Mass transfer in the affected steam generator.

Considering the explained above phenomenology a set of equations describing mass and activity conservation and transfer between the primary and secondary has been implemented into the Excel VBA application. The implementation was done considering further application in the JRODOS code which is limited to 140 isotopes and is used for estimation of radiological consequences. For each of the isotopes, the macro calculates the activity balance within the primary and the secondary circuit water (as presented in the chapter describing the balance models, in Appendix D). To calculate such values, the user must provide initial and boundary conditions. From the activity point of view, the initial activity concentration within the primary coolant, secondary steam and water and secondary feedwater must be input for each isotope. Furthermore, each isotope requires values for partitioning, flashing and bypass. Finally, the most important thing is the results of the thermal hydraulic calculations, which must be input in predefined order and in desired dimensions. Once the data is ready, the calculation can be performed. The macro creates a separate sheet for each isotope, plotting total activity in the primary circuit, total activity in the steam generator water and the total activity released through the steam dump to atmosphere.

The developed model was applied in the modelling of the DBA SGTR at VVER-1000/V-320 sequences. As part of the model validation, a short sensitivity study was conducted for three different values of partitioning coefficient (c00=1; c01=10 and c02=100) to see the impact of reduced or increased partitioning. The modified partitioning coefficients proved to have impact both on sump activity and the total release through the steam dump to atmosphere. As expected, the total activity release decreases with increasing partitioning coefficient (Figure 6) and reduced partitioning effect leads to higher concentrations in the steam generator water (Figure 7).

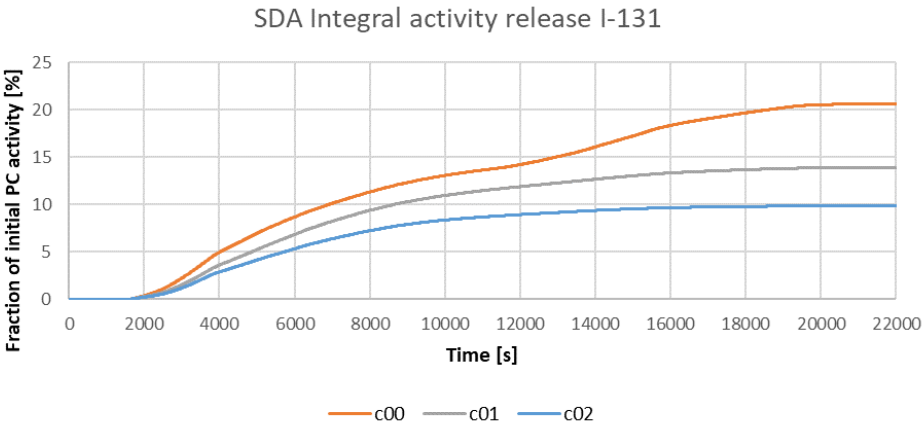

Figure 6. Sensitivity study on partitioning coefficient – SDA integral activity release.

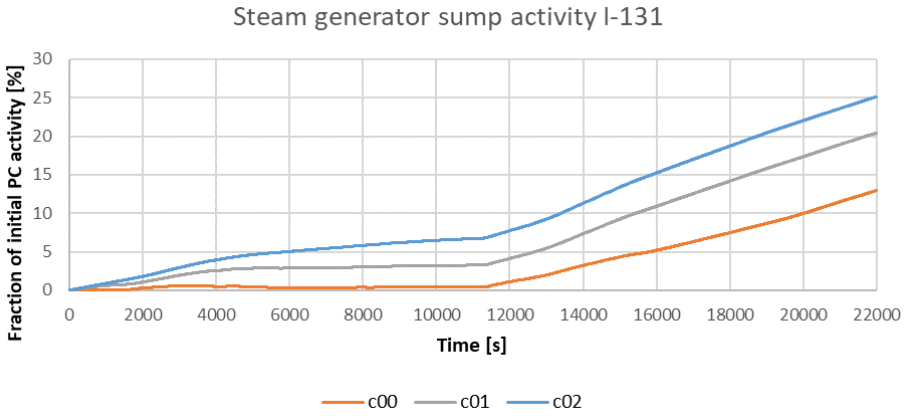

Figure 7. Sensitivity study on partitioning coefficient – SG sump activity.

The details of this assessment, model and simulation are presented in the Appendix D to this document.

CIEMAT

CIEMAT has identified and analyzed the experimental data and available open literature that might be applicable in the study of FP transport along the primary circuit and their transfer to the secondary side of the steam generator during SGTR DBA and DEC-A sequences. Particular attention has been paid to the representativeness of the initial and boundary conditions, the reliability of the experimental techniques used, and the experimental protocol adopted. The analysis of the test programs considered is summarized below and detailed in the Appendix E of this document.

Test Iod-29 (OECD THAI-2)

The Iod-29 test, conducted at the THAI facility, investigated the release of gaseous iodine from a flashing jet. Iod-29 was dimensioned both geometrically and in terms of initial and boundary conditions as anticipated in a SGTR

DBA accident. Thus, the data might be considered relevant for the scenario of investigation (discharge from the primary to the secondary side of a SG).

The iodine measurements in the THAI vessel (gas space and sump) and in the primary vessel consistently showed that there was no gaseous iodine released from the flashing jet under the investigated test conditions. Measured concentrations in the THAI vessel were very low. This observation is consistent with measurements on iodine speciation in the water of the pressure vessel, sampled during heat-up just before and just after the flashing process. Although 19.0E-03 kg of I_2 (molecular iodine) were injected before heating up, only iodide form was found. In other words, the injected I_2 reacted quickly with the steel walls of the primary vessel during heat-up and produced the non-volatile I^- form.

The conditions imposed in Iod-29 conditioned the observations as they resulted in a very low amount of iodine in the form of volatile I_2. Nonetheless, given the amount of surfaces along the primary circuit that the iodine released during iodine spiking will be exposed along its path most of iodine might be well in the form of iodide (I^-) under the conditions explored. Another important feature of the test was the pH imposed in the iodine solution, around neutral (values in between 6.9 and 7.4 should be in PWR coolant), that might be assumed not to change drastically because of addition of HPIS inventory during SGTR DBA and DEC-A transients.

ARTIST-Phase VI

The ARTIST-Phase VI (Droplet retention in the separator and dryer sections under dry conditions**)** test addressed experimentally the droplet retention and velocity field in the separator (1:1 in scale) and dryer unit (1:1 in scale) of a SG. The potential containment bypass in case of a SGTR DBA was investigated by assuming a break at the top of the tube bundle.

The gas flow rates imposed were much lower than what expected at high pressures (150 bar) in the primary circuit. The main observations of the test showed that the droplet transport downstream separators and dryers will be dependent on the carrier gas mass flow rate and on the droplet size. This said, the larger the droplet the less sensitive to the flow rate conditions (reported differences smaller than 20%). Besides, given that the flow rates imposed are estimated to be lower than the actual ones, the retention efficiency for the two highest flow rates might be applied to higher ones.

Iodine Speciation and Partitioning in PWR SGTR Accidents

A comprehensive investigation program was launched in the USA on SGTR accidents (see Appendix C) with the objective to find out as much information as possible on two key variables affecting FP transport into the SG secondary side: iodine speciation in the primary system; and iodine partitioning dependence on pH and oxygen potential.

The results of the SG iodine partitioning experiments showed the PC sensitivity to pH, although in all the cases the ratio of aqueous versus gaseous iodine was over 350; i.e., iodine in solution shows little volatility. Specifically, when considering pH in the range of coolant ones (≥ 7), one should expect even less volatility regardless other conditions of the tests. As for the effect of concentration on PC, the results showed that in aqueous solutions at 285 ˚C and 68.94 bar with concentrations in the range of 10^{-9} M a fraction of I_2 around 2% should be expected. In an SGTR accident if primary and secondary side coolants mix-up more reducing and higher pH conditions should occur, which would result in a fraction even less than such a 2%.

Additionally, to the experimental data assessment, the implemented models of MELCOR for FP transport and their applicability to SGTR sequences has been examined. The iodine models available in MELCOR are developed for conditions typical for reactor containments and could not be applied under the secondary side conditions of a SGTR sequence.

To consider the mechanisms in the transport and behavior of the iodine during SGTR sequences in DBA and DEC-A conditions (flashing of break primary water to steam, break primary water atomization and iodine partitions between liquid and vapor states and its transport with the steam, out of the steam generator and ultimately to the environment) a model, based on the MELCOR flashing model, was implemented using external MELCOR control functions.

If superheated liquid water enters a control volume at an elevation above the pool surface, some fraction of it flashes to vapor. Another fraction is dispersed as liquid droplets that are small enough to remain suspended in the atmosphere for a significant time. This effect is captured by the MELCOR flashing model. If the water is superheated at the pressure of the receiving volume, the model accounts for stagnation and equilibration at that pressure. Although the model does not explicitly account for heat transfer, at least part of the effect is captured when the partitioned water vapor, fog, and pool liquid are equilibrated with the previous contents or the volume.

The model was implemented using external control functions. The total iodine released to the environment is calculated knowing the mass of the steam released throughout the SG relief valve and the total concentration of iodine in the atmosphere of the SG (considering the flashing, atomization and partitioning contributions). It is important to point out that the model, with minor modifications is also applied in the sequences where the first release is through the breaking steam line (e.g. DEC-A SGTR sequences). Figure 8 shows a schematic representation of the model to describe the transport of iodine released in the RCS to the secondary part of the SG and to the environment.

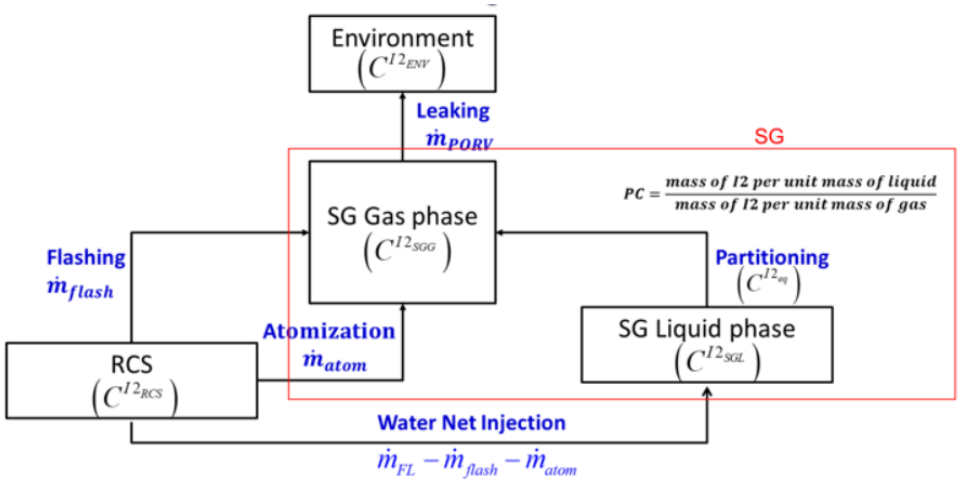

Figure 8. Schematic representation of the iodine transport model.

A sensitivity analysis of the MELCOR modelling of the water drops size in the flashing model has been conducted for the SGTR DBA sequence with a double-ended break located in the apex of the longest U-tube of one of the three SGs. In this scenario, the radioactivity release is maximised as the break remains uncovered for a longer period of time with respect to the lower part of the U-tubes. The results of the analysis showed that the droplet size affects drastically the relative importance of each phenomenon. If a droplet size between 35 and 50 μm is assumed (Figure 9), atomization became in the main mechanism of iodine release as is expected in this kind of sequences.

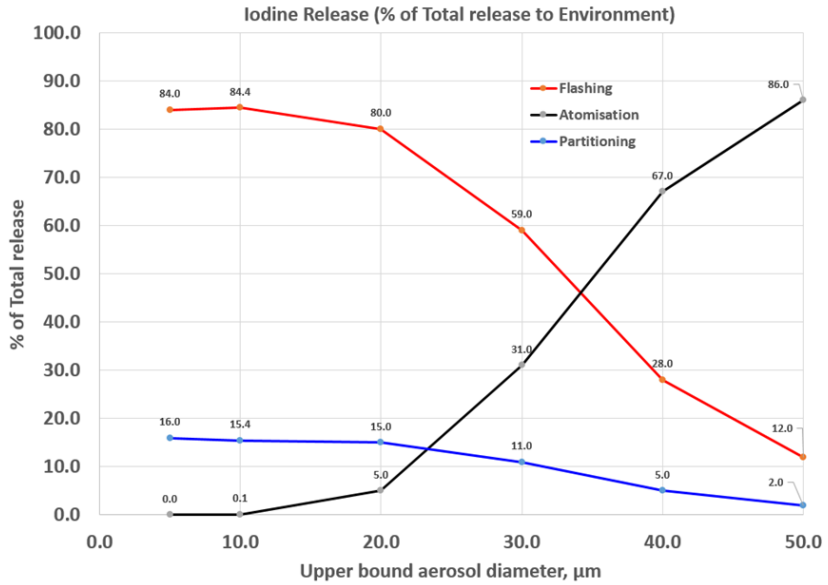

Figure 9. Impact of the droplet sizes on the total released activity to the environment.

The details of this assessment and models are presented in the Appendix E to this document.

SSTC NRS

SSTC NRS has conducted simulations with RELAP5 code to evaluate FP transport during SGTR DBA scenario at VVER-1000 plant. In such calculations it was assumed that the activity is transported with primary coolant and distributed uniformly in liquid phase of the reactor coolant over all RCS components. During the break from RCS to the secondary side of SG-1 part of the activity is transfered from the liquid phase to the vapour with a transfer coefficient, K_g. The activity that remains in the liquid phase is calculated as K_f=1-K_g.

The overall approach to activity transport is based on tracing the RCS activity dimensionless concentration with application of RELAP5 code boron tracing model with boron playing the role of the tracer. This allows to account for the dilution of radioactive coolant content by injected non-radioactive ECCS water (with tracer concentration of 0) and mixing in RCS and SG secondary side.

Figure 10 presents the simplified layout of the RELAP5 RCS to SG-1 break model and specifies the points of tracing the activity content concentration.

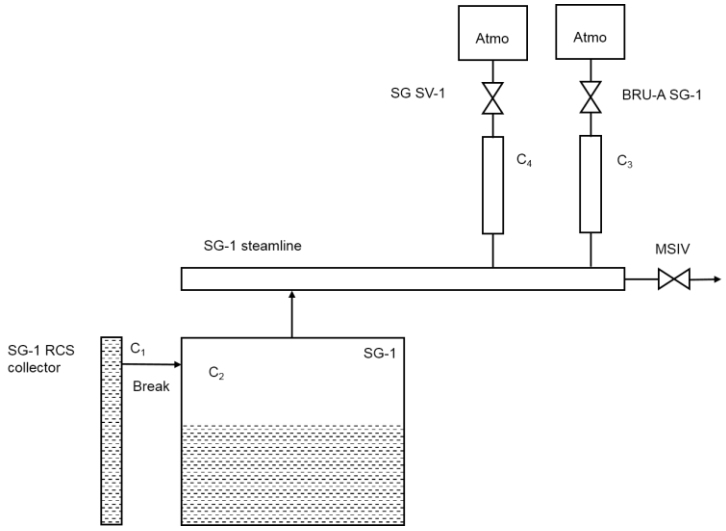

Figure 10. SGTR break simplified nodalization with target points for the analysis.

The RELAP5 code simulates boron propagation in liquid phase only, and dimensionless concentrations (in mass parts of tracer per mass part of liquid phase) are obtained as follows:

- C_1 concentration of tracer in the control volume upstream the break, initial concentration is 1;
- C_2 –concentration of tracer in the liquid phase of SG control volume downstream the break, initial concentration is equal to 0;
- C_3 –concentration of tracer in the liquid phase of the SG steam line control volume upstream the steam dump valve to atmosphere (BRU-A), initial concentration is equal to 0;
- C_4 – concentration of tracer in the liquid phase of the SG steam line control volume upstream SG safety relief valve SV-1, initial concentration is equal to 0.

As a reference of the initial activity of RCS coolant, the steady state activity plus DBA iodine spike values were used. The results of the analysis of FP release distribution for different gas transfer coefficients K_g is presented in the Appendix F of this document.

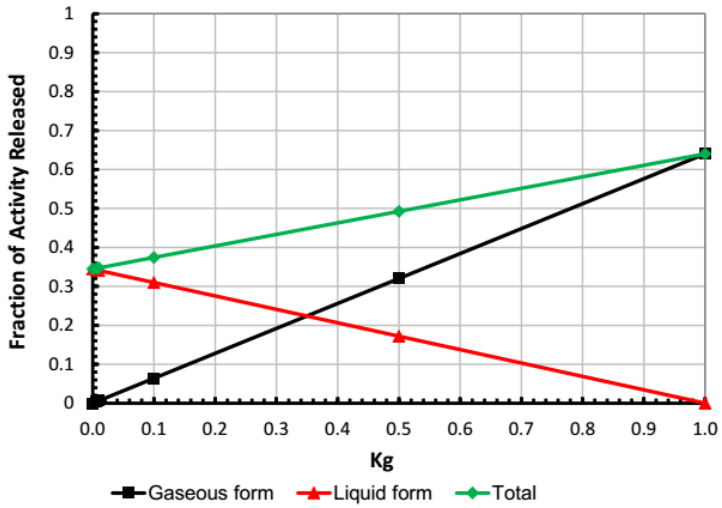

Figure 11. Activity fraction transported to SG and environment for different K_g.

The fraction of RCS initial activity released to SG and environment in both gas and liquid phases for different gas transfer coefficients K_g is presented in the Figure 11. According to the figure, the fraction of RCS activity transferred to the SG is about 0.64 and depends on the timing of operator actions on break isolation and ECCS termination/throttling (prescribed by emergency operating procedures). The total amount of activity released to environment (gas + liquid) depends on the transfer coefficient from liquid to gas phase and corresponds to the value 0.345 of initial RCS activity for $K_g = 0$ and to 0.64 of initial RCS activity for $K_g = 1$ (as for non-condensable gases).

The collector cover lift-up is the most limiting (bounding) case of the primary-to-secondary breaks for the release because the mixing with water in SG lower levels is minimal. In case of SG tube break (when the break is located below SG water level) the influence of SG water dilution and release decrease would be more substantial.

This approach is rather simple in realistic estimations of the doses because of SGTR events and might be used for operator and in the automatic's actions optimization.

The details of this assessment and models are presented in the Appendix F to this document.

3. Final remarks

Achievements on reassessment of experimental data base and on the model/code improvements for FP releases during a SGTR transient have been obtained and presented in this final report:

- RELAP5-3D capability to simulate the FP transport and behaviour during SGTR transients has been enhanced. An empirical model based on reactor power and time in fuel cycle has been proposed and several removal effects on iodine transported have been accounted for through a post-processing function.
- RELAP5 boron tracing features have been used to approximate the activity transfer between primary and secondary systems and specifying a transport coefficient from the liquid primary water to the gas phase of the secondary side of the steam generator.
- MAAP5 code has been enhanced by adding a simplified model for iodine spiking (also caesium and other FPs, except for noble gases) and by including different correlations describing the primary to secondary transfer in the steam generator. Both models have been verified by setting comparisons with the COSAQUE code, reference code for these scenarios.
- The ASTEC code capabilities to handle SGTR transients have been enlarged by adding two new modules: DROPLET to model the mechanical fragmentation and thermal fragmentation of water and flashing rates; and SAFARI to describe the radioactive transfer from the primary to the secondary circuit and, eventually, to the environment.
- MELCOR 2.2 has been also extended to deal with DBA and DEC-A SGTRs through including control functions in the scenario modelling by accounting water flashing and atomization as well as partitioning from the steam generator water inventory.
- A stand-alone model describing the primary-to-secondary activity transfer has been also built based on mass and activity preservation equations, which specific focus on DBA SGTR conditions.

Most of these developments were initially associated to a literature search on such primary-to-secondary transfer. Overall, it might be stated that not enough data were found to support any specific development concerning the transfer and further data would be certainly welcome.

Additional details from the contributing organizations may be found in the Appendixes.

References

1. Z. Hózer, Herranz L.E., Luzzi L., Leclere C., Detailed Program of Work for WP4, 2020.

2. Zoltán Hózer, et.al: Report on SGTR and LOCA available experimental data. T2.1.3. Review of experimental database, R2CA project, August, 2020.

Appendix A- BOKU Report

Contents

1. Introduction

During the course of the R2CA project, RELAP5-3D is the main programme used at BOKU for the transient calculations. Although being a thermal hydraulic system code, RELAP5-3D has limited capabilities to model radio nuclide behaviour. Target of the work of BOKU in this task is to improve the fission product transport and behaviour for RELAP5-3D during SGTR transients in the primary and secondary circuit. First, decay chains of fission products within the code were analysed, and possible shortfalls and room for improvement was identified. In order to get sufficient data to validate our fission product simulation, a literature research regarding iodine measurements at NPP was conducted (see chapter 2). During the initial transient simulation, iodine spiking values were calculated via an iodine spiking model created by the NRC (Adams J.P. and Atwood C.L. 1989). During the course of the project, it was possible to create an own empirical iodine spiking model with the obtained data (see chapter 4). This model will be used for the final calculations of the project. As RELAP5-3D is only capable of transporting fission products, but it is not possible to include any physical modification or retention effects (clean up system, radioactive decay, pool scrubbing, etc.), a post processing function was included which allows to further improve the iodine simulation. As a last step the CIAU method was applied to assess the magnitude of the mathematical uncertainties of the simulation.

2. Assessment of the experimental database of fission product transport and release

2.1. Brief description of the experimental program

In order to obtain sufficient data for the iodine spiking phenomenon, an extensive literature research was conducted. The literature review revealed that there has been very little publicly available data on this topic over the last 30 years. Therefore, most data mentioned in this chapter is from studies prior to 1990. A comprehensive study by the NRC on this topic was published in 1989 which contains 168 entries of iodine spiking events (Adams J.P. and Atwood C.L. 1989). A second study that provided several IS entries was conducted by Lewis et al (2017). In addition, data from smaller studies or reports from individual power plants were included in this report (Zoltán Hózer 2001, Smiesko et al. 2005). Considerably more data was found for PWRs produced by the American manufacturers than from Russian VVER. For VVER 1000 reactors any data was accessible. In addition, it was possible to expand the data set with entries from the US fuel reports from the years 1983 to 1988 in order to record the position in the fuel cycle on the day of the respective event (NRC, 1984; NRC, 1986; NRC, 1989). Iodine spiking data on European PWRs were not found in the open literature and were not available through R2CA partners for this review.

Development of threshold values

- According to the NRC Standard Review Plan (Section 15.6.3), for the licensing process it must be assumed that, in the event of a transient, the release rate increases by a factor of 500 in comparison to normal operation. According to this approach, in case of a SGTR transient, an iodine release of 6190 Ci/h could be assumed for an average NPP (Jennifer Uhle and Andrea D. Lee 2006). Adams and Atwood report in their study 168 iodine measurements at 26 plants before and during iodine spiking events. The average iodine concentration during the steady state is at 4.89E-2 µCi/g (coolant). According to the mentioned approach above, an average iodine spike of 24.45 µCi/g would be expected. However, in reality the measured IS values were at 7.57E-1 µCi/g (285 Ci/h), which shows that this approach is very conservative.

- In a study of the NRC, it was evaluated whether the mentioned factor of 500 is too conservative. The study analysed 168 iodine measurements at 26 NPPs. It was possible to determine a formula that allows

an elementary calculation of the expected iodine concentration during the transient by using unrestricted linear modelling. According to this formula, the iodine concentration is only dependent on the power of the reactor at the time the transient began. As the expected IS activity at a reactor with 0 MW power is 0 Ci/h, it was decided to use an unrestricted model without an intercept (Adams J.P. and Atwood C.L. 1989):

$$Activity\_IS = 0.71\ Ci/h * P\_electric$$

Activity_IS = Activity of Iodine Spike [Ci]
P_electric = Electrical Power [MW]

For the average power mentioned in Adams and Atwood, this would mean an IS of 285 Ci/h. which is significantly lower than the calculated IS with the factor of 500 mentioned in the section above. For our preliminary transient calculations, it was necessary to be able to estimate the extent of fission product releases during the accidents. Therefore, this NRC approach was used. However, it should be noted that the approach to establish this formula is rather simply as only one independent variable is included in the model (see Tab.2).

2.2. Test matrices

NRC PWR study of IS at American PWR (1989)
This study includes 168 data entries (Tab. 1) of reactor trips which were collected from 26 plants. These plants were selected from all regions of the US and from all three American PWR vendors. Until the date of the study, less than ten SGTR events have occurred in US PWRs. Thus, the iodine spiking data from these events alone are insufficient for predicting the behaviour of future iodine spiking events. However, an SGTR occurring during power operations would result in a reactor trip, which is a large power excursion. Since this power excursion causes (due to pressure and temperature reduction) the iodine spike, it can be assumed that the probability of an SGTR event leading to an iodine spike of a certain magnitude corresponds to the same probability resulting from a reactor shutdown. The assumption that it is the reactor trip that causes the iodine spike and not something else related to the SGTR itself allows for a much larger database. However, it should be noted that there are other phenomena which can affect the development of the iodine spike, like the amount of defective fuel rods for instance. The key parameters of this study can be found below. For post Iodine values the highest measurement values between 4-6 hours after the transient were taken (Adams J.P. and Atwood C.L. 1989).

Table 1: Data entries of NRC study regarding iodine spiking at PWR (Adams J.P. and Atwood C.L. 1989).

No	Plant	VENDOR	POWER %	PRE-I(µCi/g)	POST-I(µCi/g)	Ratio POST/PRE	R3 (µCi/h)
1	ANO-1	B&W	100	5.64E-01	1.44E+01	25.53	5.53E+03
2	ANO-2	B&W	75	2.46E-01	7.43E+00	30.20	2.86E+03
3	ANO-3	B&W	100	7.02E-02	3.32E+00	47.29	1.28E+03
4	ANO-4	CE	100	2.61E-01	1.11E+00	4.25	3.36E+02
5	ANO-5	CE	100	1.28E-01	3.00E-01	2.34	8.48E+01
6	ANO-6	CE	100	1.27E-01	4.39E-01	3.46	1.30E+00
7	ANO-7	CE	100	1.23E-01	1.11E+00	9.02	3.47E+02
8	ANO-8	CE	100	3.62E-01	4.81E-01	1.33	1.20E+02
9	ANO-9	CE	100	5.05E-02	1.79E-01	3.54	5.30E+01
10	ANO-10	CE	95	6.47E-02	2.46E-01	3.80	7.36E+01
11	ANO-11	CE	100	4.06E-02	1.94E-01	4.78	5.89E+01
12	ANO-12	CE	100	3.08E-02	1.53E-01	4.97	4.66E+01
13	ANO-13	CE	100	2.98E-02	1.71E-01	5.74	5.25E+01
14	ANO-14	CE	100	4.43E-02	2.36E-01	5.33	7.22E+01
15	ANO-15	CE	100	5.51E-02	3.88E-01	7.04	1.20E+02
16	ANO-16	CE	100	9.25E-02	6.83E-01	7.38	2.12E+02
17	ANO-17	CE	100	5.75E-02	9.00E-01	15.65	2.86E+02
18	ANO-18	CE	100	4.80E-02	8.74E-01	18.21	2.79E+02
19	ANO-19	CE	100	5.06E-03	6.07E-03	1.20	1.47E+00
166	Surry-2	W	100	2.00E-04	2.00E-04	1.00	4.81E-02
167	Surry-2	W	100	2.00E-04	3.00E-04	1.50	8.04E-02
168	Surry-2	W	100	2.00E-04	2.00E-04	1.00	4.81E-02
MEAN				4.89E-02	7.57E-01	26.03	2.57E+02
MIN				5.28E-05	3.90E-05	0.22	5.04E-03
MAX				5.64E-01	1.44E+01	580.34	5.53E+03
MEDIAN				1.39E-02	1.91E-01	8.27	6.10E+01

Tab. 2 includes NPPs with several data entries. It is visible that even within one specific NPP a power excursion does not always lead to a comparable IS – event. This leads to the conclusion that reactor power alone is not sufficient to predict the iodine spiking effect.

	ANO-I	ANO-2	CalClf-1	Catawba-1	Catawba-2	Cook-1	Etc.
Max (µCi/h)	5.53E+03	3.47E+02	1.66E+02	1.18E+01	6.56E-01	2.10E+02	…
Min (µCi/h)	1.28E+03	1.47E+00	3.01E-01	9.59E-01	7.23E-02	3.36E-01	…
Mean (µCi/h)	3.22E+03	1.45E+02	8.42E+01	4.59E+00	2.98E-01	9.09E+01	…
StDev (µCi/h)	2.15E+03	1.06E+02	7.61E+01	6.25E+00	2.18E-01	9.74E+01	…

Table 2: Selection of NPP with multiple data entries.

According to the data of this study, the probability that an SGTR would result in a release rate less than 0.258 Ci/h*MW(e) is 75% (Adams J.P. and Atwood C.L. 1989). It shows that the fixed value of 0.71 Ci/h*MW(e) used in the NRC iodine spiking formula is very conservative. Furthermore, it can be elaborated with this data that the mean ratio between the iodine concentration before and after the anticipated transient lies at 26. Only in two cases the ratio exceeded 230 (once at 360 and once at 580). In both cases, the iodine concentration after the anticipated transient was lower than the mean value of the study. Therefore, it can be concluded that the reason for the high ratio was rather a low iodine concentration in the normal operation and no higher risk for the environment has to be assumed. The results of this survey indicate that the NRCs prescribed value (iodine ratio of 500 between the steady state and the transient) for the licensing of nuclear power plants can be considered as extremely conservative in comparison with the measured values (Jennifer Uhle and Andrea D. Lee 2006).

Second PWR Study:
For 15 cases of reactor trips (Tab.3), data entries were collected and the escape rate calculated (B.J. Lewis et al., 2017)**:**

Table 3: US PWR Iodine SS measurements and calculated escape rate in normal operation and reactor trip conditions (B.J. Lewis et al. n.d.).

Plant	Measured Steady State Coolant Activity I_{131} (µCi/g)	Calculated Steady State Escape Rate v(s-1)	Calculated Transient Escape Rate v(s-1)
Ginna	9.10E-01	9.70E-07	5.50E-06
Ginna	7.00E-01	3.60E-07	1.40E-05
Haddam Neck	4.83E-01	8.10E-07	1.10E-05
Haddam Neck	0.35E-01	1.20E-07	5.50E-06
McGuire-1	0.15E-01	1.00E-06	1.40E-05
Mihama	1.00E-01	2.90E-06	2.80E-05
Mihama	0.50E-01	6.60E-07	1.40E-05
Oconee	0.26E-01	8.60E-07	9.40E-05
Point Beach	0.06E-01	1.50E-06	2.20E-04
Point Beach	1.27E-01	4.00E-07	5.50E-06
San Onofre	0.23E-01	3.20E-07	5.50E-06
San Onofre	1.24E-01	8.60E-07	7.90E-06
Surry-1	0.23E-01	7.30E-07	2.80E-05
Surry-1	0.33E-01	7.30E-07	3.20E-05
TMI	0.24E-01	1.40E-06	5.00E-05
Average	1.79E-01	9.08E-07	3.57E-05

The model used in this paper to calculate the escape rate during the reactor trip transients was validated by comparison with real data at NPPs. Unfortunately, the data was not published. However, it is visible that the mean of the iodine activity during the normal operation is about 3.5 times larger than the mean of the NRC PWR study.

VVER – 440

The following iodine concentrations were measured during reactor trips at the Paks power plant (Zoltán Hózer 2001):

Table 4: IS concentration measured at two units of the Paks NPP (VVER-440).

No	Unit	I_{131} concentration during steady state[1] [µCi/g]	I_{131} concentration peak during spike[1] [µCi/g]	Ratio of I_{131} increase
1	Paks 2	7.88E-05	1.08E-02	137
2	Paks 3	9.28E-05	6.97E-03	75
3	Paks 3	6.20E-05	5.69E-03	92
4	Paks 3	2.35E-04	1.88E-02	80
5	EBO 2	4.22E-04	2.11E-01	500
6	EBO 2	4.22E-05	1.05E-02	250
7	EBO 2	2.11E-03	2.74E-01	130
8	EBO 3	7.38E-05	2.10E-02	285
Mean		3.89E-04	6.98E-02	179
Median		8.58E-05	1.48E-02	172
Max		2.11E-03	2.74E-01	130
Min		4.22E-05	5.69E-03	135

[1] Table entries originate from the cited papers (Zoltán Hózer 2001; Smiesko et et al. 2005) and were converted under the following parameters: coolant pressure: 12.4 MPa; coolant temperature at core inlet: 268 °C (Gündüz et al., 1994.).

Table 1 and Table 4 show that the mean iodine concentration at the NRC PWR study is exceeding the mean measured value at the VVER-440 reactors before and after the peak with the factors 125 and 11. However, this is due to the fact that the NRC PWR study addresses a large number of reactors. Some of the western PWRs examined have similar iodine values in comparison to the Paks reactor units. This is also visible by looking at the minimum value, which is lower in the NRC study (5.3 E-5) than for the VVER-440 reactors (6.2E-5). Furthermore, at Paks 3 there are 3 data entries which differ significantly. This shows again that power alone is not sufficient to calculate the height/impact of an iodine spike. It was mentioned in the paper that each shut-down transient in Paks 3 occurred at a different fuel cycle. Therefore, the importance of the condition of the fuel rods is emphasised. Moreover, the VVER-440 study reveals that the mean ratio (90) between the iodine concentration before and after the transient is lower than the prescribed value for the licensing process (500). However, the ratio for the VVER-440 is more than 3 times as high as for the NPP in the NRC study with 168 entries (27).

VVER-1000

For VVER-1000 reactors no measurement data regarding the IS phenomenon was found in the literature. However, the regulation of Ukraine threshold values for the safety limit and the operational limit of the VVER-1000 were found (IAEA 2019).

Table 5: Safety Limit and Operational Limit for VVER-1000 in Ukraine.

	Safety limit for I131/I135 (µCi/g)	Operational limit for I131/I135 (µCi/g)
VVER-1000	5.00E+02	1.00E+03

2.3. Critical assessment of the data

Generally, it is not easy to find data on the iodine spiking phenomenon which is related to an SGTR accident. This is mainly due to the fact that in the USA, for example, only about 10 of these accidents took place until 1990 and, furthermore, not all power plants provide their data for the public. Therefore, most of the data in 2.2 originates from a large study conducted in the USA, where iodine concentrations were measured during a normal shutdown at PWRs. It was mentioned in the study that as the power reduction causing the pressure and temperature decrease is the main driver of the iodine spiking effect, it is not necessary to use only data from power transients caused by an SGTR. In addition, there is insufficient data on such incidents to conduct meaningful research (Adams J.P. and Atwood C.L. 1989). Regarding the measurement of iodine concentration at NPPs, it should be noted that the data entries are not always fully comparable. There are different reasons for this:

1) **IS development with varying velocity**
   The build-up of the Iodine spike is generally not symmetrical. This means that usually the iodine activity in the coolant increases rapidly after the initiating transient and reaches its maximum value after four or five hours. By 10 hours, the activity is dropping, but it is still elevated at 30 hours (B.J. Lewis et al. n.d.). Most studies regarding IS do not list much data at times greater than 10 h (Jennifer Uhle and Andrea D. Lee 2006). The NRC study, for instance, only includes the first 6 hours after the transient was initiated. The mean value of this study can therefore not simply be compared with mean values of other studies. Due to the short examination time, the maximum measured post-accident concentrations are not necessarily the peak concentrations, since the peak may not have occurred at the time the sample was taken. To allow for this, the maximum measured concentrations were conservatively multiplied by a factor of three to get a “bounded maximum value” (Adams J.P. and Atwood C.L. 1989). This bounded value was used to calculate the release rates. It should be noted that this approach is not optimal for obtaining exact values.

2) **Different level of power at the investigated NPP**
   In the present studies, power plants with different power levels were investigated. As the power level of the NPP has a direct influence on the spiking effect, this must be taken into account in further analysis.

3) **Varying degree of defective fuel rods**
   A higher degree of damage leads to an enhanced IS effect, as more FP are deposited on the fuel rod surface and/or are dissolved in the gap, which are washed out into the primary cycle due to the changed conditions of the transient (initiated by the pressure and temperature loss) (Eickelpasch, Seepolt, and Hock, 1978).

4) **Different iodine concentrations at the same NPP for the steady state condition as well as the transient.**
   For most NPPs, the IS phenomenon has been observed more than once, but it is clear that the iodine concentration is not constant at all measurements. This is visible in table 2.

5) **A possible second spike is not included in measurements.**

A transient caused by an SGTR might cause a second spike. In the NRC study only the first measured iodine maximum is considered in the analysis, since it is judged that the second maximum might be affected by additional transients and does not accurately reflect the effect of the trip alone. (Adams J.P. and Atwood C.L. 1989). Jennifer Uhle et al. mention that the iodine spike phenomenon is not symmetrical and is not effectively over until 30 to 40 hours have elapsed (Jennifer Uhle and Andrea D. Lee 2006). Another reason why this second spike would not be included in the data is, as already mentioned, the measurement time of most studies was too short. Since in the anticipated accident scenarios a second spike would cause an effect on the environment and the health of human, this phenomenon should be considered in further investigations.

2.4. Mayor insights

The mayor insights of this assessment are listed below:

- **It is very difficult to compare data from different studies due to alternating:**
  - primary defects,
  - types of the reactors,
  - power levels of the reactors,
  - measurement time and location.

- **Little data has been published since 1990**
  - Since measurement methods/approaches may have improved over the past 30 years, this situation is not favourable, especially because no publicly available data has been found for the newer reactor systems, such as VVER-1000 or modern western PWR designs that are being studied in the R2CA project.

- **The NRC Standard Review Plan benchmark for licensing, which assumes that during an accident the iodine concentration increases up to 500 times in comparison to normal operation, is too conservative (see Tab.1 and Tab. 3).**

- **The NRC formula, which was created to correct the benchmark, is too conservative as well (see Tab.1 and Tab. 3). Furthermore, it uses a model which only uses one explanatory variable (power), which is not ideal if the deviations in IS measurements at the same reactors (with the same power) are viewed (see Tab. 2).**

- **There is little comparative material between European/American PWR and Russian VVER because too little VVER data is available and European PWR data are not available at all.**

3. Assessment of the IS phenomenon in code models

3.1. Brief description of the code

RELAP5-3D is a successor to RELAP5/MOD3. The code is used primarily for the analysis of potential accidents and transients in water-cooled nuclear power plants, and for the analysis of advanced reactor systems. RELAP5-3D provides a multi-dimensional thermal- hydraulic and kinetic modelling capability, which distinguishes the code from its predecessors (INL 2012a). The multi-dimensional component in RELAP5-3D allows the user to model the multi-dimensional flow behaviour more accurately, thus removing any restrictions on the applicability of the code to the full range of postulated reactor accidents. RELAP5-3D is a highly generic code that, in addition to the calculation of the behaviour of a reactor coolant system during a transient, can be used for the simulation of a wide

variety of hydraulic and thermal transients in both nuclear and nonnuclear systems involving mixtures of steam, water, non-condensable, and solute (Müllner 2010). RELAP5-3D is developed and maintained at the Idaho National Laboratory (INL) for the United States Department of Energy (US DOE). The first version (1.0.0) was released in July 1997. The most recent version is 4.4.2, released in June 2018 (INL 2012b). RELAP5-3D is written in FORTRAN 95 for 32- and 64-bit computers.

3.2. Description of the code models for transport and release

Although being a thermal hydraulic system code, RELAP5-3D has limited capabilities to model radio nuclide transport. RELAP5-3D does not calculate fuel behaviour, instead general tables or control variables are utilized. With those it is possible for example to determine the release of a radionuclide specie from fuel rods due to bursting during a transient or through pinhole leaks that develop due to erosion, fretting, or manufacturing defects in the fuel rod cladding or through leaching of the nuclide from the structural material in the reactor system (INL 2012c). However, the accuracy of this approach is not considered as adequate, because Relap5-3D is not capable to compute any decay or physical retention effects on nuclear species during the runtime of the code.

An Eulerian radionuclide transport model is applied to simulate the transport of radioactive or fertile nuclides in the reactor coolant systems. In connection with the nuclear detector model, this model can be applied to describe the response of the control and safety systems to the existence of radioactive species in the coolant systems. The radionuclide species may be transported by either the liquid or vapor/gas phases. It is possible to create a radioactive specie by either neutron absorption in a fertile specie or by injection into the coolant system using general tables or control variables (INL 2012c). The concentrations of radionuclide species are assumed to be sufficiently dilute that the following assumptions are valid:

- The fluid properties (liquid or vapor/gas) are not affected by the presence of radionuclide substances.
- Energy absorbed by the transporting phase from the decay of radionuclide species is negligible.
- The radionuclide species are well mixed with the transporting phase so that they are transported at the phase velocity (INL 2012c).

Under these assumptions, the equation for the conservation of mass for a radionuclide substance is:

$$\frac{\partial C}{\partial t} + \frac{1}{A}\frac{\partial}{\partial x}(CvA) = S$$

Where:

C… density (concentration) of the radionuclide specie in atoms per unit volume (atoms/m^3),
v… velocity of the transporting phase,
A… cross sectional area of the flow duct,
S… source of the radionuclide specie in units of atoms per unit volume per second (INL 2012c).

The density (concentration), C, may be converted to the mass density using:

$$\rho = \frac{C \bullet Mw}{N_a}$$

Where:

ρ… mass density of the radionuclide specie in units of mass per unit volume (kg/m^3),
N_a… Avogadro's number (atoms/kg-mole),
Mw… molecular weight of the radionuclide specie (kg/kg-mole) (INL 2012c).

3.3. Critical assessment of the model's applicability

The transport model of RELAP5-3D works and provides realistic results. It has already been used for the initial calculations during the project. However, as Relap5-3D utilizes general tables or control variables to calculate fuel behaviour, it is only possible for the user to define which substances are present in which form (fluid/gaseous) (INL 2012c). Nevertheless, during the runtime of the code, the characteristics of the substances are not affected in any way. As a result, transported fission products do not experience any material conversion. In theory, the programme provides a function where parent and daughter nuclides can be defined. However, this function has almost never been used in the literature and is not sufficiently validated (Honaiser and Anghaie 2004). An own assessment was conducted to analyse whether RELAP5-3D is capable of simulating fission product behaviour in a simple environment. It became evident that no decay of I_{131} to Xe_{131} occurs nor decay into any other nuclide. I_{131} was reduced due to half-life, but no daughter nuclides emerged.

4. Description of the model enhancements

4.1. Creation of an empirical IS Model

The aim of BOKU at this WP was to collect as many data as possible regarding IS phenomena and create an empirical model that not only considers the power as explaining variable (like the NRC model) but also the current position (amount of days) of the fuel cycle. The current position in the fuel cycle is an important indicator as an IS only can take place if there are small breaks at the fuel rods. Those defects develop over time. Therefore, it can be assumed that if the reactor is further in the fuel cycle it is more likely to have defects at the fuel rods. For this reason, the dataset was expended by including information regarding the fuel cycle of the different reactors of the US nuclear fuel annual reports (Tab. 6).

Table 6: Dataset extended with days in fuel cycle

No	Plant	VENDOR	POWER %	Days in Fuel Cycle	PRE-I(µCi/g)	POST-I(µCi/g)	Ratio POST/PRE	R3 (µCi/h)
1	ANO-1	B&W	100	**509**	5.64E-01	1.44E+01	25.53	5.53E+03
2	ANO-1	B&W	75	**517**	2.46E-01	7.43E+00	30.20	2.86E+03
3	ANO-1	B&W	100	**485**	7.02E-02	3.32E+00	47.29	1.28E+03
4	ANO-2	CE	100	**485**	2.61E-01	1.11E+00	4.25	3.36E+02
5	ANO-2	CE	100	**267**	1.28E-01	3.00E-01	2.34	8.48E+01
6	ANO-2	CE	100	**297**	1.27E-01	4.39E-01	3.46	1.30E+00
7	ANO-2	CE	100	**505**	1.23E-01	1.11E+00	9.02	3.47E+02
8	ANO-2	CE	100	**141**	3.62E-01	4.81E-01	1.33	1.20E+02
9	ANO-2	CE	100	**236**	5.05E-02	1.79E-01	3.54	5.30E+01
10	ANO-2	CE	95	**264**	6.47E-02	2.46E-01	3.80	7.36E+01
11	ANO-2	CE	100	**443**	4.06E-02	1.94E-01	4.78	5.89E+01
12	ANO-2	CE	100	**476**	3.08E-02	1.53E-01	4.97	4.66E+01
13	ANO-2	CE	100	**515**	2.98E-02	1.71E-01	5.74	5.25E+01
14	ANO-2	CE	100	**574**	4.43E-02	2.36E-01	5.33	7.22E+01
15	ANO-2	CE	100	**3**	5.51E-02	3.88E-01	7.04	1.20E+02
16	ANO-2	CE	100	**193**	9.25E-02	6.83E-01	7.38	2.12E+02
17	ANO-2	CE	100	**375**	5.75E-02	9.00E-01	15.65	2.86E+02
18	ANO-2	CE	100	**444**	4.80E-02	8.74E-01	18.21	2.79E+02
19	ANO-2	CE	100	**365**	5.06E-03	6.07E-03	1.20	1.47E+00
166	Surry-2	W	100	**242**	2.00E-04	2.00E-04	1.00	4.81E-02
167	Surry-2	W	100	**285**	2.00E-04	3.00E-04	1.50	8.04E-02
168	Surry-2	W	100	**227**	2.00E-04	2.00E-04	1.00	4.81E-02
MEAN				**3.57E+02**	4.89E-02	7.57E-01	26.03	2.57E+02
MIN				**3.00E+00**	5.28E-05	3.90E-05	0.22	5.04E-03
MAX				**5.74E+02**	5.64E-01	1.44E+01	580.34	5.53E+03
MEDIAN				**3.70E+02**	1.39E-02	1.91E-01	8.27	6.10E+01

In a next step, a restricted linear regression model was constructed as in the US NRC study by Adams and Atwood (see section 2.2). However, in our model we used two explanatory variables, the “power [MW]” of the reactor and the “time in fuel cycle [days]” instead of only “power” alone. In the summary statistic of the regression, it is visible that both coefficients are significant (Fig. 1). Power is significant at the 5% level and the time in the fuel cycle at the 10% level. According to the formula, an iodine spike of 695.68 Ci/h is expected for a transient scenario at a reactor at 1000 MW, which is already one and a half years running. In comparison the model of the NRC which only considers power as determining factor would result into an iodine spike of 710 Ci/h under the same circumstance. Therefore, it can be assumed that the result of the developed model is in the correct size of magnitude. However, our model allows a wider range of analysis as it is now possible to conduct several calculations at different points of time in the fuel cycle. Therefore, it is possible to make a more accurate prediction of the severity of an accident where iodine reaches the environment. However, it has to be said that the issue regarding the small dataset still remains as not for all reactors data regarding the fuel cycle was available.

	Dependent variable:
	iodine spike [Ci/h]
power [MW]	0.286**
time in fuel cycle [days]	0.750*
R^2	0.241
Adjusted R^2	0.227
Residual Std. Error	840.830 (df = 104)
F Statistic	16.541*** (df = 2; 104)
Note:	*p<0.1; **p<0.05; ***p<0.01

Figure 2: Summary Statistic of empirical IS Model

4.2. Fission product post processing function

For our further calculations, the model described in 4.1 can be used. However, as was already described, the fission product transport model of RELAP5-3D is not capable of considering reductive effects on iodine. Therefore, in the next step we try to include several retention effects via a postprocessing function. As we are analysing both Russian VVER and Western CONVOI reactor, we established two versions of the function with specific input parameters.

The following effects are included in the function:

- Primary side coolant purification system.
- Secondary side pool-scrubbing effects.
- Containment retention effect.

4.2.1 Primary side coolant purification system

The reactors have the possibility to filter the coolant at the PS on a regular basis. For the PWR, for instance, the clean-up system is able to process up to 30 kg of coolant per second. Therefore, a clean-up coefficient of 0.01225 was calculated for this reactor type. However, it has been shown that the impact of such a system in the first hours of a transient scenario is only moderate (Fig. 2). The shown values originate of our VVER-1000 DEC-A SGTR scenario.

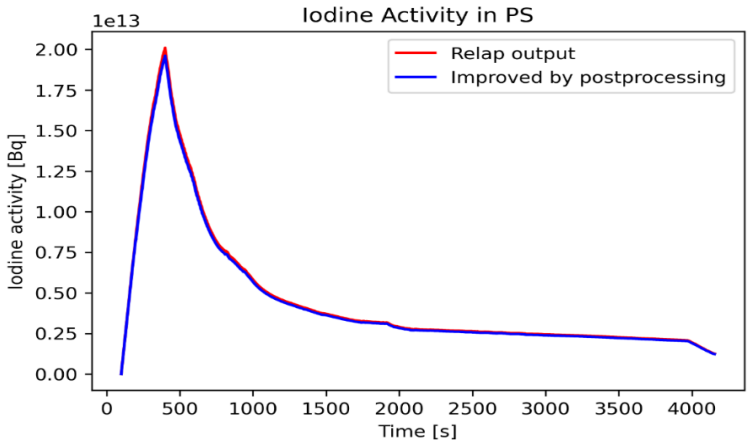

Figure 3: Effect of clean-up system on iodine

4.2.2 Secondary side pool-scrubbing effects

On the secondary side of the steam generator of the affected loop, a pool may form instead of the usual steam. This restricts the iodine mass flow which results from the steam generator tube rupture. This is especially the case as 90% of the iodine is transported as CsI in aerosol form. In the literature, several references can be found that describe how pronounced the retention effect on aerosols is in dependence on the water level above the break (NRC, 1995; Porcheron et al., 2019). One of the most important models in this regard was developed by Pich and Schütz (1991). The main equations of the model are presented below:

$$\eta_{Pich} = 1 - exp\left[-\left(5.1 \cdot \left(\frac{D}{U_b \cdot d_b^3}\right)^{\frac{1}{2}} + \frac{3 \cdot g \cdot \tau}{2 \cdot U_b \cdot d_b} + \frac{18 \cdot U_b \cdot \tau}{d_b^2}\right) \cdot H\right]$$

Where:
η_{Pich} is the collection efficiency,
D ($m^2.s^{-1}$) is the Brownian diffusion coefficient,
U_b is the bubble rising velocity ($m.s^{-1}$),
τ is the particle relaxation time (s),
g accounts for the gravitational acceleration ($m.s^{-2}$).

The particle relaxation time τ and the Brownian diffusion coefficient D are expressed respectively by the relations 2 and 3 for a spherical particle:

$$\tau = \frac{\rho_P \cdot {d_p}^2 \cdot Cu}{18 \cdot \mu_g}$$
$$D = \frac{k_b \cdot T \cdot Cu}{3 \cdot \pi \cdot \mu_g \cdot d_p}$$

Where:

P_p is the particle density ($kg.m^{-3}$),
μ_g the dynamic viscosity of the gas (Pa.s),
k_b the Boltzmann constant ($J.K^{-1}$),
T the gas temperature (K),
and Cu the Cunningham coefficient.

Porcheron et al. (2019) implemented the pool scrubbing model of Pich and Schütz (1991) for their analysis. The Input values for the calculations originate of the performed experiments at the DELIA facility operated by the CEA (Chagnot et al. 2010) and in the TOSQAN facility operated by IRSN (Porcheron et al. 2006).
Their results regarding the aerosol retention potential of pools are depicted in Tab. 7.

Table 7: Retention effect on aerosols of different pool depths (Porcheron et al. 2019)

Water depth	**1m**	**2.5 m**	**5.6m**
Scrubbing efficiency for aerosols	15%	35%	60%
Aerosol fraction transferred to the gas	85%	65%	40%

The results of Porcheron et al. were used by BOKU to derivate the retention effect in the steam generator. Therefore, it was important for our simulation to examine the water level in the affected steam generator. As an example, the water level (Fig. 3) of one of our scenarios (VVER-1000 DEC_A SGTR) and the liquid void fraction (Fig. 4), to assure that a pool is present are shown.

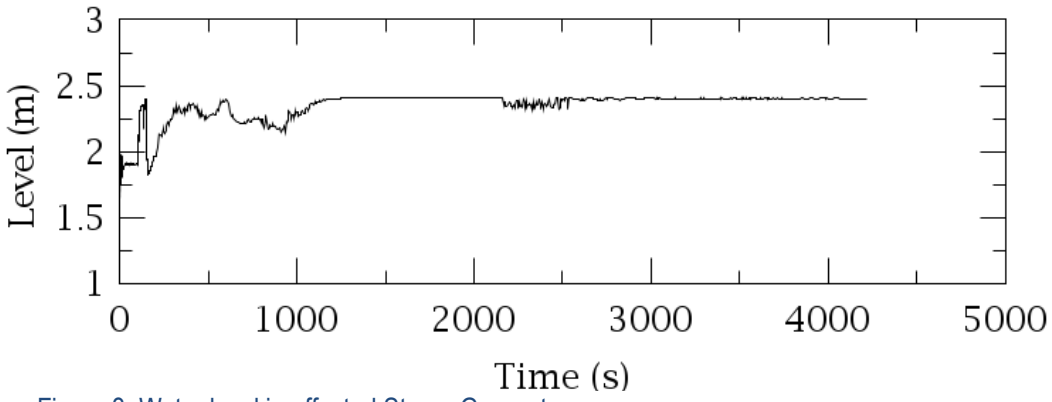

Figure 3: Water level in affected Steam Generator

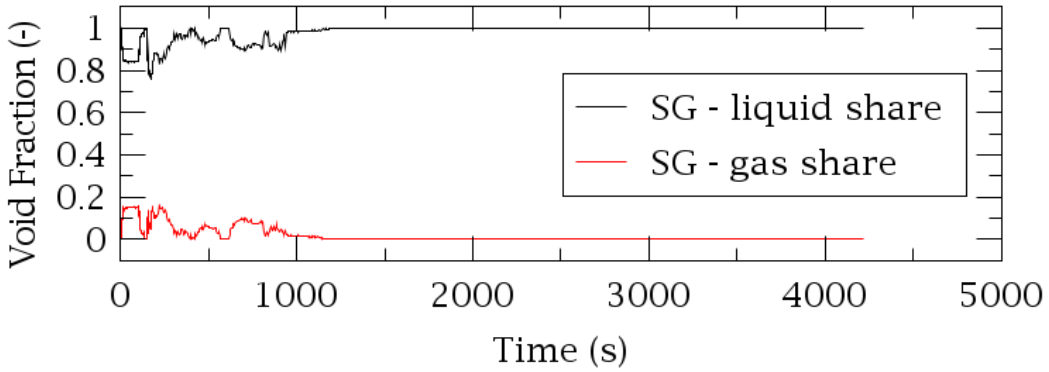

Figure 4: Liquid/Gas share in affected Steam Generator

In Figure 5 the impact of the pool scrubbing effect on the iodine concentration at the secondary side is visible. As was mentioned above the size of the impact is dependent on the pool height, the liquid fraction at the bottom of the affected steam generator and the retention at the PS. A significant retention effect on iodine can be seen.

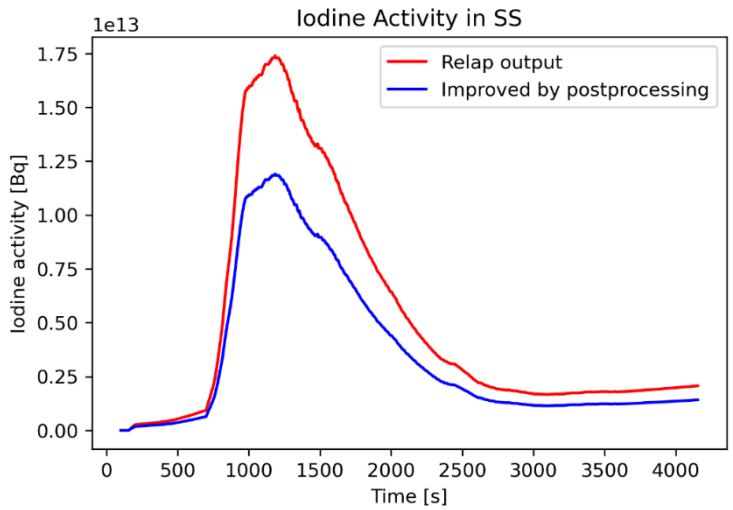

Figure 5: Effect of pool – scrubbing on iodine concentration.

4.2.3 Containment venting / containment spray system

The containment is designed to retain 99%/s of the air/substances inside (design leakage: 1%). Furthermore, in the containment a spray system is installed which is capable of precipitating the steam in the containment. This effect leads to the retention of fission products in the containment sump. However, in our scenario, there is no iodine pathway into the containment, therefore no figure is included.

4.2.4 Environment

As the main path in this scenario leads through the SGTR and the defect relief valve at the secondary side (containment bypass), the iodine concentration that reaches the environment is reduced in dependency to the PS and the SS retention effect (Fig. 6)

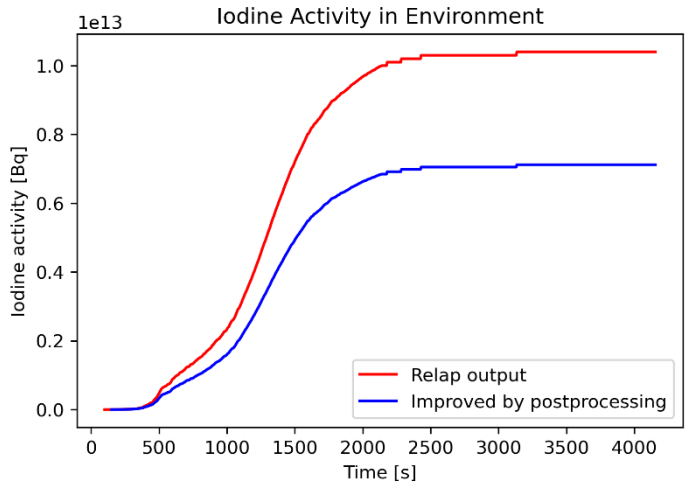

Figure 6: Iodine concentration in environment

4.3. Implementation of the CIAU method to evaluate the uncertainty of the transient simulation

Thermohydraulic simulations of transients are always subject to uncertainties. For licensing purposes in principle an uncertainty analysis has to be conducted, whenever a best estimate method is applied (D'Auria 2002). Therefore, several methods have been developed to determine this uncertainty, including the GRS method, the UMAE and the CIAU (Code with capability of Internal Assessment of Uncertainty) of the University of Pisa. Since the CIAU method is currently maintained by NINE, BOKU decided to perform this analysis together with NINE to determine the uncertainty of the transient calculations.

Description of the CIAU Method:
Compared to the GRS method, the CIAU approach requires only one (best estimate) simulation and afterwards the results are compared with the weighted average of a set of experimental data. The main ideas of the methodology are:

1. Any transient scenario assumed in the reference systems can be characterized by the time and by a limited number of variables. The boundaries of variation for those variables and the time are identified.
2. The ranges of variation for those variables and the transient time are subdivided into intervals. Hypercubes result from the combination of variables intervals.
3. The NPP status is formed by the combination of one hypercube and one time interval.
4. It is assumed that uncertainty can be associated to any NPP status.

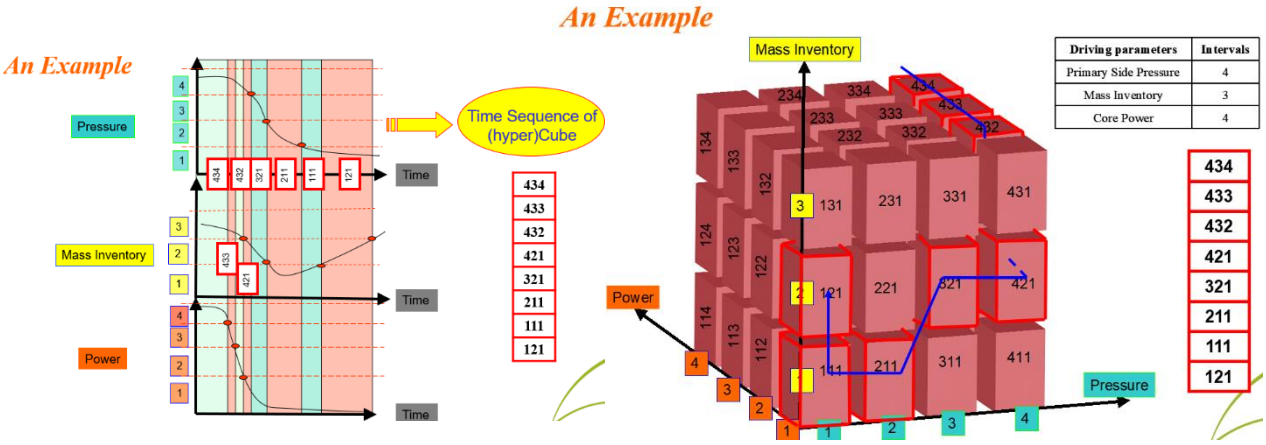

Figure 7: Allocation of simulation results to hypercubes

In Figure 7 a (hyper)cube is included. Furthermore, it is shown, how the alternating values of each parameter lead to the sequence of the (hyper) cube.

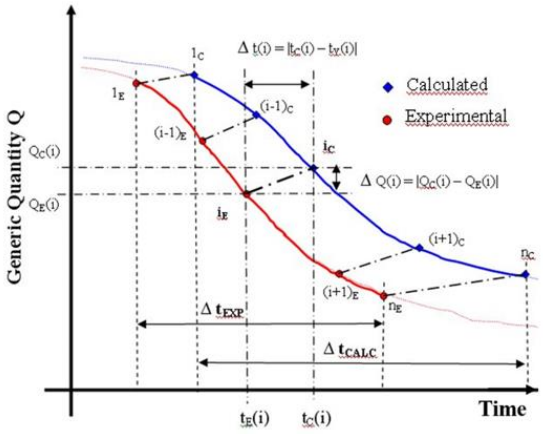

Figure 8: Schema of CIAU Results

The CIAU method is capable to assess quantitative and time errors to create uncertainty bands (FIG. 8/9)

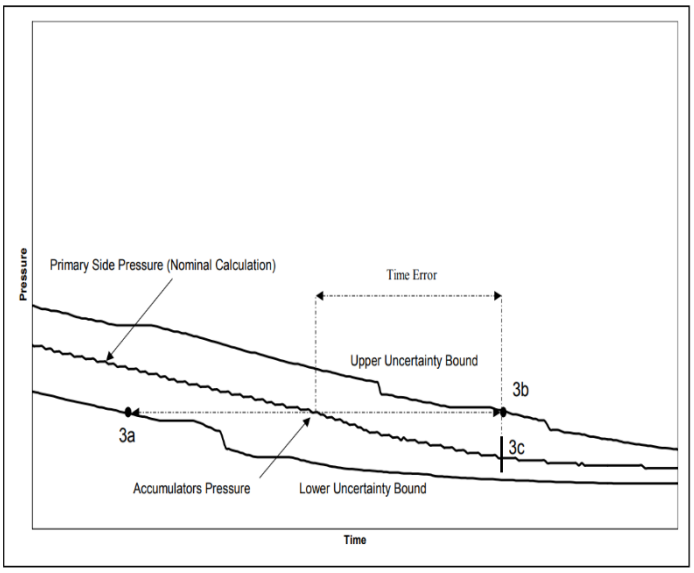

Figure 9: Example result of the CIAU method (D'Auria, 2002)

Uncertainty of IS simulation:

The standard CIAU procedure assesses the uncertainty of the following 6 parameters:

- Upper plenum pressure
- Steam generator pressure
- Primary side mass
- Reactor power
- Steam generator downcomer level
- Cladding Temperature at 60% core height

In principle any parameter could be included in the analysis if there are sufficient experimental data in the developed databank. However, for iodine transport this is not the case as up to now not enough studies are published, that address this parameter. Therefore, it was considered how the uncertainty of the iodine concentration could be derived from the basic parameters of the CIAU method. Since in our scenarios the iodine transport to the environment occurs always via a containment bypass over the secondary side, the pressure difference between the steam generator and the environment is mainly responsible for the contamination of the environment. Therefore, it would be reasonable to consider the uncertainty of the secondary side pressure as the main driver for the uncertainty of the iodine transfer into the environment.

Results:
Currently BOKU cooperates with NINE on the calculations of the uncertainty. The results will be delivered as soon as possible.

5. Conclusions and remarks

In the course of the analyses the following conclusions could be reached:

- To be able to analyse the IS phenomenon in more detail, it would be beneficial to have more data at NPP, in particular to obtain more recent data. Especially the comparability between reactor types is not given, as no data of VVER-1000 reactors is publicly available.

- By adding an additional explanatory variable (point of time in the fuel cycle), the NRC's IS model was significantly improved. Nevertheless, the validation of a theoretical IS models via NPP data is difficult as very often there is no data about the damage of the fuel rods, or the point of time in the fuel cycle available, although this parameter is essential for the calculation of an IS spike.

- By implementing a post-processing function that includes the effects on iodine during the transient, it is possible to significantly improve the transport model of Relap5-3D. In interaction with the new IS model, more meaningful results can therefore be generated.

References

Adams J.P. & Atwood C.L. (1989). PROBABILITYOF THE IODINE SPIKE RELEASE RATE DURING AN SGT.

B.J. Lewis, F.C. Iglesias, A.K. Postma, & D.A. Steininger. (n.d.). Iodine spiking model for pressurized water reactors.

F. D 'Auria (2002). Ciau method for uncertainty evaluation

Giinduz, O. (n.d.). Analysis of VVER-440 Fuel Performance Under Normal Operating Conditions, 4.

Honaiser, E., & Anghaie, S. (2004). *FPTRAN: A volatile fission products and structural materials transport code for SCDAP/RELAP5. Proceedings of the 2004 International Congress on Advances in Nuclear Power Plants, ICAPP'04*.

IAEA. (2019). Review of Fuel Failures in Water Cooled Reactors (2006–2015).

INL. (2012a). RELAP5-3D - Home. https://relap53d.inl.gov:443/SitePages/Home.aspx. Accessed 22 April 2020.

INL. (2012b). RELAP5-3D - RELAP5-3D Released Versions. https://relap53d.inl.gov:443/SitePages/RELAP5-3D%20Released%20Versions.aspx. Accessed 22 April 2020.

INL. (2012c). *RELAP5-3D© Code Manual Volume I: Code Structure, System Models and Solution Methods - Revision 4.0* (No. INEEL-EXT-98-00834) (p. 645). Idaho Falls: Idaho National Laboratory.

Jennifer Uhle & Andrea D. Lee. (2006). Results of Initial Screening of Generic Issue 197, "Iodine Spiking Phenomena.," 31.

Müllner, N. (2010). *Simulation of Beyond Design Basis Accidents - a Contribution to Risk Analysis of Nuclear Power Plants*. University of Vienna.

Pich, J. and Schütz, W. (1991). On the theory of particle deposition in rising gas bubbles: the absorption minimum. J. Aerosol Sci. 22: 267–272.

Porcheron et al. (2019). Fukushima Dai-ichi fuel debris retrieval: aerosol pool scrubbing efficiency applied to underwater laser cutting.

US NRC (1984). Fuel Performance Annual Report for 1983.

US NRC (1986). Fuel Performance Annual Report for 1985.

US NRC (1989). Fuel Performance Annual Report for 1988.

Zoltan Hozer (2001). Prediction of Iodine Activity Peak During Refuelling.

Appendix B- EDF Report

Contents

1. Introduction

During a SGTR (Steam Generator Tube Rupture) accident occurring in a PWR reactor, some of the Fission Products (FPs) that are present in the water of the RCS (Reactor Coolant System) will flow to the SG water and hence be released to the environment.

It is essential to be able to estimate the activity that would be released to the environment for the different types of FPs. The MAAP5 (Modular Accident Analysis Program) code, developed by EPRI (Electric Power Research Institute) enables to model such SGTR transients and evaluate the FPs released.

In the frame of the R2CA project, EDF has modified the equations that are implemented in the MAAP code in order to better estimate those releases. Those modifications have been validated against the EDF reference code for FP activity calculation: COSAQUE.

Moreover, a model related to the iodine spiking has been added to the EDF MAAP5 code in order to model the phenomenon that has a not negligible impact on transients initiated at non-zero power. This new model has equally been validated against COSAQUE reference code.

This document presents the modifications implemented in the EDF MAAP5 code for both the generic model of SGTR FPs activity release and the iodine-spiking model as well as their validations against COSAQUE.
All the modifications are embedded in the EDF Crisis Tool that is in use within the EDF Crisis teams.

2. Assessment of the in code models

2.1. Brief description of the code

The Modular Accident Analysis Program, Version 5 (MAAP5) is a computer code that simulates the response of light water reactor (LWR) power plants during severe accidents. MAAP5 treats the full spectrum of important phenomena that could occur during an accident, simultaneously modeling those that relate to the thermal-hydraulic and the fission products. It also simultaneously models the primary system, core, containment, and reactor/auxiliary building. Thus, given a set of initiating events and operator actions, MAAP5 predicts both the thermal-hydraulic and fission product response of the entire plant as the accident progresses. For these reasons, MAAP is often referred to as an *integral severe accident analysis code*.

The purpose of MAAP is to provide an accident analysis that can be used with confidence by the nuclear industry in all phases of severe accident studies, including accident management, for current reactor/containment designs and for advanced LWRs and that can be used to do the following:

- Predict the timing of key events (for example, core uncovery, core damage, core relocation to the lower plenum, and vessel failure).
- Evaluate the influence of mitigative systems, including the impact of the timing of their operation.
- Evaluate the effects of operator actions.
- Predict the magnitude and timing of fission product releases.
- Investigate uncertainties in severe accident phenomena.
- Investigate spent fuel pool (SFP) accident scenarios.
- Calculate in-plant and ex-plant radiation doses using MAAP5-DOSE.

MAAP5 results are primarily used to determine Level 1 and 2 success criteria and accident timing for PRAs. They are also used for investigating accident management strategies, equipment qualification analyses, fission product large early release frequency (LERF) determinations, integrated leak rate test evaluations, emergency planning

and training, simulator verification, analyses to support plant modifications, generic plant issue assessments (such as significance determinations), and other similar applications.

Parallel versions of MAAP5 support boiling water reactors (BWRs) and pressurized water reactors (PWRs). Other unique versions of the MAAP code exist for CANDU (Canadian deuterium/uranium), VVER (Russian Federation PWR), and advanced thermal reactor designs. In addition, MAAP5 is applicable to both current and advanced LWR designs, with models that represent the passive features of the latter.

MAAP5 treats the spectrum of physical processes that could occur during an accident including steam formation, core heat-up, cladding oxidation and hydrogen evolution, vessel failure, core debris-concrete interactions, ignition of combustible gases, fluid (water and core debris) entrainment by high velocity gases, and fission product release, transport, and deposition. MAAP5 treats all of the important engineered safety systems such as emergency core cooling, containment sprays, fan coolers, and power-operated relief valves. In addition, MAAP allows operator interventions and incorporates these in a flexible manner, permitting the user to model operator behavior in a general way. Specifically, the user models the operator by specifying a set of variable values and/or events which are the operator intervention conditions combined with associated operator actions. Lastly, the auxiliary or reactor building can be modeled for sequences in which it is important.

The PWR primary system model calculates the thermal-hydraulic conditions in the reactor pressure vessel, the hot legs, the cold legs, and the primary side of the steam generators. (The pressurizer is treated in a separate model.) The primary system is divided into a user specified number of loops.

MAAP5 uses separate nodalization schemes for the loop flows and the mass and energy balance flows. These nodalizations allow for the individual loop modeling of the cold leg, downcomer, lower plenum, core, upper plenum, hot leg, inlet SG plenum, SG hot tube bundle, SG cold tube bundle, crossover leg, as well as the reactor dome.

The PWR RCS heat sinks are modeled as vertical, two-dimensional steel slabs. Separate heat transfer coefficients and fluid temperatures are applied to each heat sink for the covered (by water) and uncovered portions. Fission product heating is also modeled based on the amount of fission products deposited on the heat sink. Fission product heat is supplied to the surfaces of the nodes uniformly.

The thermal-hydraulic model calculates water transport, gas transport, steaming, and heat transfer to the structures that interface with the secondary side and the containment. In addition to condensation onto the inside surfaces of the steam generator tubes, steam can condense on cold emergency core cooling system (ECCS) water injected into the primary system. When the accident progresses to core uncovery, the level of detail in the calculations increases, and the modeling includes such phenomena as natural circulation of superheated gases in the vessel and in the hot leg (countercurrent flow).

At each time step, the code calculates the influx of water through makeup flow; accumulator flow; and high pressure, low pressure, and charging pump injection systems, as appropriate. It also calculates water and gas flow from the primary system through breaks, steam generator tube ruptures (SGTRs), and other user-specified openings, as well as fluid transport between the primary system and the pressurizer through the surge line.

2.2. Description of the code models for transport and release

2.2.1. Radionuclides and Fission Products groups considered in MAAP5

EPRI MAAP5 enables to follow the activity released to the environment for 65 radionuclides that are presented in Table 8 below (ref. [1]):

i	Isotope	i	Isotope	i	Isotope	i	Isotope
1	Kr-85	18	Cs-137	35	Te-132	52	Ce-144
2	Kr-85m	19	Rb-86	36	Te-134	53	Pu-238
3	Kr-87	20	Rb-88	37	Sb-127	54	Pu-239
4	Kr-88	21	Rb-89	38	Sb-129	55	Pu-240
5	Xe-131m	22	Y-90	39	Sr-89	56	Pu-241
6	Xe-133	23	Y-91	40	Sr-90	57	Np-239
7	Xe-133m	24	Y-92	41	Sr-91	58	La-140
8	Xe-135	25	Y-93	42	Sr-92	59	La-141
9	Xe-135m	26	Zr-95	43	Ba-139	60	La-142
10	Xe-138	27	Zr-97	44	Ba-140	61	Nd-147
11	I-131	28	Nb-95	45	Ru-103	62	Pr-143
12	I-132	29	Mo-99	46	Ru-105	63	Am-241
13	I-133	30	Te-127	47	Ru-106	64	Cm-242
14	I-134	31	Te-127m	48	Rh-105	65	Cm-244
15	I-135	32	Te-129	49	Tc-99m		
16	Cs-134	33	Te-129m	50	Ce-141		
17	Cs-136	34	Te-131m	51	Ce-143		

Table 8: 65 radionuclides tracked in the MAAP5 code.

The evaluation of the mass of FPs transferred from the RCS to the SGs at each time step is not performed radionuclide by radionuclide but thanks to grouping of FPs depending on their volatility. Table 9 (ref. [1]) below shows the 18 FPs groups that are tracked with MAAP5 code.

1.	Nobles (Xe, Kr)
2.	CsI + RbI
3.	TeO_2
4.	SrO
5.	MoO_2, TcO_2, RhO_2
6.	CsOH + RbOH
7.	BaO
8.	La_2O_3, Pr_2O_3, Nd_2O_3, Sm_2O_3, Y_2O_3, ZrO_2, NbO_2, AmO_2, CmO_2
9.	CeO_2, NpO_2, PuO_2,
10.	Sb
11.	Te_2
12.	UO_2 (fuel, not fission product)
13.	Ag (Group 13 is not a fission product. It is reserved for silver, a structural material active in iodine chemistry.)
14.	I_2 (iodine in elemental form)
15.	CH_3I (iodine in organic form)
16.	Cs_2MoO_4
17.	RuO_2
18.	PuO_2

Table 9: 18 FPs groups within MAAP5.

2.2.2. FPs releases during a SGTR transient-New model

The model developed by EDF in the EDF version of MAAP5 in the frame of the R2CA project does embed different correlations depending on the status of the affected SG: the SG is overflowing or not. The MAAP5 RCS for a PWR can model up to 4 loops (parameter IL below).

2.2.2.1. The affected SG is not overflowing

If the affected SG is not overflowing, the following correlation is used to transfer the FPs from the primary circuit to the SG and from the SG to the environment:

$$WFPSG(J_G, IL) = FENTRAIN(K_G).WFVLKSG(IL).MFPWPS(J_G) + FDEGAZAGE(K_G).WFVSTEAMSG(IL).MFPWSG(J_G)$$
$$IL \in [\![1,4]\!], J_G \in [\![1,18]\!] \; et \; K_G \in [\![1,4]\!]$$

With:

$$WFVLKSG(IL) = \frac{WWSGTR(IL)}{MWPS}$$

And:

$$WFVSTEAMSG(IL) = \frac{WSTEAMSG(IL)}{MWSG(IL) * NSG(IL)}$$

The different variables are described below:

- $WFPSG(J_G, IL)$: total FPs flow to the environment of group J_G and loop IL.
- $WWSGTR(IL)$: water flow from the RCS to the SG of loop IL,

- $MWPS$: total mass of water in the RCS (pressurizer excluded),
- $WSTEAMSG(IL)$: flow of steam flowing out of the SG of loop IL,
- $MWSG(IL)$: mass of water in the SG of loop IL,
- $NSG(IL)$: number of SGs in loop IL (1 SG per loop for French reactors),
- $MFPWPS(J_G)$: mass of FP group J_G in the water of the RCS,
- $MFPWSG(J_G)$: mass of FP group J_G in the water of the SG of loop IL.

Parameters $FENTRAIN(K_G)$ and $FDEGAZAGE(K_G)$ are defined as described below:

- $FENTRAIN(1)$: entrainment coefficient for the Noble Gases,
- $FENTRAIN(2)$: entrainment coefficient for Iodine,
- $FENTRAIN(3)$: entrainment coefficient for Cesium,
- $FENTRAIN(4)$: entrainment coefficient for all other FPs.
- $FDEGAZAGE(1)$: partition coefficient for the Noble Gases,
- $FDEGAZAGE(2)$: partition coefficient for Iodine,
- $FDEGAZAGE(3)$: partition coefficient for Cesium,
- $FDEGAZAGE(4)$: partition coefficient for all other FPs.

Those parameters can be modified by the user and adapted to his plant configuration. Table 10 shows the values considered in the validation of this model against COSAQUE.

Parameter	Typical value
$\boldsymbol{FENTRAIN(1)}$	*1*
$\boldsymbol{FENTRAIN(2)}$	*0.1*
$\boldsymbol{FENTRAIN(3)}$	*0.0025*
$\boldsymbol{FENTRAIN(4)}$	*0.0025*
$\boldsymbol{FDEGAZAGE(1)}$	*1*
$\boldsymbol{FDEGAZAGE(2)}$	*0.01*
$\boldsymbol{FDEGAZAGE(3)}$	*0.01*
$\boldsymbol{FDEGAZAGE(4)}$	*0.01*

Table 10 : typical values for entrainment and partition coefficient

2.2.2.2. The affected SG is overflowing

As soon as the affected SG is overflowing, it is considered that all the FPs transferred from the RCS to the affected SG through the break are released to the environment.

The following correlation is hence considered in this case (same notations than in §2.2.2.1)

$$WFPSG(J_G, IL) = WFVLKSG(IL).MFPWPS(J_G) + WFVSTEAMSG(IL).MFPWSG(J_G)$$

$$IL \in [\![1,4]\!],\ J_G \in [\![1,18]\!]$$

It has to be noted that once the affected SG is not flowing anymore, the correlations presented in §2.2.2.1 are anew applied.

2.2.3. Iodine spiking model-New model

After a significant power change in a reactor, a temporary increase in the primary coolant iodine concentration is observed in PWR plants (ref. [2]). Iodine is not the only fission product impacted, as other FP elements have a temporary concentration increase (Cs, Te…).

EPRI MAAP 5 does not natively model this phenomenon. A simplified model has been developed in the EDF MAAP 5 code in the frame of the R2CA project so that users can take into account this physical phenomenon during accident transients' simulations. Theoretically, as presented in Figure 4, an increase in the source term appears after the reactor scram and lasts for a duration noted Δt (a few hours generally).

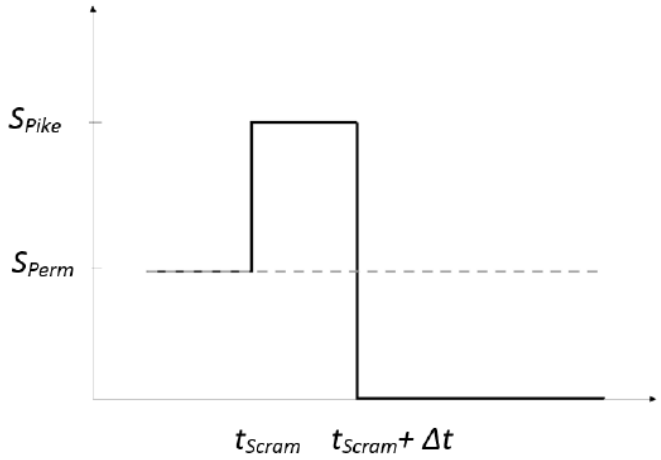

Figure 4: Source term increase during an iodine spiking.

The following model is considered in the EDF MAAP5 version:

- The activity of Noble Gases in the water of the RCS is not affected by this phenomenon,
- For the other FPs it is supposed that the activity in the water of the RCS increases linearly from the initial activity at the scram time for around 1.5 hours. Then a natural decrease of activity is considered.

Some new coefficients are added to the code and can be set up by the users:

- FPICIODEI: multiplication factor for iodine,
- FPICIODECS: multiplication factor for cesium,
- FPICIODEAUTRES: multiplication factor for all the other FPs (except noble gases).

2.3. Validation of the new release models

In order to validate the models described in §2.2.2 (new release model for SGTR transients) and §2.2.3 (iodine spiking model) some transients have been run with both EDF MAAP5 and the EDF reference code COSAQUE on 2 different French plant types: a PWR 3-Loop plant (900MWe) and a PWR 4-Loop plant (1450MWe – N4).

More precisely, 2 transients have been run on each type of plant (3-Loop & 4-Loop)

- A transient initiated in hot shutdown state (pre-established iodine spiking),
- A transient initiated at full power (for the iodine spiking model).

Based on the results of the 3-Loop plant, the transients that have been run on the 4-Loop plant have slightly different assumptions that are detailed hereafter.

For each transient, the activity of Noble Gases, Iodine and Cesium released to the environment are shown for both MAAP and COSAQUE. The COSAQUE data are obtained using MAAP5 thermal hydraulics data (break flow, RCS water inventory, SG flows…).

All the data presented hereafter are normalized for confidentiality purpose.

2.3.1. Transient initiated in Hot Shutdown State– 3 Loop-plant (PWR 900 MWe)

2.3.1.1. Transient description

The modelled transient is a SGTR initiated under Hot Shutdown conditions. It is supposed that the iodine spiking has already been developed before the initialization of the SGTR. Therefore,the activity of FPs in the RCS is initially increased compared to a transient initialized at full power.

The break opening in the RCS leads to a loss of pressure: the High Pressure Injection (HPI) system is activated once the pressure reaches the activation threshold. The activation of this system leads to an increase of the water inventory in the RCS and the affected SG (through the primary/secondary leakage). HPI is supposed to stop after around 43 % of the scenario run time after reaching an insufficient Net Positive Suction Head (NPSH). MAAP5 evaluates that the affected SG sees an overflow after around 5 % (early) of the scenario run time.

2.3.1.2. Results

2.3.1.2.1. Noble gases

Figure 5 below shows the Noble gases activity released to the environment versus time for both EDF MAAP5.04 and COSAQUE codes. A good agreement is obtained between the 2 codes: the kinetics of the release is quite the same and the total activity released is within a few percent between the codes.

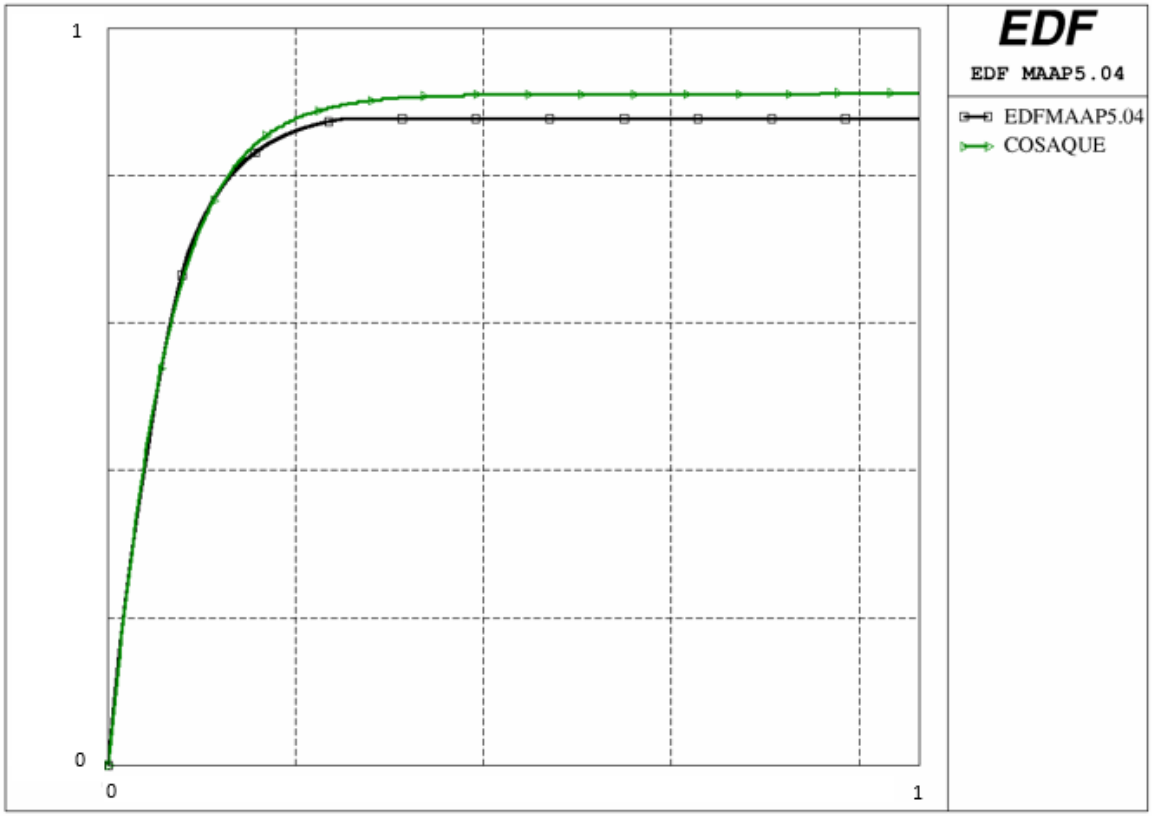

Figure 5: Noble gases activity released to the environment vs time.

2.3.1.2.2. Iodine

Figure 6 shows the iodine activity released to the environment versus time for both EDF MAAP5.04 and COSAQUE codes. The level of activity released increases rapidly for the 2 codes after around 5 % of the total transient calculation time, when the affected SG starts overflowing. The kinetics of release is quite the same.

After around 45 % of the calculation time, an increase in the activity of iodines released to the environment appears in the EDF MAAP5.04 calculation, which is not the case in COSAQUE. At this time, the affected SG stops overflowing: a larger steam flow is hence observed leading to an increase in the activity released. The final activity released is around 6% higher in EDF MAAP5.04 compared to COSAQUE, which seems to be acceptable.

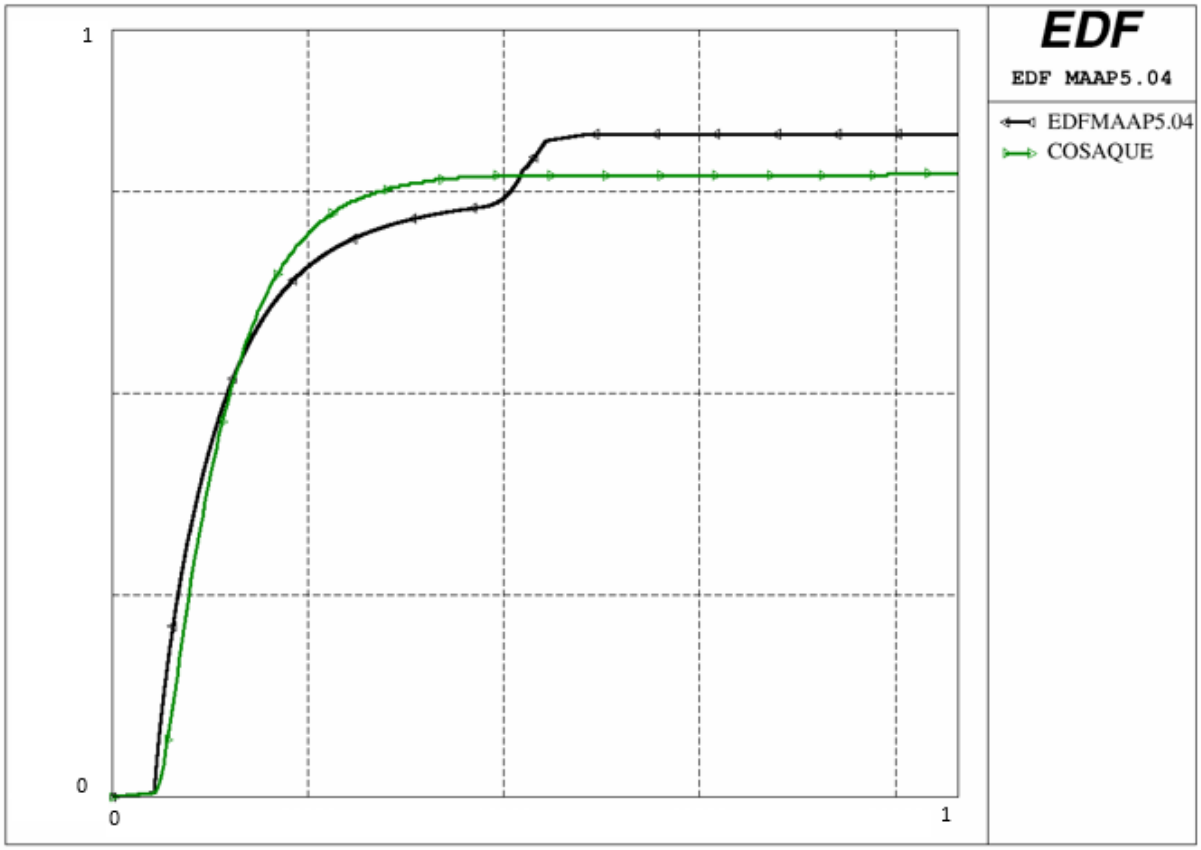

Figure 6: Iodine activity released to the environment vs time.

2.3.1.2.3. Cesium

Figure 7 shows the Cesium activity released to the environment versus time for both EDF MAAP5.04 and COSAQUE codes. In the same way as previously, a very good agreement is observed between the 2 codes. The steam flow increase at the break after the affected SG is not overflowing any more leads to a smaller increase in the activity released. The final Cesium activity released is identical between the calculations.

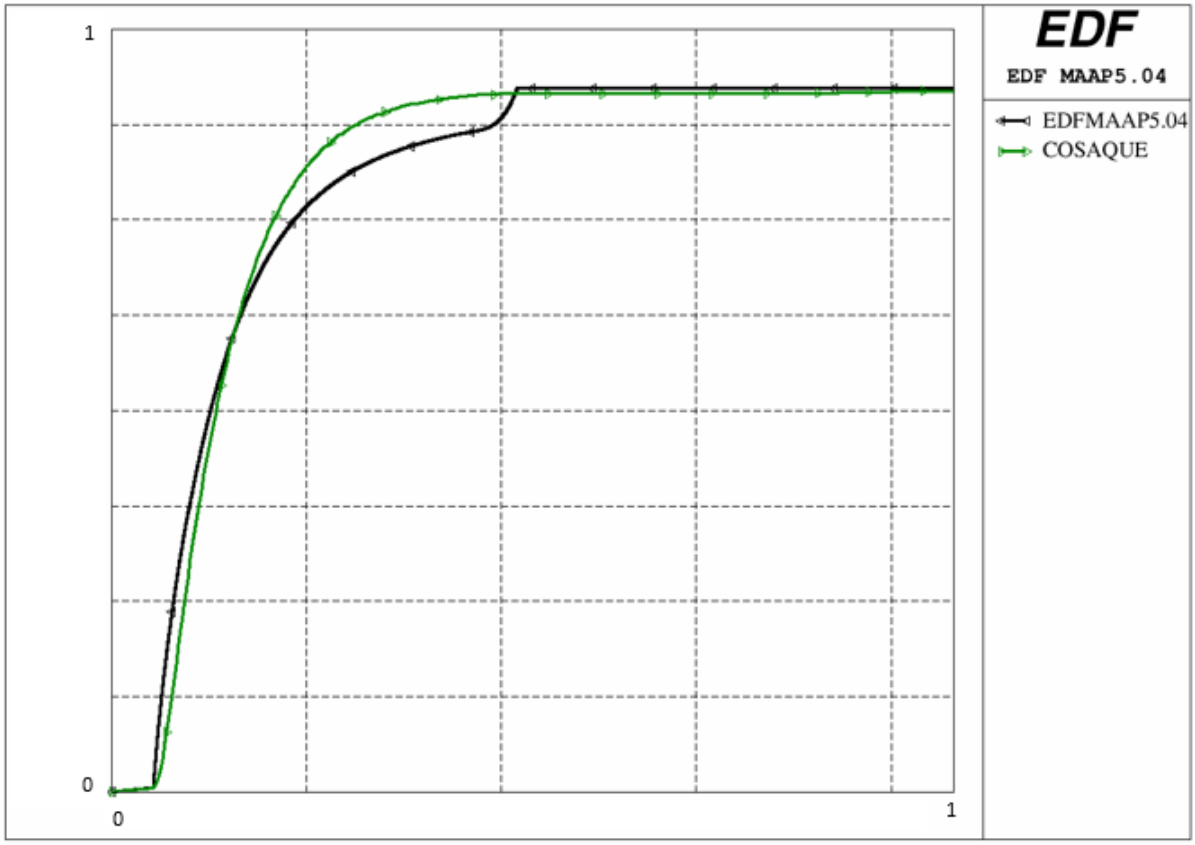

Figure 7: Cesium activity released to the environment vs time.

2.3.2. Transient initiated at full power – 4 Loop-plant (PWR 1450 MWe)

2.3.2.1. Transient description

The modelled transient is a SGTR initiated under Hot Shutdown conditions. It is supposed that the iodine spiking has already been developed before the initialization of the SGTR. Therefore, the activity of FPs in the RCS is initially increased compared to a transient initialized at full power.

The break opening in the RCS leads to a loss of pressure. In order to evaluate the model behavior, it is assumed that an injection of water is present in the primary circuit that exactly compensates the break flow to the broken SG. By this way, the global water inventory in the primary circuit is constant during all the transient. This assumption allows to avoid any FP dilution in the RCS as well no water release to the environment from the affected SG (only a steam release is calculated by MAAP).

2.3.2.2. Results

2.3.2.2.1. Noble gases

Erreur ! Source du renvoi introuvable. below shows the Noble gases activity released to the environment versus time for both EDF MAAP5.04 and COSAQUE codes. A good agreement is obtained between the 2 codes: the kinetics of the release is almost identical and the total activity released is within a few percent between the codes.

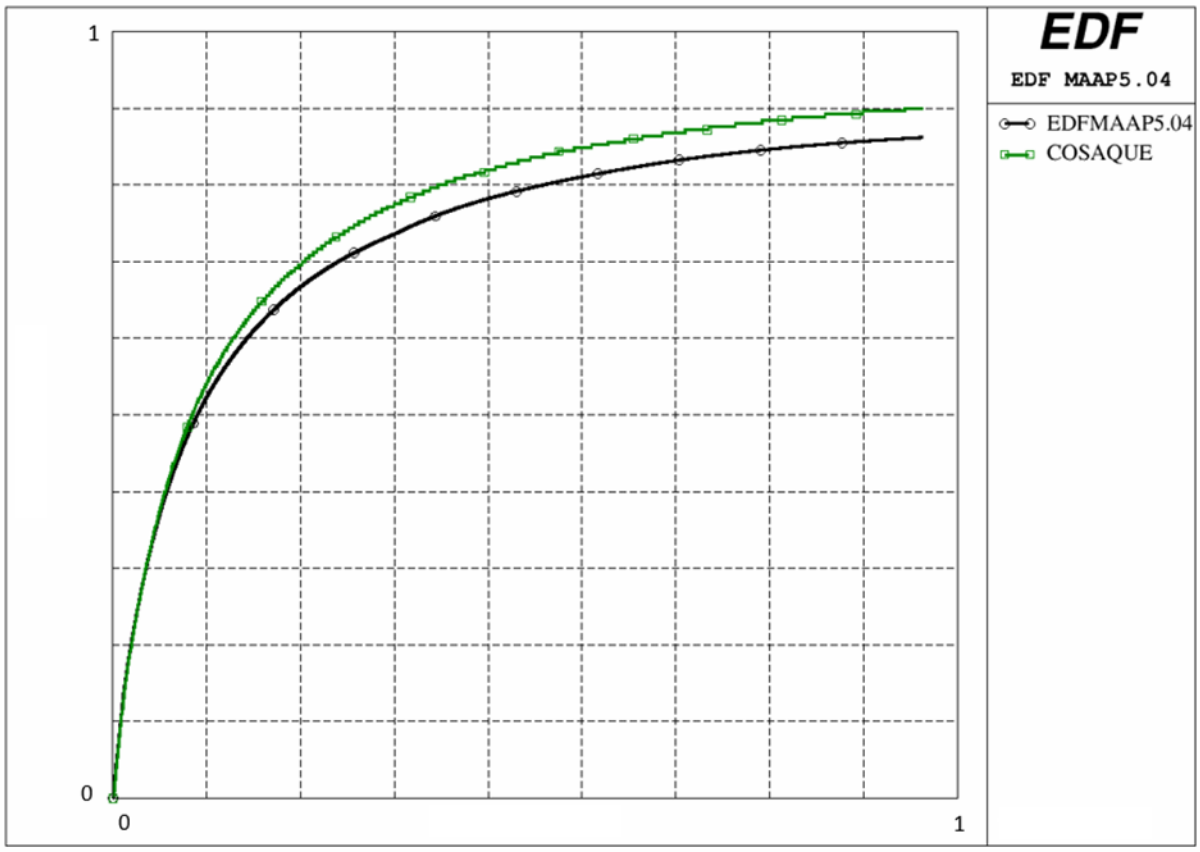

Figure 8: Noble gases activity released to the environment vs time.

2.3.2.2.2. Iodine

Erreur ! Source du renvoi introuvable. shows the iodine activity released to the environment versus time for both EDF MAAP5.04 and COSAQUE codes. The level of activity released increases immediately after the SG tube rupture because of the steam release. No big increase can be observed as was observed in the PWR 900 MWe (cf. §**Erreur ! Source du renvoi introuvable.**) case, again explained by only a steam released to the environment in this scenario.

After around 50% of the transient, a slight discrepancy can be seen between the 2 codes increasing along with time. MAAP is around 5% more penalizing at the end of the calculation. It has to be noted that since only steam is released, the activity released is low and the absolute value of the discrepancy between the 2 calculations is low as well.

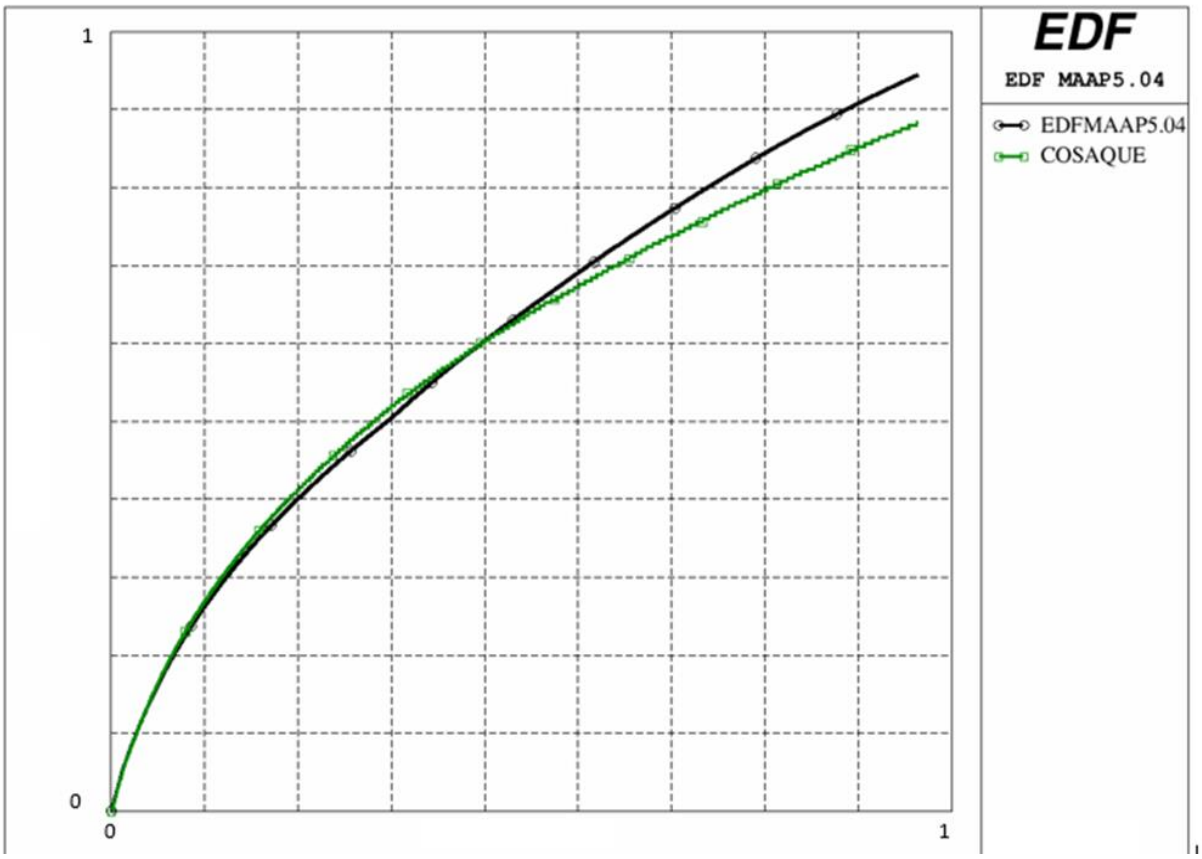

Figure 9: Iodine activity released to the environment vs time.

2.3.2.2.3. Cesium

Figure 7 shows the Cesium activity released to the environment versus time for both EDF MAAP5.04 and COSAQUE codes. In the same way as previously, a very good agreement is observed between the 2 codes. The same tendency is observed as for the Iodine with an increasing discrepancy along with time. At the end of the calculation, the discrepancy is around 8%, with MAAP a little bit penalizing. As explained, the absolute activity value difference is small (only steam is released from the affected SG).

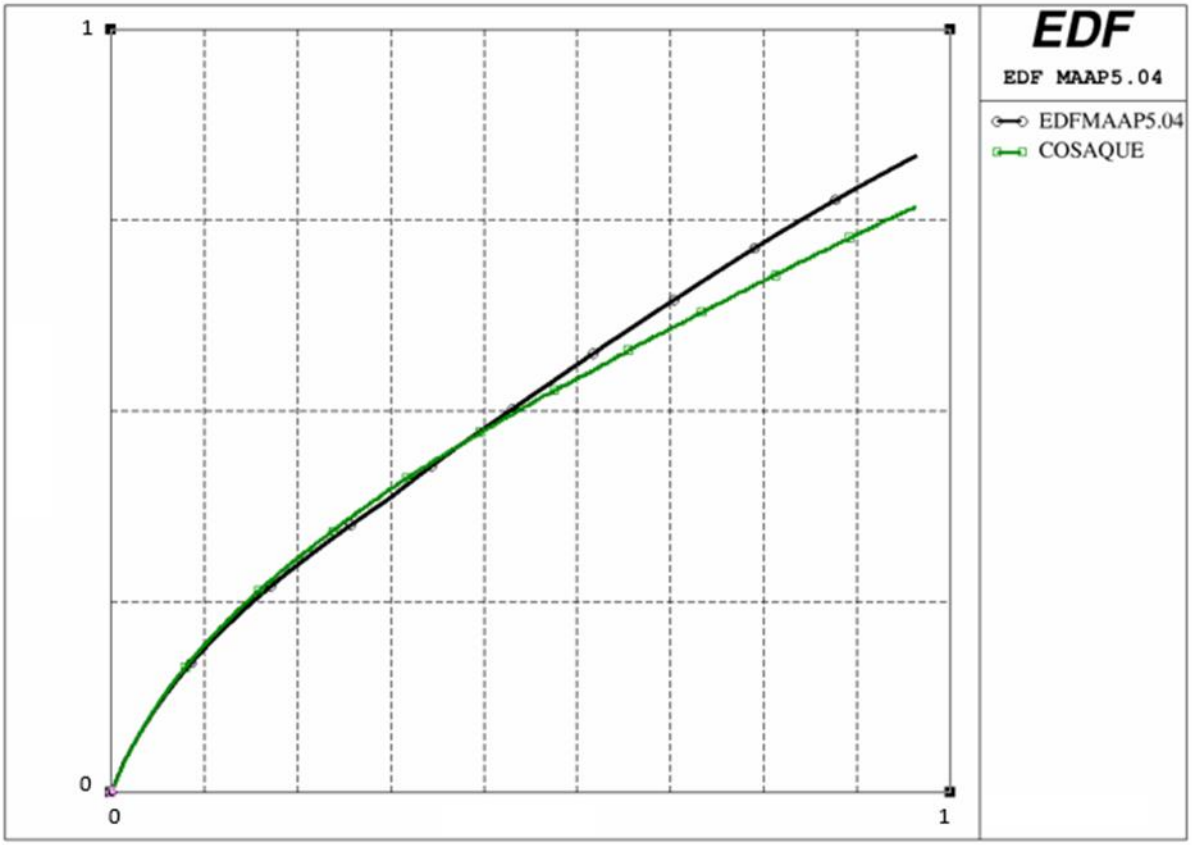

Figure 10: Cesium activity released to the environment vs time.

2.3.3. Transient initiated at full power – 3 Loop-plant (PWR 900 MWe)

2.3.3.1. Transient description

The modelled transient is a SGTR initiated at full power. It is supposed that the iodine spiking develops during the transient after the scram. The scram in itself is reached on a low pressure signal in the pressurizer almost immediately after the initiator (0.35 % of the simulated transient time).

The HPI system threshold is reached rapidly after the scram (almost concomitantly). It leads to an increase of water in the RCS and in the affected SG causing this last one to overflow after around 4% of the transient calculation time.

The HPI stops after 55 % of the transient because of an insufficient NPSH.

2.3.3.2. Results

2.3.3.2.1. Noble gases

Figure 8 below shows the Noble gases activity released to the environment versus time for EDF MAAP5.04. COSAQUE result is not presented but is very close to MAAP results.

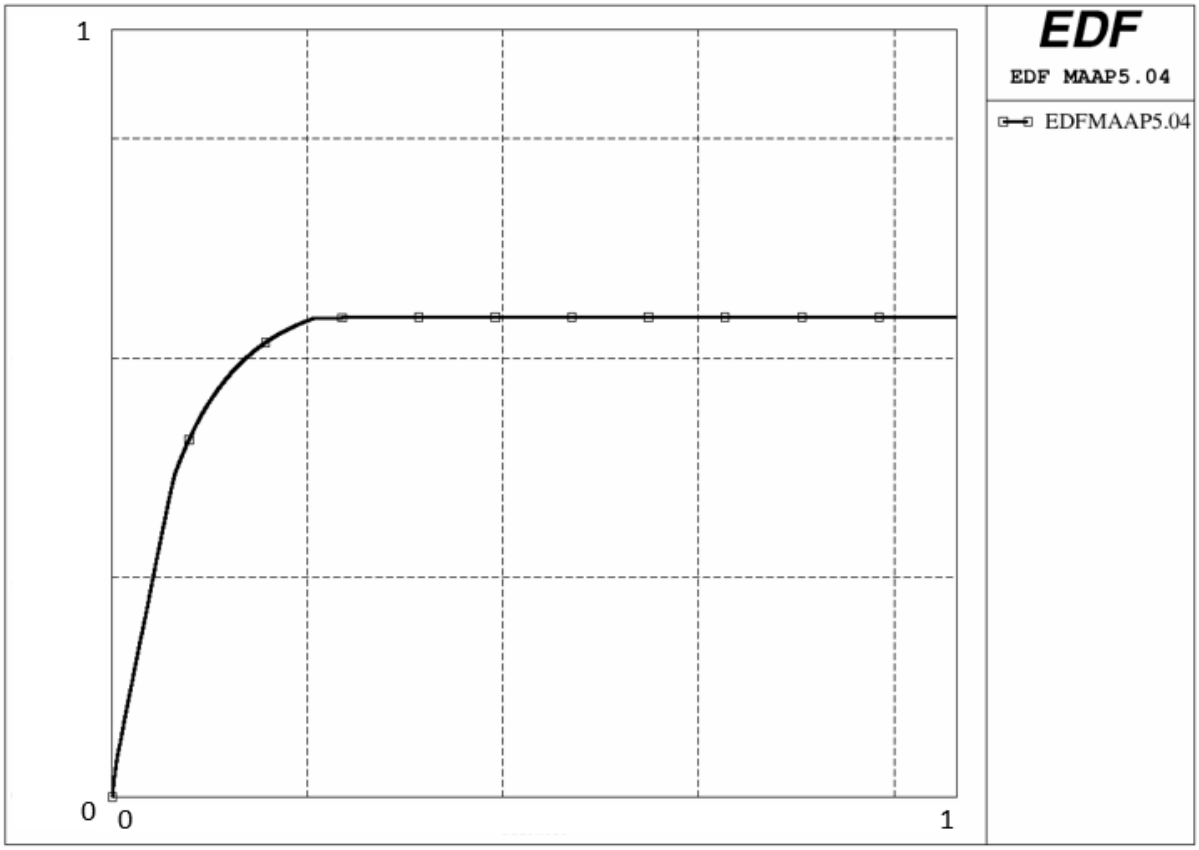

Figure 11: Noble gases activity released to the environment vs time.

2.3.3.2.2. Iodine

Figure 9 shows the iodine activity released to the environment versus time for both EDF MAAP5.04 and COSAQUE codes. The level of activity released increases rapidly for the 2 codes after around 4% of the total transient calculation time, when the affected SG starts overflowing. The kinetics of release is close.

After around 70 % of the calculation time, an increase in the activity of Iodines released to the environment appears in the EDF MAAP5.04 calculation, which appears to be smaller in COSAQUE. At this time, the affected SG stops overflowing: a larger steam flow is hence observed leading to an increase in the activity released. The final activity released is around 3 % lower in EDF MAAP5.04 compared to COSAQUE, which seems to be acceptable.

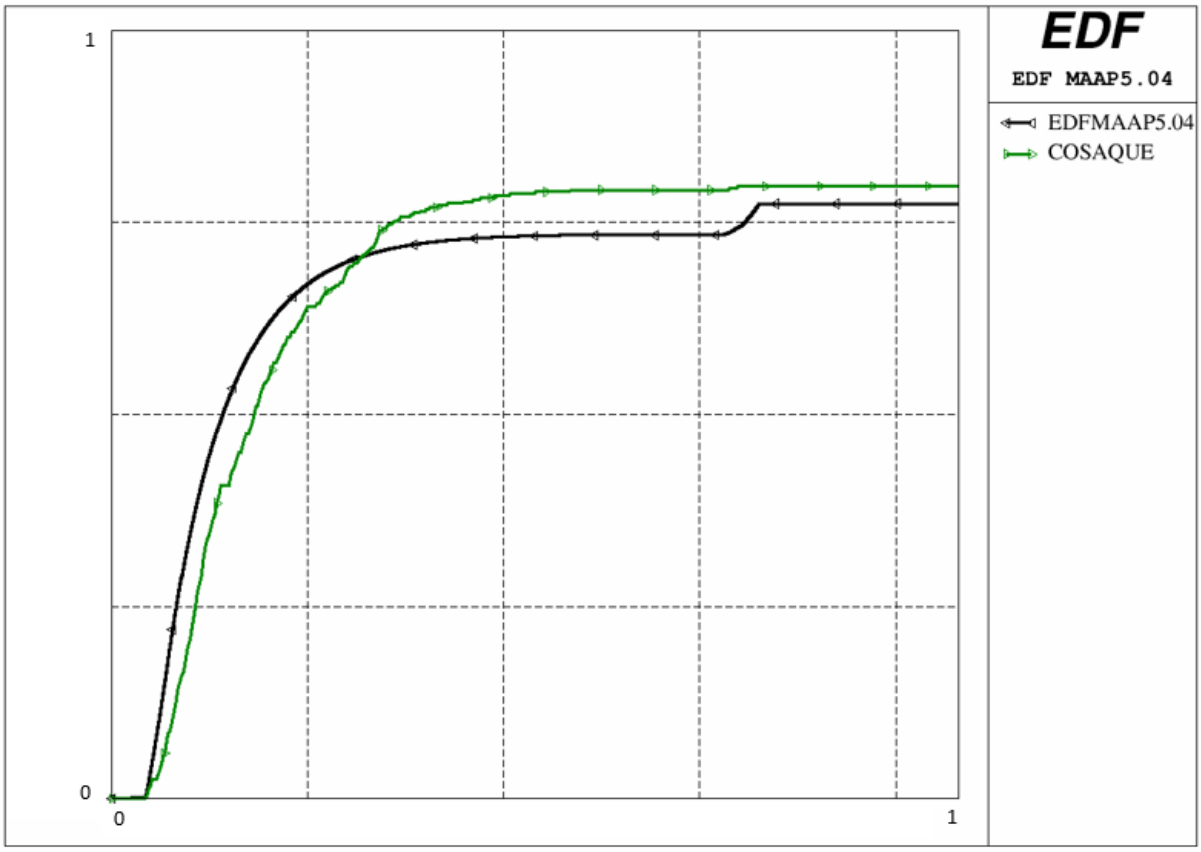

Figure 12: Iodine activity released to the environment vs time.

2.3.3.2.3. Cesium

Figure 10 shows the Cesium activity released to the environment versus time for both EDF MAAP5.04 and COSAQUE codes. In the same way than previously, a rather good agreement is observed between the 2 codes. The steam flow increase at the break after the affected SG is not overflowing any more leads to a smaller increase in the activity released. The final Cesium activity released is 5 % higher in EDF MAAP5.04 compared to COSAQUE, which is fair.

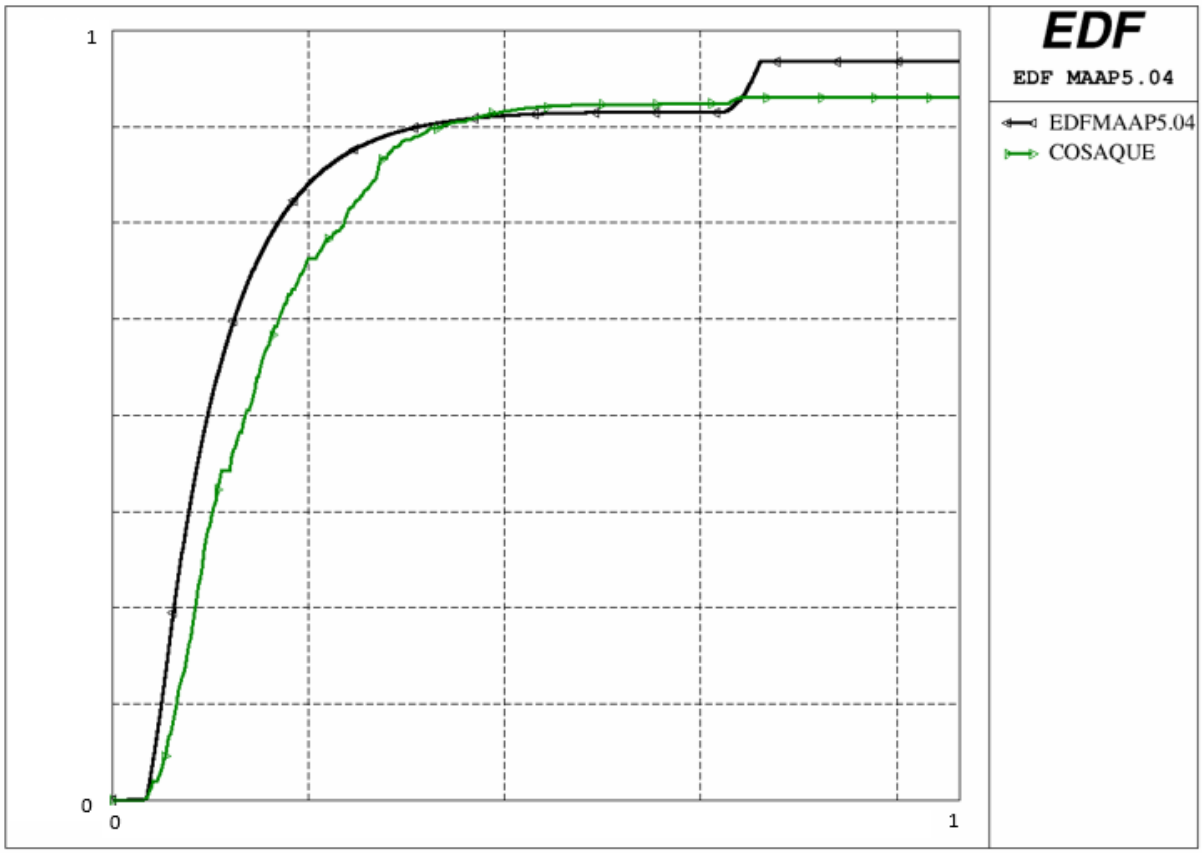

Figure 13: Cesium activity released to the environment vs time.

2.3.4. Transient initiated at full power – 4 Loop-plant (PWR 1450 MWe)

2.3.4.1. Transient description

The modelled transient is a SGTR initiated at full power. It is supposed that the iodine spiking develops during the transient after the scram. The scram in itself is reached on a low pressure signal in the pressurizer rapidly after the initiator (0.08 % of the simulated transient time).

The break opening in the RCS leads to a loss of pressure. In order to evaluate the model behavior, it is assumed that an injection of water is present in the primary circuit that exactly compensates the break flow to the broken SG. By this way, the global water inventory in the primary circuit is constant during all the transient. This assumption allows to avoid any FP dilution in the RCS as well no water release to the environment from the affected SG (only a steam release is calculated by MAAP).

2.3.4.2. Results

2.3.4.2.1. Noble gases

Figure 14 below shows the Noble gases activity released to the environment versus time for both EDF MAAP5.04 and COSAQUE codes. A good agreement is obtained between the 2 codes: the kinetics of the release is almost identical and the total activity released is within a few percent between the codes.

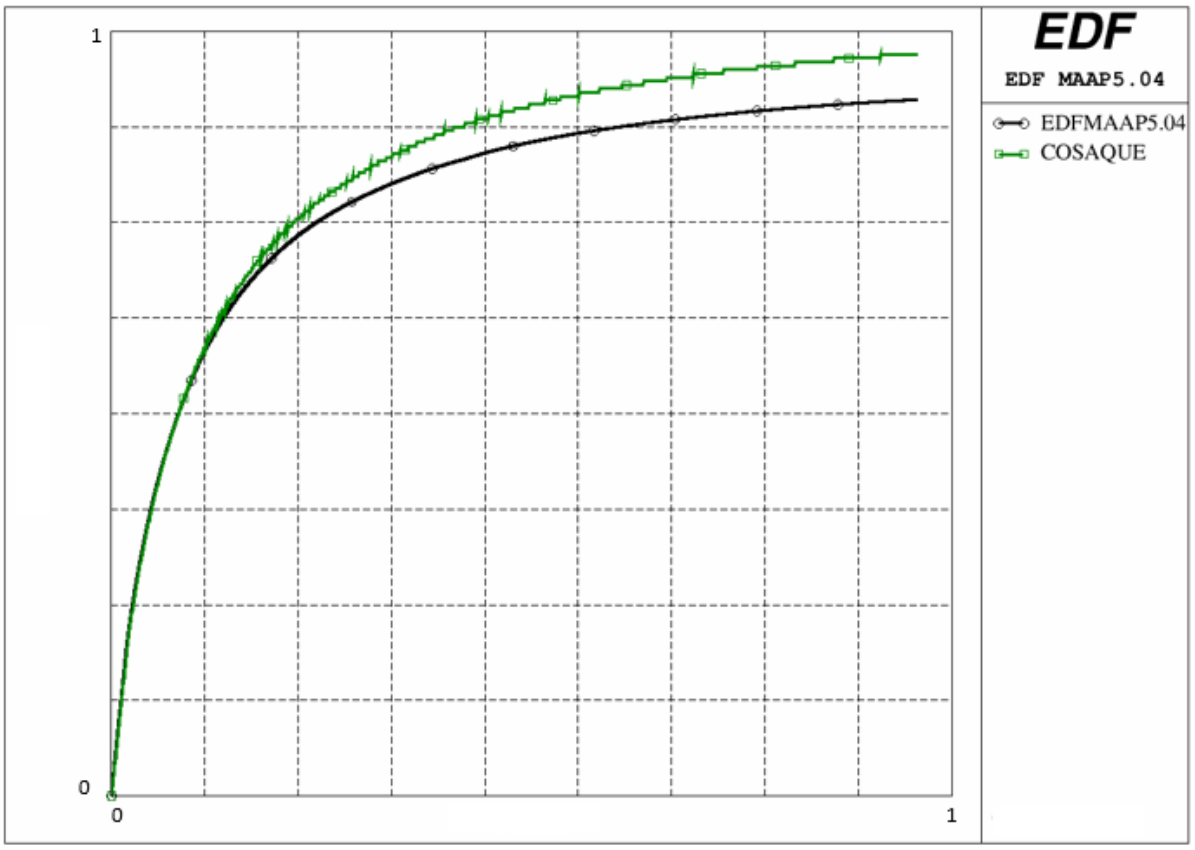

Figure 14: Noble gases activity released to the environment vs time.

2.3.4.2.2. Iodine

Figure 15 shows the iodine activity released to the environment versus time for both EDF MAAP5.04 and COSAQUE codes.

Some discrepancies appear along with time but stay quite small. MAAP is around 20% more penalizing than COSAQUE at the end of the calculation. Those discrepancies are linked to the relatively simple model that is implemented in the EDF version of MAAP5.04 (a user coefficient for the activity increase in the water of the RCS). This model still gives reasonable results compared to COSAQUE especially for a crisis use of the code.

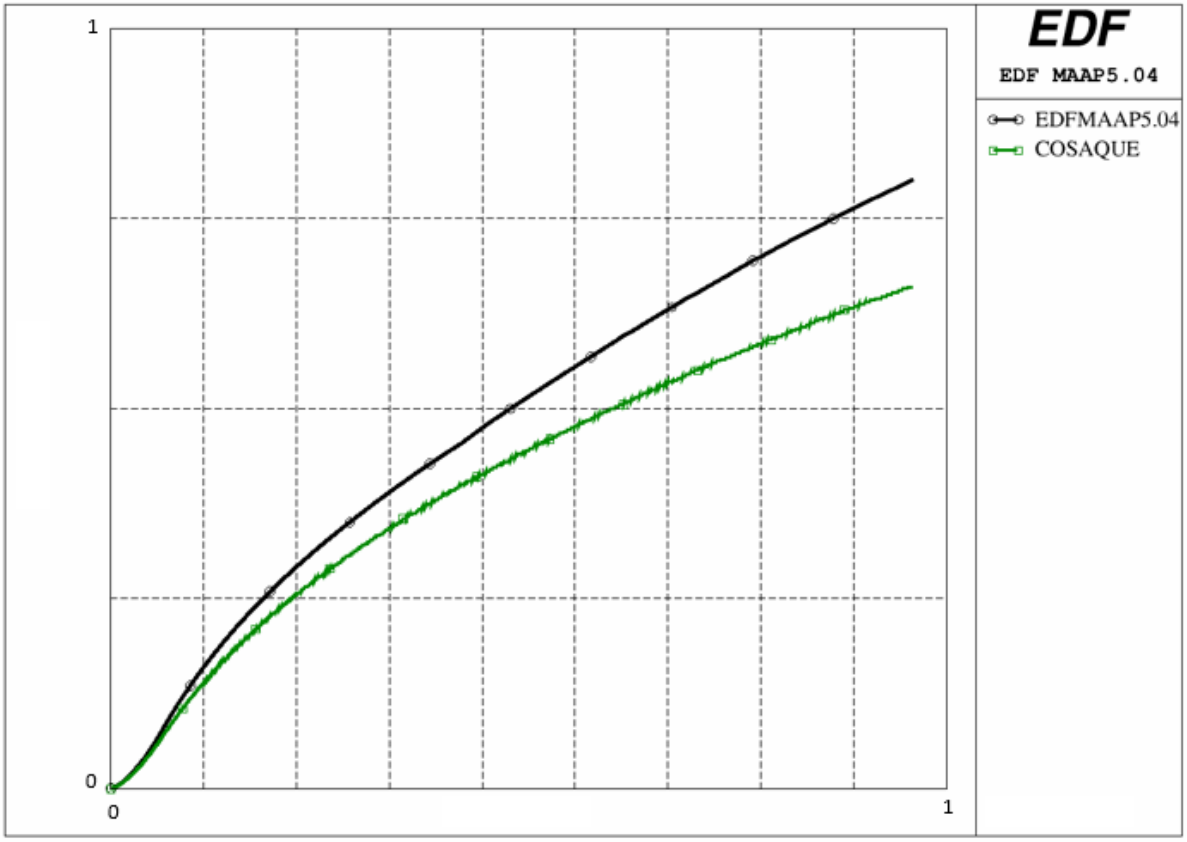

Figure 15: Iodine activity released to the environment vs time.

2.3.4.2.3. Cesium

Figure 16 shows the Cesium activity released to the environment versus time for both EDF MAAP5.04 and COSAQUE codes. Again, a rather good agreement is observed between the 2 codes with discrepancies increasing along with time for the same reasons as exposed in §2.3.4.2.2 MAAP is around 30% more conservative than COSAQUE at the end of the calculation.

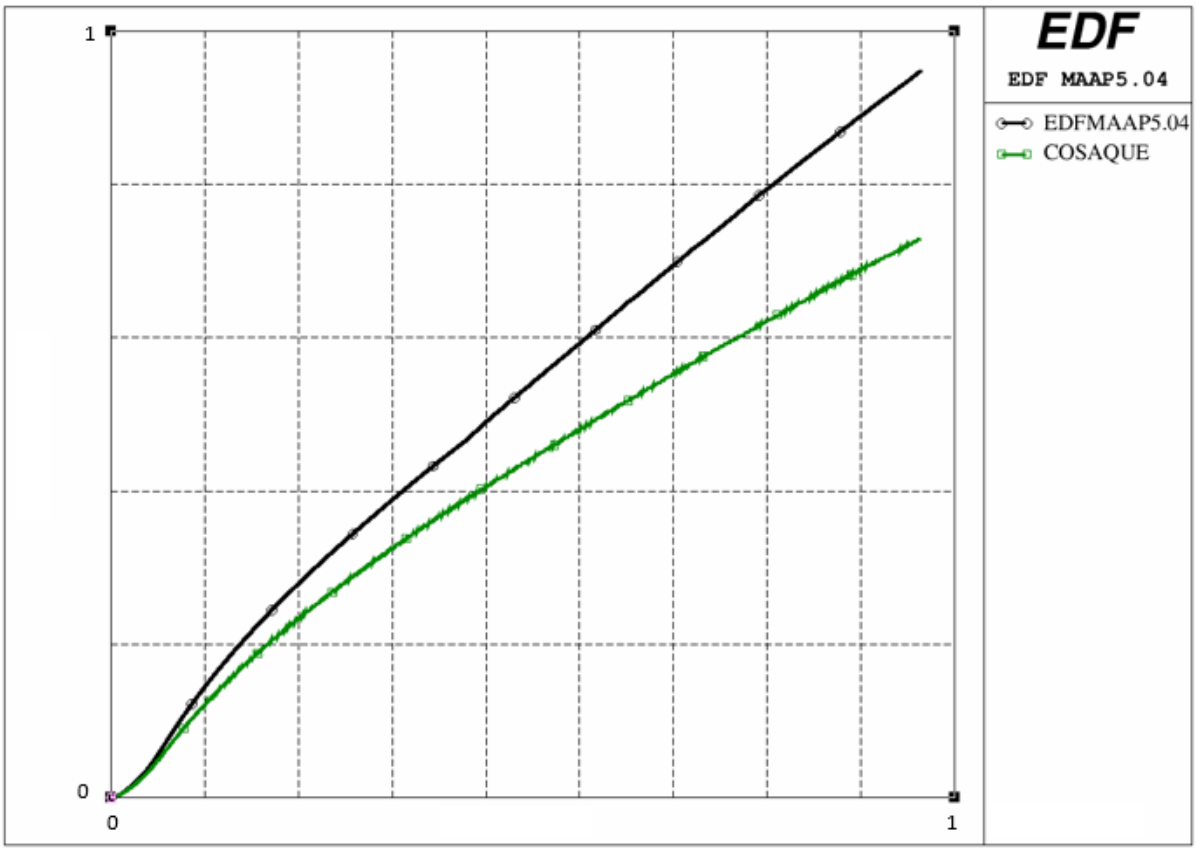

Figure 16: Cesium activity released to the environment vs time.

3. Conclusions and remarks

The development in EDF MAAP5.04 of new models for the activity released to the environment during a SGTR transient appears to be relevant against the COSAQUE reference code results.

The initial model embedded in EPRI MAAP5.04 does not allow to select the entrainment and partition coefficients which are highly impacting the FP releases to the environment. The new EDF MAAP5.04 model, validated against COSAQUE and embedding the dilution of the FP in the water of the RCS gives consistent results to the COSAQUE reference code.

Iodine spiking model, that was not modelled within the EPRI version of MAAP allows evaluating more precisely the releases of transients initiated at high power. The model implemented in EDF MAAP5.04 appears as a little be conservative against COSAQUE for some transients of the N4 reactor but stays acceptable for a crisis use.

Those developments realized in the frame of the R2CA project will be used by crisis experts within EDF crisis organization units.

References

3. MAAP User Guidance Phase 3.

4. W.F. PASEDAG, “Iodine spiking in BWR and PWR coolant systems”, Thermal reactor safety meeting; Sun Valley, ID, USA; 31 Jul - 5 Aug 1977, American Nuclear Society (1977).

Appendix C- IRSN Report

Contents

Abbreviations

FP	Fission products
RCS	Reactor Coolant System
SGTR	Steam Generator Tube Rupture

1. Model assessment

1.1. Brief description of the code

The V3.1 version of the IRSN ASTEC code used for the simulation was released in November 2022 for IRSN partners.

The ASTEC integral code aims at modelling all the phenomena which occur during a severe accident in water cooled reactors, from the initiating event to the releases of FPs into the environment. In a single calculation it is then possible to characterize the core thermal behaviour, the number of failed rods if any and the associated FP release, the FP transport in RCS up to the containment and their environmental releases (i.e., the Source Term).

1.2. Description of the code models for FP transport and release

ASTEC is divided in several modules, each one simulating a specific set of physical phenomena or related to a given reactor zone. Each module can be used in coupled or stand-alone mode. The main modules related to FP transport and release are listed below:

- ISODOP module: simulation of FPs and actinide isotopes decay in different zones of the reactor and the containment.
- ELSA module: simulation of release of FPs from the fuel and of structure materials
- SOPHAEROS module: simulation of FPs and structure materials transport and chemistry in the whole reactor plant (reactor cooling systems and containment).
- DOSE module: computation of the dose rate in the containment (liquid/gas phase and inner walls).
- MDB module: the Material Data Bank shared by all ASTEC modules.
- DROPLET module: activated to simulate the flashing phenomenon during a SGTR transient.
- SAFARI module: calculation of the FP mass transport and activities in a reactor, associated to a simplified modelling of the reactor different zones, in order to improve the computing times.

1.3. Critical assessment of models applicability

The modules listed above contain some limitations regarding the specificities of FP transport and release during a SGTR accident. The first limitation concerns the phenomenology of iodine flashing at the SGT breach, which is not taken into account in SOPHAEROS. The second limitation concerns the estimation of activity in the different components of the RCS, and in the different phases (liquid, gaseous…) of each of these components. The ISODOP module of ASTEC was not designed to reach this level of detail.

2. Improvement of the modeling

In an effort to address the aforementioned limitations of FP models of ASTEC, two new modules were developed: DROPLET and SAFARI.

2.1. DROPLET

The DROPLET model was developed and implemented in the ASTEC code system. Its goal was to model the iodine transfer and release into the environment, in the thermal-hydraulic conditions generated by a SGTR event occurring in the SG's dry part downstream the tube break. The pressurized primary water bursting out of the break

undergoes a mechanical fragmentation and an adiabatic expansion, thus forming overheated droplets with vapour germs, which reach equilibrium through droplet-atmosphere exchanges and germ growth. and potentially lead to droplet thermal fragmentation Under such conditions the transfer of iodine to the gaseous phase of the SG (so-called 'iodine flashing rate') depends on the following parameters:

- The hydraulic flashing rate (splitting of the vapour and liquid phases) at the break, leading to an iodine transfer in gaseous form and in liquid form by the droplets;
- The droplet-size distribution;
- The iodine chemical speciation at the break.

DROPLET calculates an iodine flashing rate until the break is reflooded, following the modelling pattern displayed on Figure 17 below. It models the following mechanisms [1]:

- Mechanical and thermal fragmentation of droplets;
- Depressurization and vapour germ formation;
- Iodine transfers toward vapour germs and at the droplet surface;
- Germ growth.

The fragmentation models require the thermohydraulic conditions of the primary and secondary circuit. Such information is provided by the ASTEC/CESAR module. Furthermore, the iodine mass transfer from liquid to gas phase depends on the presence of volatile species in the droplet composed of water from primary circuit. The iodine speciation is provided by the ASTEC/SOPHAEROS module which calculates the iodine chemistry in the primary circuit over the duration of the SGTR transient.

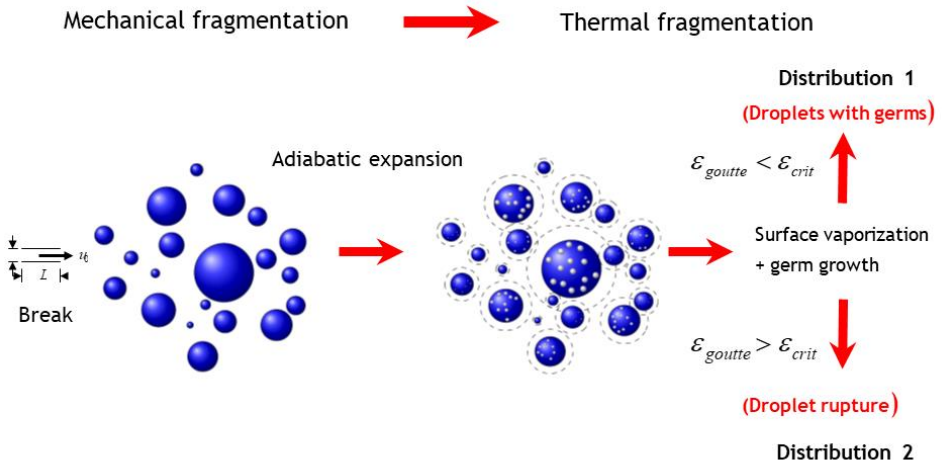

Figure 17. DROPLET main modelling diagram.

2.2. SAFARI

SAFARI (SGTR Accident Fission product Activity and Release Inventory) was developed and implemented in the ASTEC code system to calculate the mass and activity transfer of FP from a reactor's primary circuit to its secondary circuit, and the releases to the environment, in case of a SGTR accident. SAFARI calculates the FP transport, the isotopic inventory, and its associated activities in each defined zone – basically the coarse-meshed RCS main zones, plus a zone to simulate the environment. SAFARI has been chosen over the ISODOP module, because of its ability to discriminate each steam generator, and the liquid and gaseous phases in each one, when providing activity calculation results.

Like DROPLET and when in coupled mode, SAFARI uses the thermal-hydraulic conditions of the primary and secondary circuits provided by the ASTEC/CESAR module. Furthermore, the partition of iodine at SGT breach calculated by DROPLET is provided to SAFARI. As an illustration, the simplified nodalization of a PWR 900 Mwe is provided in Figure 18 below. In each zone, the element masses are calculated in liquid phase, gaseous phase, or deposited on the surfaces. Filters can be defined in the junctions and connexions linking the different zones. In order to reduce the computing time, one SAFARI zone corresponds to a main part of the primary circuit, and another one corresponds to the environment and correspond to the CESAR volumes in the following way:

- The VESSEL zone represents the core. In the design basis accident scenarios and also in order to reduce the computing time it is not modelled in SAFARI but only its inventory is limited to the fission and corrosion products found in the primary circuit, which quantities are based on the French reactors feedback is taken into account ;
- The PRIMARY zone includes all the primary circuit volumes defined in the CESAR module;
- A SGi (GVi in the graph) and a STLi zone represents each of the three steam generators and steam lines;
- A STH and a RCV zone represent respectively the steam header and the “volumetric and chemical control system”. In the database used for this current work, the condenser was not modelled; as a consequence, the isotopes arriving in the steam header remain here or are released from the GCTas. The RCV is also not modelled.

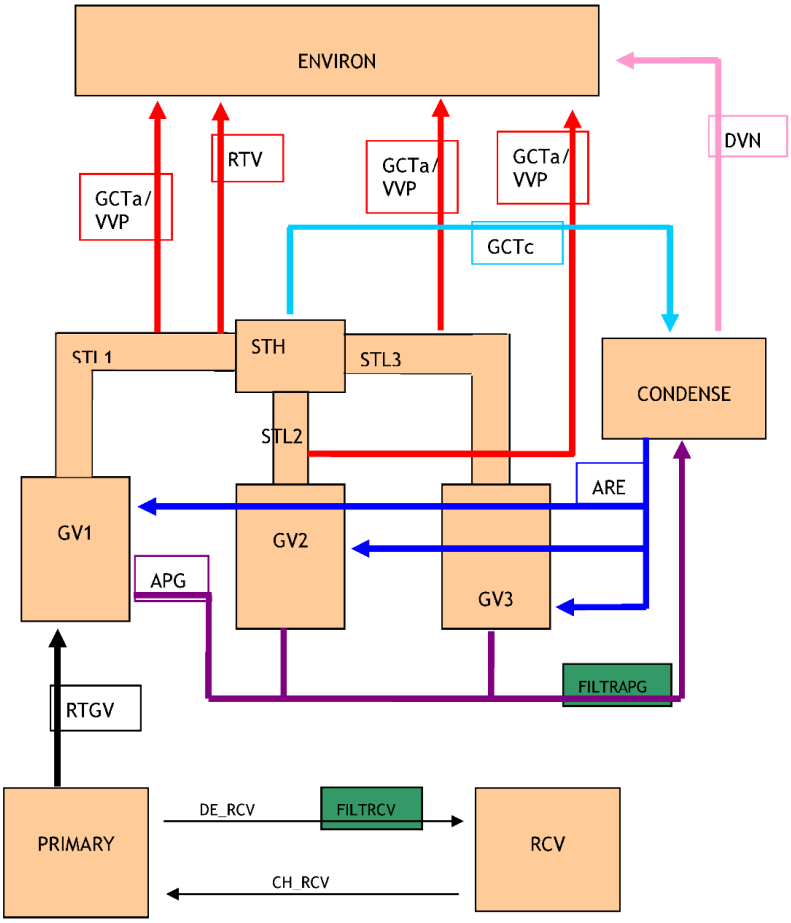

Figure 18: Example of SAFARI nodalization for SGTR accidents.

The activity increase during the reactor shutdown (sometimes referred to as “iodine spiking”) is not yet calculated by SAFARI. The start time and the duration of the peak are input data provided by the user, as well as the initial and peak isotope activities.

References

5. A. Cartonnet, « Contribution à l’étude du rejet à l’environnement de l’iode radioactif lors d’une séquence accidentelle de type RTGV » - Thèse, Université Lille 1, 17/12/2013.

Appendix D- UJV Report

Contents

Abbreviations

DBA	Design basis accidents
PC	Primary circuit or partition coefficient
SC	Secondary circuit
SG	Steam generator
SGTR	Steam generator tube rupture
SDA	Steam dump to atmosphere
SLB	Steam line break
VBA	Visual basic for applications

1. Introduction

The UJV's contribution is aimed at complex approach to the computation of radiological consequences during SGTR, emphasizing the DBA events. Up to now, there was no common methodology or approach in the Czech Republic to determine the SGTR source term. The previously proposed idea to use ATHLET-CD for fission product transport simulation in the primary and secondary circuit was abandoned due to lack of appropriate validation experiments and NPP models. The newly proposed idea is to create a standalone computational tool using balance equations. Such approach will be code-independent and able to use existing and future thermal hydraulic calculations as initial and boundary conditions. Furthermore, the proposed computational tool can create standardized XML source terms, which can be used directly by codes for radiological consequences evaluation, such as JRODOS.

In general, the UJV contribution can be split into following sections:

- Literature survey on SGTR activity transport phenomena.
- Proposal of new methodology.
- Proposal on computational approach based on system TH calculation.
- Implementation of the developed methodology and computational model into a VBA macro.
- Application to a DBA SGTR event at VVER-1000/V-320 and sensitivity study.

2. Literature survey on SGTR activity transport phenomena

2.1. Description of the general approach

The scope of the review was to find a general description of the processes, recommendations and finally some specific information on partition coefficients. Most of the information in the literature aim at iodine, which is a dominant contributor to radiological consequences.

NRC renowned documents from the Regulatory Guides series provide tremendous amount of information. The R.G. 1.183 **Erreur ! Source du renvoi introuvable.** and R.G. 1.195 **Erreur ! Source du renvoi introuvable.** bring general information on activity release and transport. The activity is assumed to be mixed homogenously within the primary circuit. For the affected steam generator, the thermal hydraulic conditions govern the activity transport. During phases with steam generator dry-out, where the leak is directed into the steam generator atmosphere only, the primary to secondary leak is assumed to be released into the environment with no mitigation. In other situations, where portion of the non-flashed primary to secondary leak is present, it is assumed to mix with the bulk water. The flashed content rises through the water column and scrubbing may occur. The recommended scrubbing models are presented in NUREG-0409 **Erreur ! Source du renvoi introuvable.**. A scheme of the transport model is given in Figure 19.

The activity release from steam generator water due to evaporation is assumed to happen at a rate that is the function of the steaming rate and the partition coefficient. For iodine, a partition coefficient of 100 may be assumed. The description of the partition coefficient is given in Equation 1 **Erreur ! Source du renvoi introuvable.**.

$$PC = \frac{mass\ of\ I_2\ per\ unit\ mass\ of\ liquid}{mass\ of\ I_2\ per\ unit\ mass\ of\ gas} = 100 \qquad (1)$$

Regarding the noble gas activities, the release from primary circuit is directed into the environment with no mitigation and reduction. Chemical composition of released iodine should be assumed to be 97 % elemental and 3 % organic **Erreur ! Source du renvoi introuvable.**.

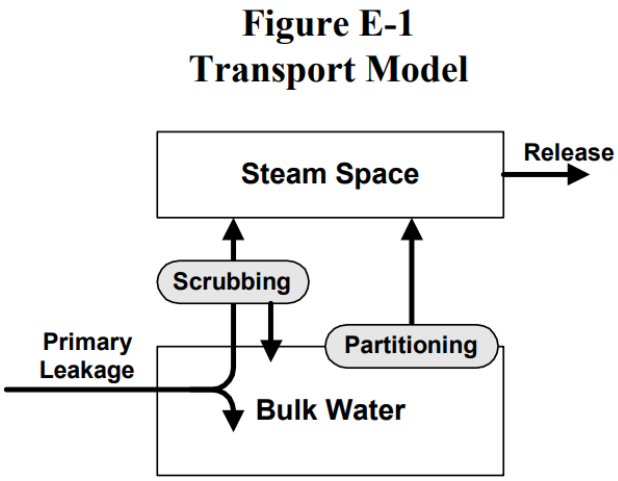

Figure 19. Iodine transport model for SLB and SGTR **Erreur ! Source du renvoi introuvable.**.

The report 0 defines three main activity transport phenomena occurring during SGTR, extending slightly the simplified description provided in **Erreur ! Source du renvoi introuvable.**, cf. Figure 20. The released mass from primary circuit may either enter the secondary side as steam (bypass), as immediately evaporating water (flashing) and finally as water mixing with the steam generator bulk water, which later evaporates.

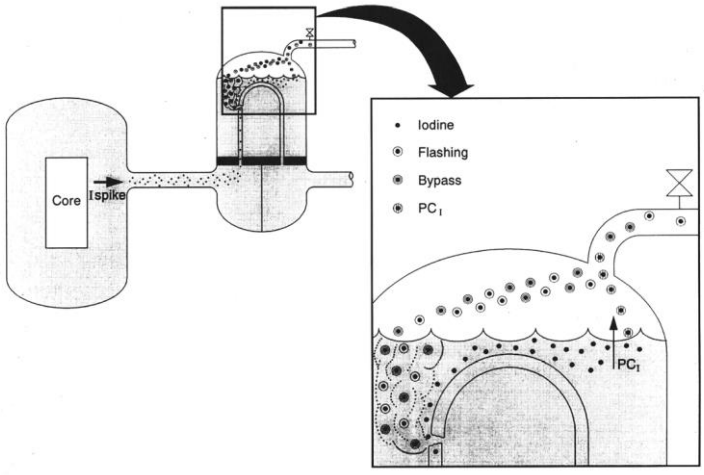

Figure 20. Iodine transport model for SGTR from Attwood.

The report **Erreur ! Source du renvoi introuvable.** provides information of general approach in Belgium, France, Germany, UK and Italy. In general, noble gasses are assumed to be released from the steam generator directly into the atmosphere with no retention or mitigation. The partition coefficient ranges from 10 to 100, where the first value is used in France to incorporate flashing phenomena, the second should be used for intact steam generator. Italy and Belgium use the same 100 partitioning coefficient for iodine. Furthermore, Italian approach assumes partition coefficient for non-volatile species to be 1000.

Other documents and paper complement the general information. Document **Erreur ! Source du renvoi introuvable.** recommends use of PC = 35 due to the pH values in SGs. This value is valid for recirculating SGs. Document **Erreur ! Source du renvoi introuvable.** notices that the partition coefficient depends on boric acid concentration rather than on pH. The partition coefficients should be between 1000 and 14000. Document **Erreur ! Source du renvoi introuvable.** summarizes that for pH 6-10 and temperatures 118°C, 143°C and 179°C with pressure below 1 MPa reaches values between 17 to 25000. These values were obtained after several hours. This time frame may exceed the duration of the investigated SGTR event. Paper **Erreur ! Source du renvoi introuvable.** mentions that with pH 6.5 the partitioning coefficient is 197.

3. Description of the model enhancements

3.1. Proposed methodology

The newly proposed methodology is based on the literature survey. Furthermore, demands of the Czech regulatory body were incorporated as well, namely the demand on conservative approach for DBA events **Erreur ! Source du renvoi introuvable.**.

1) Conservative initial inventory of primary and secondary activities (e.g. corrosion products, leaked fission products from fuel).
2) Spiking phenomena is assumed.
3) Radioactive decay may be modelled.
4) Activities are homogenously distributed between the volumes and phases.
5) Release of the activities from the primary circuit to the secondary circuit is equivalent to the coolant mass release through the steam generator tube rupture, where:
   a) Fraction of the primary coolant entrains the secondary side as steam (bypass), carrying 100 % of the activities of the evaporated water, i.e. PC = 1.
   b) Fraction of the primary coolant entraining the secondary side flashes immediately once it reaches the secondary side (flashing). It is assumed that 100 % of the activities of the evaporated water are further carried by the evaporated steam, i.e. PC = 1.
   c) The activities in the steam generator sump are increased by the activities leaked with water from the primary circuit.
6) Pool scrubbing is not modelled.
7) Retention of activities in the SG structures are not modelled.
8) Release through SDA.
   a) Main steam line is not modelled, i.e. the release from steam generator goes directly to the SDA.
   b) Noble gasses – If the SDA is opened, the available activities in the SG are released into the environment. If the SDA is closed, it is assumed that the activities are transported further to the secondary side.
   c) Other fission products – If the SDA is opened, the activities from the steam space are released into the environment. If the SDA is closed, it is assumed that the activities are transported further to the secondary side. The steam evaporated from the steam generator water (partitioning) takes fraction of the activities of the equivalent water mass, where the maximum value of the PC should be 100.
   d) The released iodine is composed of 97 % elemental and 3 % organic form.

3.2. Proposed computational approach

In general, the coolant from the primary can enter the secondary side either as a steam (bypass) or as a water. Once the water enters the secondary side, fraction of this release is not mixed with the steam generator water content, but thanks to thermal hydraulic conditions it flashes immediately (flashing). The remaining water mixes

with the steam generator water volume. Due to the heating of the steam generator water content, evaporation of the water can occur. The steam from the SG steam space then advances through the steam line.

Regarding the fission products, as in the previous case, three main pathways may be assumed for activity release from steam generator to the steam line. Firstly, the fission products entraining the steam generator with steam from primary coolant. Depending on the position of the SGTR, the release can be covered (under water) or uncovered. For the covered case, pool scrubbing may occur. Second path, related to flashing, defines the activity, which is torn off with the flashing content. The remaining activity is assumed to be mixed with bulk water. Finally, due to evaporation, fraction of the activities may enter the steam space (partitioning). Depending on the thermal hydraulic conditions, some of the effects may not take effect. A scheme of the relevant processes is given in

Figure 21.

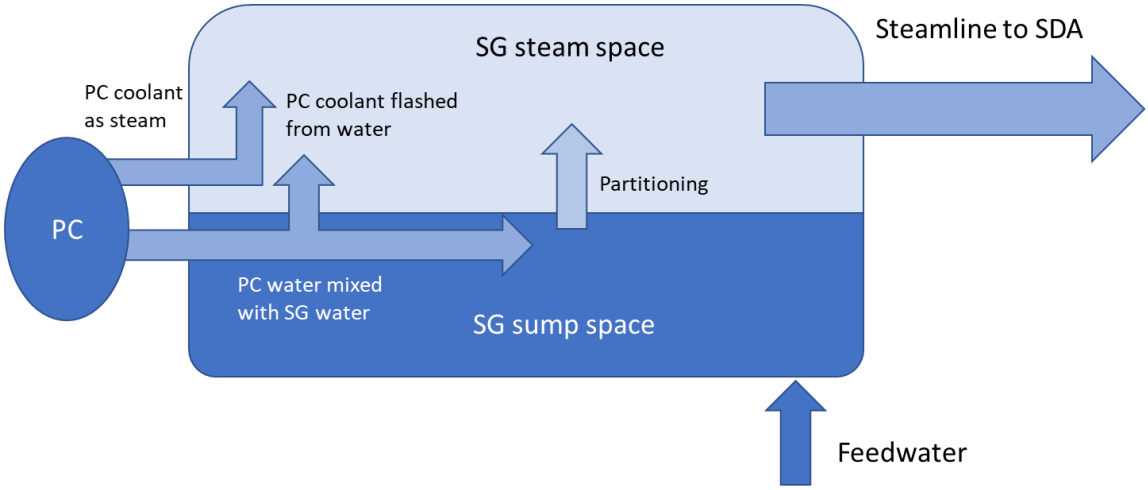

Figure 21. Mass transfer in the affected steam generator.

3.2.1. Balance models

Following the description of phenomenology, a set of equations describing mass and activity conservation and transfer between the primary and secondary has been introduced. The equations calculate the values of next time step based on the values from the previous step. The length of the time step is based on the thermal hydraulic calculation.

For the primary circuit coolant mass, the balance is following.

$$m_{I.O,t+1} = m_{I.O,t} - \dot{m}_{break,t}\Delta t_{t,t+1} - \dot{m}_{rem,t}\Delta t_{t,t+1} + \dot{m}_{ECCS,t}\Delta t_{t,t+1} \quad (2)$$

Where

$m_{I.O,t}$	mass of the PC coolant at time t [kg]
$m_{I.O,t+1}$	mass of the PC coolant at time t + 1 [kg]
$\dot{m}_{break,t}$	SGTR break mass flow at time t [kg.s^{-1}]
$\dot{m}_{rem,t}$	total mass release through primary relief systems at time t [kg.s^{-1}]
$\dot{m}_{ECCS,t}$	total primary coolant injection at time t [kg.s^{-1}]
$\Delta t_{t,t+1}$	time step length t, t+1 [s]

The balance of the activities in the primary circuit is following

$$A_{I.O,t+1} = A_{I.O,t} - \dot{A}_{break,t}\Delta t_{t,t+1} - \dot{A}_{rem,t}\Delta t_{t,t+1} \quad (1)$$

Where

$A_{I.O,t}$	activity of the primary coolant at time t [Bq]
$A_{I.O,t+1}$	activity of the primary coolant at time t+1 [Bq]
$\dot{A}_{break,t}$	activity release through SGTR at time t [Bq.s^{-1}]
$\dot{A}_{rem,t}$	activity removed by primary relief systems at time t [Bq.s^{-1}]
$\Delta t_{t,t+1}$	time step length t, t+1 [s]

The balance of coolant mass inside the steam generator sump is following.

$$m_{PG,t+1} = m_{PG,t} + (1 - f_{bypass,t} - f_{flashing,t})\dot{m}_{break,t}\Delta t_{t,t+1} - \dot{m}_{steamline,t}\Delta t_{t,t+1} + \dot{m}_{feed,t}\Delta t_{t,t+1} \quad (2)$$

Where

$m_{PG,t}$	SG coolant mass at time t [kg]
$m_{PG,t+1}$	SG coolant mass at time t + 1 [kg]
$\dot{m}_{break,t}$	mass flow through SGTR at time t [kg.s^{-1}]
$\dot{m}_{steamline,t}$	mass flow to the steamline at time t [kg.s^{-1}]
$\dot{m}_{feed,t}$	feedwater mass flow at time t [kg.s^{-1}]
$f_{bypass,t}$	fraction of the SGTR leak bypassing SG at time t [-]
$f_{flashing,t}$	fraction of the SGTR leak flashing immediately after reaching the SG at time t [-]
$\Delta t_{t,t+1}$	time step length t, t + 1 [s]

For the activities inside the steam generator water, the balance is following.

$$A_{PG,t+1} = A_{PG,t} + \dot{A}_{break,liquid,t}\Delta t_{t,t+1} - \dot{A}_{evap,t}\Delta t_{t,t+1} + \dot{A}_{feed,t}\Delta t_{t,t+1} \quad (3)$$

Where

$A_{PG,t}$	activity in the SG water at time t [Bq]
$A_{PG,t+1}$	activity in the SG water at time t + 1 [Bq]
$\dot{A}_{break,liquid,t}$	activity flow through SGTR into SG water at time t [Bq.s^{-1}]
$\dot{A}_{evap,t}$	activity evaporated with steam at time t [Bq.s^{-1}]
$\dot{A}_{feed,t}$	activity flow from SG feedwater at time t [Bq.s^{-1}]
$\Delta t_{t,t+1}$	time step length t, t + 1 [s]

The most important thing is modelling of the activity transport within the affected steam generator and release through corresponding SDA. The adopted simplifications do not allow modelling of mass transfer delay between the SG and SDA. Two possible simplified scenarios may be observed:

1. The mass flow through SDA is equal or lower than the steam mass flow from SG bypass and flashing. In this case, the partitioning effect is neglected ($\dot{A}_{evap,t} = 0$), and the total activity release is maintained by the SG bypass and flashing only.

$$\dot{A}_{SDA,t} = f_{flashing,t}\frac{1}{PC_{flashing}}c_{PC,t}\dot{m}_{break,t} + f_{bypass,t}\frac{1}{PC_{bypass}}c_{PC,t}\dot{m}_{break,t} \quad (4)$$

Where

$f_{bypass,t}$	fraction of the SGTR leak bypassing SG at time t [-]
$f_{flashing,t}$	fraction of the SGTR leak flashing immediately after reaching the SG at time t [-]
PC_{bypass}	partition coefficient for bypass [-]
$PC_{flashing}$	partition coefficient for flashing [-]
$c_{PC,t}$	activity concentration in the primary circuit water at time t [Bq.kg^{-1}]
$\dot{m}_{break,t}$	mass flow through SGTR at time t [kg.s^{-1}]

2. The mass flow through SDA is higher than the steam mass flow from SG bypass and flashing. In this case, the "missing" release is complemented by the release from evaporation and the total activity released through SDA is a sum of activities from bypass, flashing and partitioning.

   The activity released by evaporation is following.

$$\dot{A}_{evap,t} = (1 - f_{bypass,t}\frac{\dot{m}_{break,t}}{\dot{m}_{SDA,t}} - f_{flashing,t}\frac{\dot{m}_{break,t}}{\dot{m}_{SDA,t}})\frac{1}{PC_{part}}c_{SG,t}\dot{m}_{SDA,t} \quad (5)$$

   The activity released through SDA is following.

$$\dot{A}_{SDA,t} = \dot{A}_{evap,t} + f_{bypass,t}\frac{1}{PC_{bypass}}c_{PC,t}\dot{m}_{break,t} + f_{flashing,t}\frac{1}{PC_{flashing}}c_{PC,t}\dot{m}_{break,t} \quad (6)$$

Where

$\dot{A}_{SDA,t}$	activity release through SDA at time t [kg.s^{-1}]
$\dot{m}_{SDA,t}$	mass flow through SDA at time t [kg.s^{-1}]
$\dot{m}_{break,t}$	mass flow through SGTR at time t [kg.s^{-1}]
$c_{SG,t}$	activity concentration in SG sump at time t [Bq.kg^{-1}]
$c_{PC,t}$	activity concentration in primary circuit water at time t [Bq.kg^{-1}]
PC_{part}	partition coefficient for partitioning [-]
PC_{bypass}	partition coefficient for bypass [-]
$PC_{flashing}$	partition coefficient for flashing [-]
$f_{bypass,t}$	fraction of the SGTR leak bypassing SG at time t [-]
$f_{flashing,t}$	fraction of the SGTR leak flashing immediately after reaching the SG at time t [-]

3.3. Implementation into EXCEL VBA

The implementation was done bearing in mind further application in the JRODOS code, which is used for estimation of radiological consequences. JRODOS is limited to 140 isotopes, which are presented in Table 11. For each of the isotopes, the macro calculates the activity balance within the primary and the secondary circuit water as

presented in the chapter describing the balance models. To calculate such values, the user must provide initial and boundary conditions. From the activity point of view, the initial activity concentration within the primary coolant, secondary steam and water and secondary feedwater must be input for each isotope. Furthermore, each isotope requires values for partitioning, flashing and bypass. For noble gasses such as krypton and xenon the values are obsolete. Finally, the most important thing is the results of the thermal hydraulic calculations, which must be input in predefined order and in desired dimensions. Once the data is ready, the calculation can be performed. The macro creates a separate sheet for each isotope, plotting total activity in the primary circuit, total activity in the steam generator water and the total activity released through SDA.

Isotopes used for calculation of radiological consequences						
Ag-110	Co-60	I-135	Np-238	Rb-89	Sn-127	U-235
Ag-110m	Cr-51	Ir-192	Np-239	Rh-103m	Sn-128	U-237
Ag-111	Cs-134	Kr-83m	Pd-109	Rh-105	Sr-89	U-238
Am-241	Cs-134m	Kr-85	Pm-147	Rh-106	Sr-90	W-185
Ba-137m	Cs-135m	Kr-85m	Pm-148	Ru-103	Sr-91	W-187
Ba-139	Cs-136	Kr-87	Pm-148m	Ru-105	Sr-92	Xe-131m
Ba-140	Cs-137	Kr-88	Pm-149	Ru-106	Tb-160	Xe-133
Ba-141	Cs-138	La-140	Pm-151	Sb-122	Tc-99m	Xe-133m
Br-82	Cu-64	La-141	Po-210	Sb-124	Te-125m	Xe-135
Br-83	Eu-154	La-142	Pr-142	Sb-125	Te-127	Xe-135m
Br-84	Eu-155	Mn-54	Pr-143	Sb-126	Te-127m	Xe-138
C-11	Eu-156	Mn-56	Pr-144	Sb-127	Te-129	Y-90
Ce-141	F-18	Mo-99	Pr-144m	Sb-128	Te-129m	Y-91
Ce-143	Fe-59	N-13	Pu-238	Sb-129	Te-131	Y-91m
Ce-144	I-129	Na-24	Pu-239	Sb-131	Te-131m	Y-92
Cf-252	I-130	Nb-95	Pu-240	Se-75	Te-132	Y-93
Cm-242	I-131	Nb-95m	Pu-241	Sm-153	Te-133	Yb-169
Cm-243	I-132	Nb-97	Ra-226	Sn-121	Te-133m	Zn-65
Cm-244	I-133	Nd-147	Rb-86	Sn-123	Te-134	Zr-95
Co-58	I-134	Nd-149	Rb-88	Sn-125	U-234	Zr-97

Table 11. List of isotopes calculated by JRODOS **Erreur ! Source du renvoi introuvable.**.

3.4. Application to VVER-1000/V-320 DBA SGTR and sensitivity study

The developed macro was applied to DBA SGTR at VVER-1000/V-320. This accident was previously investigated within the Task 2.3. The source thermal hydraulic calculation was done with ATHLET 3.1. The initiation event is a double ended guillotine break of single steam generator tube. Further information about the thermal hydraulic calculation can be obtained from **Erreur ! Source du renvoi introuvable.**. Timing of the main events is presented in Table 12.

Event	Timing [s]	Further information
Start of the calculation	-500 s	Steady state calculation
Initiating event	0 s	SG4 tube rupture 2x D13 mm leak
Reactor SCRAM	1663	2 s delay after low pressurizer water level signal
Loss of off-site power LOOP	1663	Main circulation pumps failure
Minimal DNBR	1664	
SDAs opened	~1667	SDA4 remains locked in open position
DG available	1683	
SG4 rupture signal	1756	SG4 armature close
First operator action	1800	
PTTQ start	1865	3/3 available
VTTQ start	1943	3/3 available
Steam bubble under the reactor cover	1955	
End of the Tk refill	2012	Depletion of water supply
Renewal of the TK refill	2400	Operator action
End of the calculation	220000	

Table 12. Timing of the DBA SGTR at VVER-1000/V-320 **Erreur ! Source du renvoi introuvable.**.

The activity release into the environment starts at 1667 s after the initiating event. The SDA of the affected steam generator remains opened. The activity from the primary circuit enters the secondary side both in water and gas phase. All three phenomena, namely the bypass, flashing and partitioning occur during the accident. Following the literature research, a short sensitivity study was conducted for three different values of partitioning coefficient to see the impact of reduced or increased partitioning. The variants including results at the end of the calculation are presented in
Table 13. I-131 was chosen as a representative isotope. For simplification and lucid evaluation, the values are standardized to the fraction of initial total activity of the primary circuit.

Case	Partitioning coefficient	Released I-131 activity as fraction of PC initial inventory [%]	Difference from c00 [%]
c00	1	20.7	-
c01	10	13.9	-32.9
c02	100	9.8	-52.4

Table 13 Calculated variants and results.

The modified partitioning coefficients proved to have impact both on sump activity and the total release through SDA. As expected, the total activity release decreases with increasing partitioning coefficient, cf. Figure 22. On the other hand, reduced partitioning effect leads to lower concentrations in the steam generator water, cf. Figure 23.

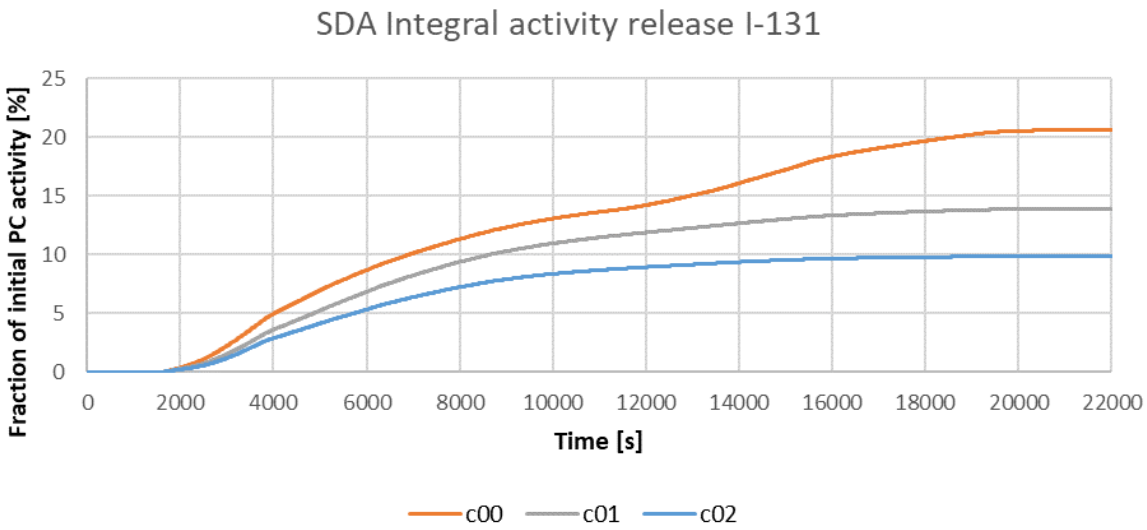

Figure 22. Sensitivity study on partitioning coefficient – SDA integral activity release.

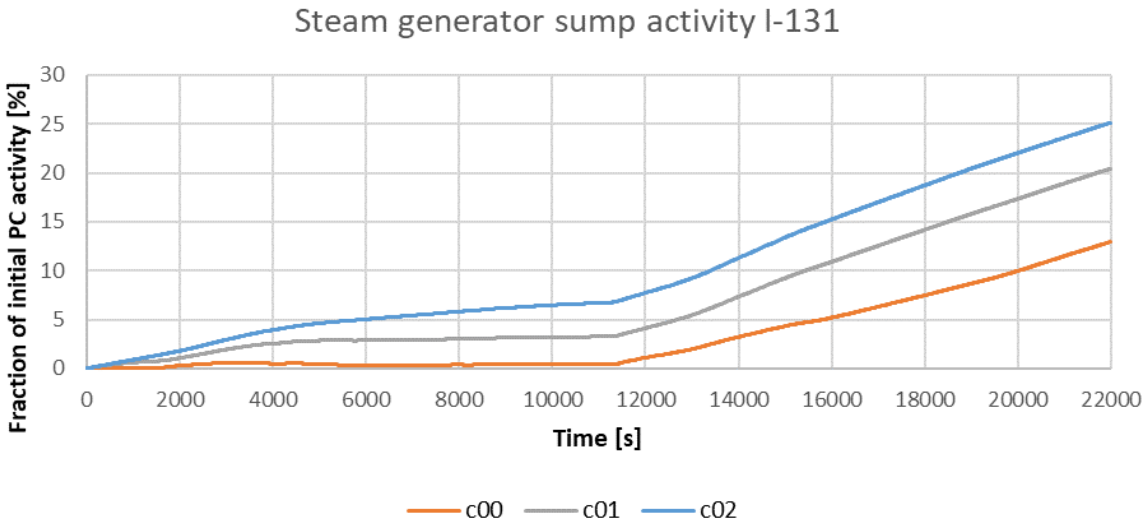

Figure 23. Sensitivity study on partitioning coefficient – SG sump activity.

Change of the partitioning coefficient changes the ratio between the three activity release phenomena occurring during the SGTR. For c00 case with PC = 1, partitioning is the dominant release phenomena, cf.

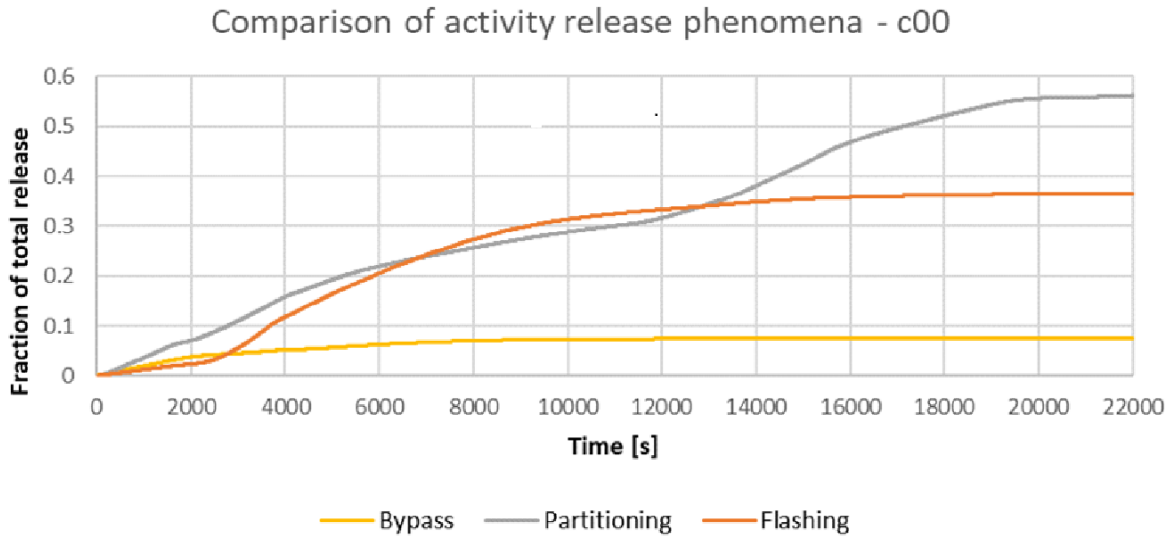

Figure 24. With increasing value of partitioning coefficient to PC = 10, the flashing effect becomes dominant, cf.

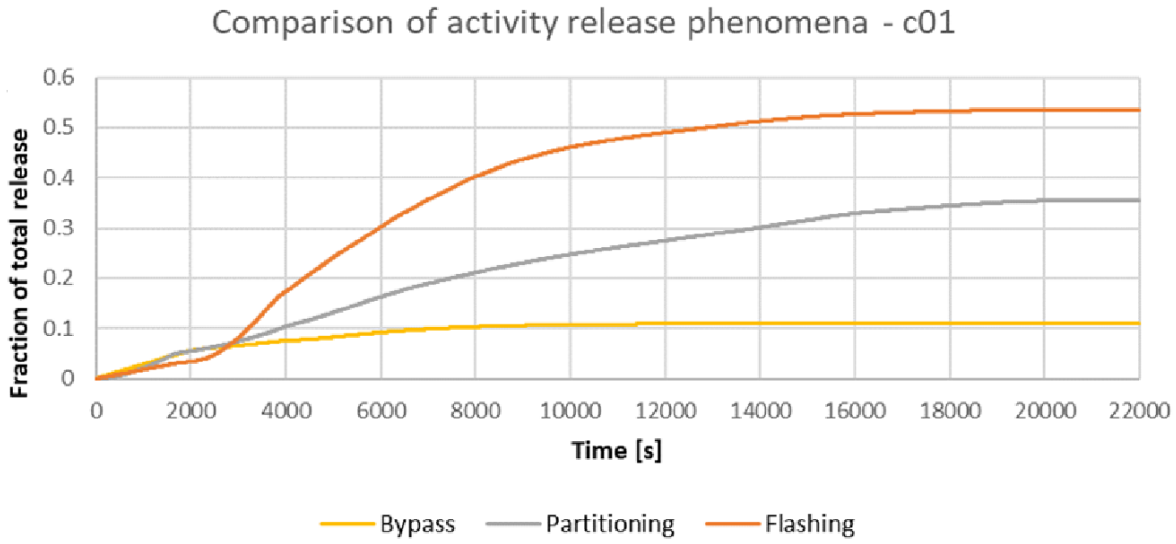

Figure 25. Finally, if the partition PC = 100 (the value proposed in the methodology and documents like **Erreur ! Source du renvoi introuvable.**), partitioning becomes the minor contributor to the activity release, cf.

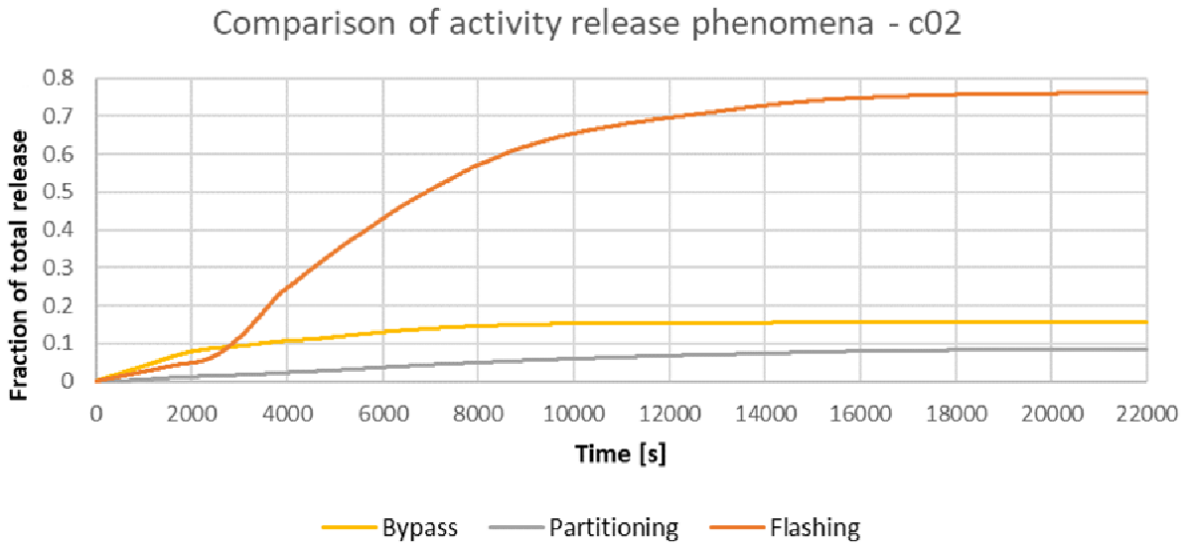

Figure 26.

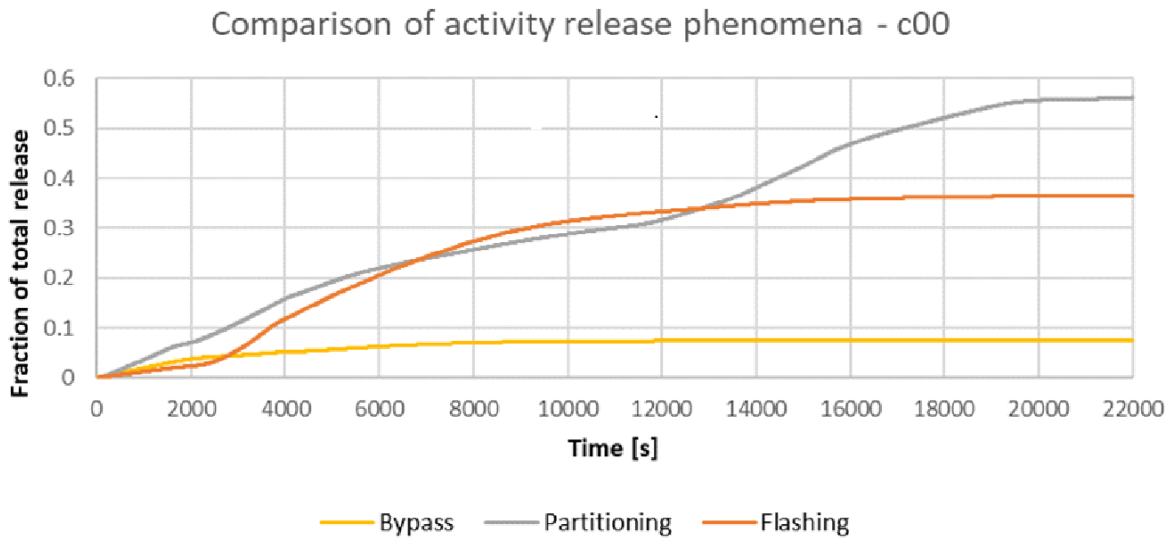

Figure 24. Sensitivity study on partitioning coefficient – comparison of activity release phenomena, c00.

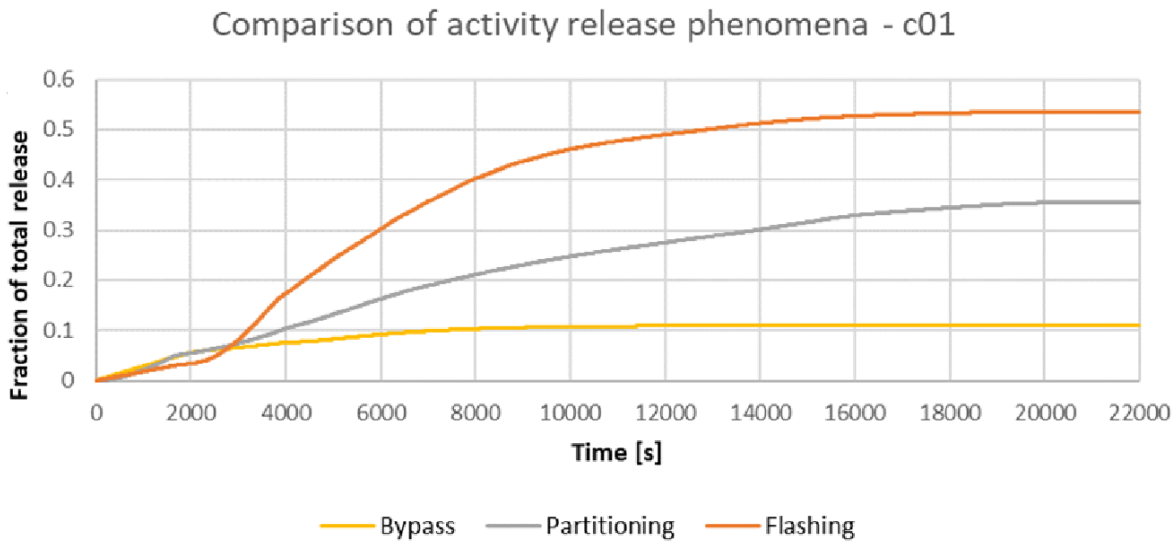

Figure 25 Sensitivity study on partitioning coefficient – comparison of activity release phenomena, c01.

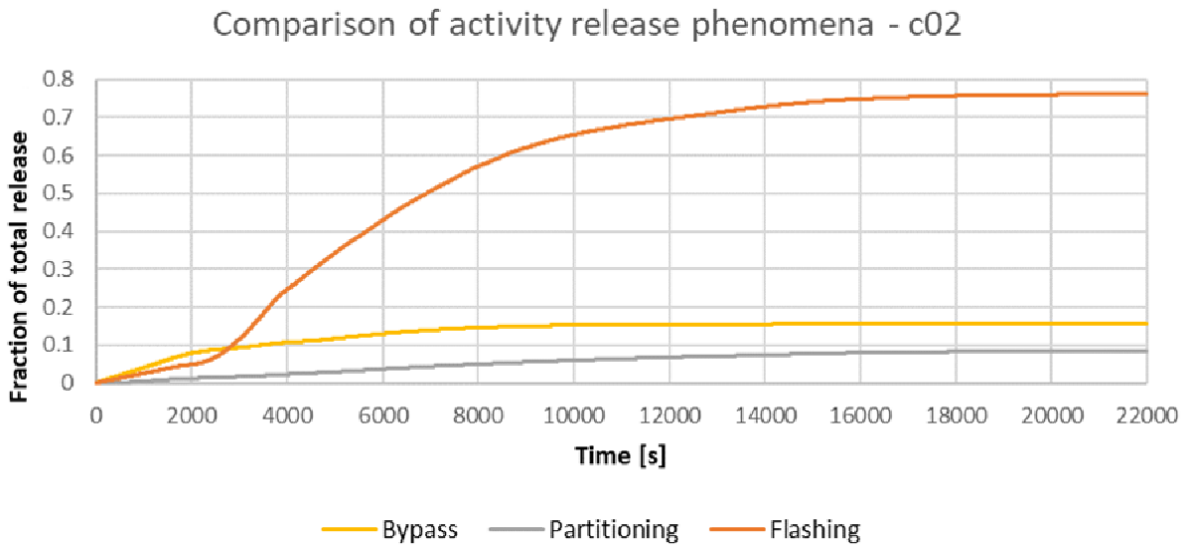

Figure 26. Sensitivity study on partitioning coefficient – comparison of activity release phenomena, c02.

4. Conclusions and remarks

The conducted literature research revealed that the general approach assumes three possible phenomena of activity release from primary to secondary circuit. This approach is valid for all activities except noble gasses, where simplified approach, thank to chemical and physical nature, may be adopted. Important part of the phenomena description is the value of partitioning coefficient, which defines the fraction of activity present released into evaporated steam. The value ranges from 10 to thousands, depending on the thermal hydraulic and chemical

conditions inside the steam generator. For volatile species, lower values of PC, ie. larger release fractions are expected.

The literature research created a cornerstone for development of a computational tool, which calculates the activity transport and estimates SGTR source term based on balance equation and separate thermal hydraulic calculation. This approach is code independent and suitable both for previous and future calculations.

The developed computational tool is tailored for further radiological consequence calculation with JRODOS code, i.e. 140 isotopes implemented JRODOS are considered for transport. The output file can be directly mounted into the JRODOS code.

The computational tool was for testing purposes applicated to a SGTR event at VVER-1000/V-320, where hydraulic calculations were done by ATHLET code. This event was previously investigated within the Task 2.3. The application brought satisfactory results. To understand the behaviour of the proposed approach, a short sensitivity study was conducted. The base case with PC = 1 revealed strong impact of the partitioning effect, which becomes less important with reduction of the partitioning coefficient. Using partitioning coefficient 10 and 100, flashing becomes the main contributor to the total activity release.

The developed approach will find its application in current and future analyses of NPPs. Further research may be aimed at bypassing and flashing phenomena and related partition coefficients.

References

6. James P. Adams. Iodine release during a steam generator tube rupture. Nuclear Technology, August 1994.

7. US NRC: Regulatory Guide 1.183, Alternative Radiological Source Terms for Evaluating Design Basis Accidents at Nuclear Power Reactors, U.S. Nuclear Regulatory Commission, July 2000.

8. US NRC: Regulatory Guide 1.195, Methods and Assumptions for Evaluating Radiological Consequences of Design Basis Accidents at Light Water Nuclear Power Reactors, U.S. Nuclear Regulatory Commission, July 2003.

9. Gorman, R., 2000. FOIA/PA-2000-0255 – Resolution of GI 67.5.1, "Reassessment of SGTR Radiological Consequences", 6-30-94 E. S. Beckjord memo, Letter, ML003720028. Humphreys, 1998. https://www.nrc.gov/docs/ml0037/ML003725812.pdf.

5. Dutton, L. M. C.; Smedley, C.; Handy, B. J.; Herndlhofer, S.R.: Realistic methods for calculating the release of radioactivity following steam generator tube rupture faults, A consensus document, Report EUR 15615 EN, European Commission, 1994.

6. USNRC, “Iodine Behavior in a PWR Cooling System Following a Postulated Steam Generator Tube Rupture Accident,” NUREG-0409, May 1985. https://www.nrc.gov/docs/ML1926/ML19269F014.pdf.

7. Clinton, S D, and Simmons, C M. 1987. "Iodine partition coefficient measurements at simulated PWR steam generator conditions: Interim data report". United States. https://www.nrc.gov/docs/ML2023/ML20236K038.pdf.

8. Hopenfeld, J. (1985). Radioactivity transport following steam generator tube rupture (NUREG--1108). United States https://www.nrc.gov/docs/ML2010/ML20100E507.pdf.

9. Changdong Lu, Zhidong Le, Yonggang Shen, Wei Cai, Jiang Yang, Wenying Ji, Ying Zhang: The prediction of steam generator secondary pH under SGTR condition of HPR1000, Progress in Nuclear Energy, Volume 134, 2021, 103673, ISSN 0149-1970, https://doi.org/10.1016/j.pnucene.2021.103673.

10. USNRC, "Steam Generator Tube Integrity," Draft Regulatory Guide DG-1074, December 1998.

11. USNRC, "Steam Generator Tube Rupture Analysis Deficiency," Information Notice 88- 31, May 25, 1988.

12. Bixler, N.E; Erickson, C.M.; Schaperow, J.H.: INVESTIGATION OF A STEAM GENERATOR TUBE RUPTURE SEQUENCE USING VICTORIA. https://inis.iaea.org/collection/NCLCollectionStore/_Public/27/051/27051657.pdf.

13. Adams, J P, and Peterson, E S. 1991. "Steam generator secondary pH during a steam generator tube rupture". United States. https://doi.org/10.2172/5375670. https://www.osti.gov/servlets/purl/5375670.

14. SÚJB (2020). Safety guide BN-JB-2.10 (Rev. 0.0) deterministic safety analyses of abnormal operation and design basis accidents, Bezpečnostní návod BN-JB-2.10 (Rev. 0.0) Deterministické bezpečnostní analýzy událostí abnormálního provozu a základních projektových nehod. State Office for Nuclear Safety, Prague, Czechia.

15. Husťáková, H.: Zadávání zdrojových členů do kódu JRODOS, ÚJV Z5605, ÚJV Řež, a. s. červen 2021.

16. Kecek, A.; Kral, P.; Denk, L.: Summary report on VVER 1000 /V320 LOCA calculations, R2CA Consortium, February 2021.

Appendix E- CIEMAT Report

Contents

Abbreviations

AECL	Atomic Energy of Canada Limited
DBA	Design Basis Accident
DEC	Design Extension Conditions
FGR	Fission Gas Release
FP	Fission Product
LOCA	Loss Of Coolant Accident
LWR	Light Water Reactor
PC	Partition Coefficient
PIE	Post-Irradiation Examination
PV	Pressure Vessel
PWR	Pressurized Water Reactor
R2CA	Reduction of Radiological Consequences of design basis and design extension Accidents
SG	Steam Generator
SGTR	Steam Generator Tube Rupture

1. Introduction

In the framework of the R2CA project (Work Package 2), the experimental databases available on fuel failure, fission products (FP) release and activity transport up to the environment during LOCA and SGTR events were reviewed [1]. Based on this material, the present report identifies and analyzes the experimental data that might be applicable in the study of FP transport along the primary circuit and their transfer to the secondary side of the steam generator during SGTR DBA and DEC-A sequences. Particular attention has been paid to the representativeness of the initial and boundary conditions, the reliability of the experimental techniques used and the experimental protocol adopted. Additionally, the implemented models of MELCOR for FP transport and their applicability to SGTR sequences has been assessed and a new model has been developed for the consideration of the mechanisms of flashing, atomization and partitioning in the transport of the iodine to the environment.

2. Assessment of the experimental database of fission product transport and release

2.1. Test Iod-29 (OECD THAI-2)

The OECD THAI-2 project, conducted at the THAI facility from August 2011 to July 2014, was aimed to address open questions concerning the behavior of hydrogen, iodine and aerosols in the containment of water-*cooled* reactors during design basis or severe accident conditions. As for the purpose of this report, the experiment Iod-29 explored the release of gaseous iodine from a flashing jet under conditions simulating the interface of primary and secondary circuit during a SGTR DBA accident.

2.1.1. Brief description

In case of a SGT DBA a fraction of the iodine inventory in the primary circuit (to a good extent resulting from iodine spiking) would be released to the secondary side of the SG through the leak in the form of a two-phase flashing jet. Thus, Iod-29 investigated the release of gaseous iodine from a flashing jet [2].

Figure 1 shows the configuration of the test with the specific iodine instrumentation [2]. A droplet separator inside the THAI vessel immediately behind the inlet of the pipeline simulating the primary circuit leak, removed the droplet-bound iodine and thus enabled measurement of a gaseous iodine fraction. The iodine measurement was based upon the gas scrubber technique and other THAI instrumentation, measuring iodine in any arriving form.

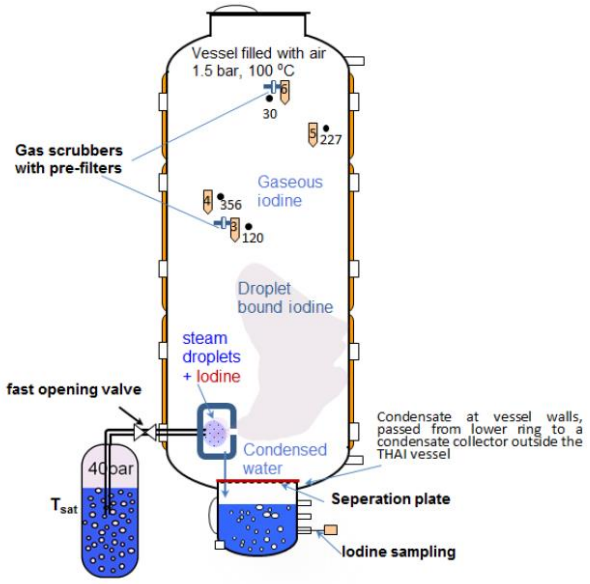

Figure 27. Iod-29 test configuration with iodine specific instrumentation [2].

2.1.2. Test conditions and protocol

The dimensions of the experimental facility (release line and PV operating parameters) were selected to get fluid velocities representative of flashing jet conditions. A pressure drop during flashing of about 40 bar was realized by flashing water containing iodine from a high-pressure primary vessel through a pipeline of 9 mm ID into the THAI vessel at a pressure of only 1.5 bar. The water temperature in the pressure vessel was 250 ˚C and pressure attained 40 bar at the end of the heating phase previous to the depressurization. The Iod-29 test conditions as achieved at start and end time of the flashing are given in the Table 1.

The THAI vessel (60 m^3) was initially filled with dry air at 1.5 bar and 100 ˚C. The pressure vessel was filled with 0.750 m^3 of water and 19.0E-03 kg of I_2 (molecular iodine) were injected into the cold primary vessel. The water was buffered by a phosphate at a pH = 7.2 before heating up. At high temperature, flashing conditions were expected to yield a significant gaseous iodine fraction in the form of hypoiodous acid (HOI).

During the flashing period of 3.03 min, about 178 kg of water was discharged from the PV corresponding to a mean mass flow rate of 0.98 kg/s. Out of this, about 41 kg of steam was generated and about 137 kg of water was directly transferred to the THAI sump. The amount of condensate from THAI gas atmosphere was about 4.0 kg. At the end of the flashing period, the generated steam and associated temperature rise resulted in an absolute pressure level of 2.85 bar in the THAI vessel which relaxed back to about 2.6 bar within 10 min after flashing. Based on the generated steam amount, a flashing evaporation ratio of approximately 23% was estimated [2].

Test parameter	Specified	Measured	Measured
Preconditioning			**End of Flashing***
THAI vessel pressure [bar]	1.50	1.497	2.848
THAI vessel fluid temperature [°C]	100	100.3	122.9
THAI vessel wall temperature [°C]	100	101.45	-
PV pressure [bar]	40	40.17	38.64
Water temperature in PV [°C]	250	247	245.6
Chemical boundary conditions (pressure vessel)			
pH at ambient conditions	7.2	7.0 - 7.2	
Buffer concentration [mol/L] NaOH KH_2PO_4	 6.0E-3 1.0E-2	 6.67E-3 1.0E-2	
I_2 injected into PV water [g] I_2 inv. before flash. based on sampl. [g]	19.0	19.1 13.9	
Iodine concentration in PV water [mol/L] Based on sampl. [mol/L]	1.0E-4	1.0E-4 0.73E-4	

* Flashing duration: 3.03 min

Table 14. Test conditions as achieved at start and end time of the flashing [2]

2.1.3. Critical assessment of the data

Iod-29 was dimensioned both geometrically and in terms of initial and boundary conditions as anticipated in a SGTR DBA accident. Thus, the data might be considered relevant for the scenario of investigation (discharge from the primary to the secondary side of a SG).

2.1.4. Major insights

The iodine measurements in the THAI vessel (gas space and sump) and in the primary vessel consistently showed that there was no gaseous iodine released from the flashing jet under the investigated test conditions [2]. Measured concentrations in the THAI vessel were very low.

This observation is consistent with measurements on iodine speciation in the water of the pressure vessel, sampled during heat-up just before and just after the flashing process. Although 19.0E-03 kg of I_2 (molecular iodine) were injected before heating up, only iodide form was found. In other words, the injected I_2 reacted quickly with the steel walls of the primary vessel during heat-up and produced the non-volatile I^- form.

In short, the conditions imposed in Iod-29 conditioned the observations as they resulted in a very low amount of iodine in the form of volatile I_2. Nonetheless, given the amount of surfaces along the primary circuit that the iodine released during iodine spiking will be exposed along its path most of iodine might be well in the form of iodide (I^-) under the conditions explored. Another important feature of the test was the pH imposed in the iodine solution, around neutral (values in between 6.9 and 7.4 should be in PWR coolant), that might be assumed not to change drastically because of addition of HPIS inventory during SGTR DBA and DEC-A transients.

2.2. ARTIST-Phase VI

2.2.1. Brief description of the experiments program

Aerosol Trapping In Steam GeneraTor (ARTIST) project was an international collaborative project developed in two stages, between 2003 and 2011. The primary objective of the project was the experimental determination of aerosol retention in the steam generator during a SGTR accident sequence through an eight-phase program. Even though, the program was mainly focused on aerosol retention and severe accident conditions, droplet retention in the separator and dryer sections (Phase VI) was also investigated under SGTR DBA conditions.

The ARTIST facility is a scaled-down model of the FRAMATOME 33/19 type steam generator in operation at the Swiss power plant Beznau which is a 1136 MWth pressurized water reactor. It consists of a tube bundle, one separator unit (1:1 in scale) and one dryer cell (1:1 in scale). The bundle section is composed of a scaled-down 0.57 m diameter tube bundle comprised of 270 straight tubes with an outer diameter of 19.08 mm and a height of 3.8 m. The scaling ratio for the number of tubes and free flow area is approximately 1:20 [3].

Phase VI: **Droplet retention in the separator and dryer sections under dry conditions.**

Phase VI addressed experimentally the droplet retention and velocity field in the separator (1:1 in scale) and dryer unit (1:1 in scale) of a SG. The potential containment bypass in case of a SGTR DBA was investigated by assuming a break at the top of the tube bundle. Fine liquid droplets were sprayed upwards towards the separator and dryer. Since droplets contain the dissolved activity, quantification of their potential retention in the secondary side determines the radiological consequences of the accident.

The droplets for the experiments are generated with a two-fluid, air-assist, full-cone spraying nozzle projecting upwards. The nozzle was mounted in the axis of the inlet section of the test section (Figure 2).

For the droplet retention experiments, a known mass of Di-Ethyl-Hexyl-Sebacat (DEHS) was injected by means of the spraying nozzle at the bottom of the test section. The retention in the swirl vane unit, the upper section of the droplet separator and the dryer occurs by droplet impingement on surfaces and formation of a downward flowing film [4].

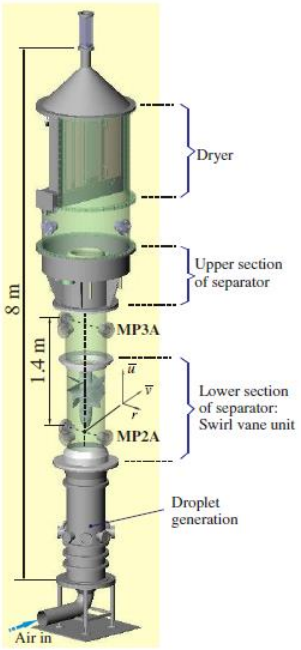

Figure 28. Test section for droplet retention tests in separator and dryer [4].

2.2.2. Test matrices

Two series of tests were conducted [4]:

- Type A tests: the droplet retention was measured by collecting this film for each component separately during the experiments and additionally for 10 h after the experiments into buckets. From the collected DEHS-mass a retention coefficient (RET), RET=retained/input, was calculated for each component and the whole test section.
- Type B tests: additional information was obtained by the local droplet size and velocity measurements with standard phase-Doppler anemometer system (PDA) and a laser-Doppler anemometer (LDA).
- The parameters investigated in the experiments were the droplet carrier gas mass flow rate (air) in the range from 50 to 800 kg/h fed to the test-section inlet; and the operational parameters of the spraying nozzle to generate different droplet-size spectra with initial aerodynamic mass median diameters (AMMD) of 20, 30 and 50 µm, respectively, entering the swirl vane unit.

2.2.3. Critical assessment of the data

Facility dimensions of the separator and dryer were fully representative of real ones. However, the gas flow rates imposed were much lower than what expected at high pressures (150 bar) in the primary circuit.

The main observations were:

- The integral retention in the separator and dryer increases with increasing droplet size.
- Higher carrier gas mass flow rates have a lower retention than lower flow rates.
- The retention for carrier gas mass flow rates of 400 kg/h and 800 kg/h nearly coincide (Figure 3).

At the lowest gas flow rate of 10 kg/h, the droplets were retained in the separator-dryer section due to gravitational settling, and with increasing flow rate a larger fraction of droplets were transported through the test section.

However, the droplet transmission through the components gets to an asymptotic behavior at flows higher than 400 kg/m^3. The DF varied from DF = 2 for the smallest droplets of AMMD = 21.5 µm at the highest flow rate of 800 kg/h to DF = 90 for the largest droplets of AMMD = 51.5 µm at the lowest flow rate of 10 kg/h.

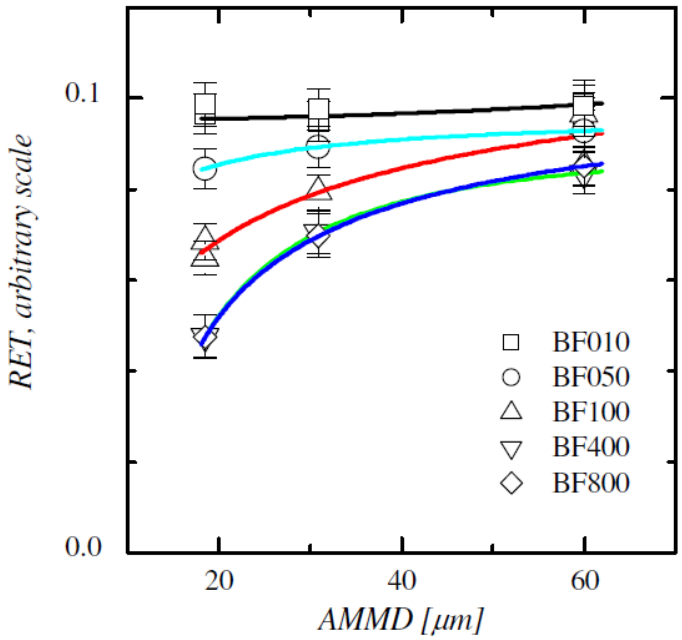

Figure 29. Retention in the separator and dryer as a function of initial AMMD and carrier gas mass flow rate [4].

2.2.4. Major insights

The droplet transport downstream separators and dryers will be dependent on the carrier gas mass flow rate and on the droplet size. This said, the larger the droplet the less sensitive to the flow rate conditions (reported differences smaller than 20%). Besides, given that the flow rates imposed are estimated to be lower than the actual ones, the retention efficiency for the two highest flow rates might be applied to higher ones.

2.3. Iodine Speciation and Partitioning in PWR SGTR Accidents

Back in the 80's of last century, a comprehensive investigation program was launched in the USA on SGTR accidents [5]. The goal set was to find out as much information as possible on two key variables affecting FP transport into the SG secondary side: iodine speciation in the primary system; and, iodine partitioning dependence on pH and oxygen potential.

Two USA PWRs were sampled to know the volatile fraction of radioiodine isotopes present in primary coolant of PWRs**.** Sampling was conducted at full power, during power reduction at the start of an outage, and up to 48 h after shutdown. Those data provided a basis for assessing the effects of operational changes on iodine species dynamics. It was found that a significant fraction of the radioiodine injected into the coolant from the fuel appears to be in the form of elemental iodine (20% near the time of shutdown; higher fractions, 30% - 40%, were found at later times). More information about the measurements and analyses can be found in [5].

The second test program related with the iodine partitioning under simulated conditions of a SGTR accident is analyzed below.

2.4.1. Brief description of the experiments program

The experimental system consisted of a large (152-cm-long, 8.9-cm-diam) stainless steel autoclave, which is heated electrically in three zones along its length and is connected to a separate condenser vessel via an orifice and air-operated valve. A schematic diagram of the system is shown in Figure 4.

Sufficient orthoboric acid to give a concentration of 0.05 to 0.5 M (usually 0.2 M) was dissolved in 1.2 liters of demineralized-distilled water (some tests were carried out with 1.75 or 4.0 liters of feed solution). The I^{131} tracer was diluted and added to the feed solution in the form of "carrier free" NaI^{131} in 0.1 M of NaOH solution to give approximately 1.10^{-6} Ci/ml. This gave a total iodine concentration in each of the experiments of 1.10^{-9} M to 5.10^{-9} M (the primary coolant in PWRs would have iodine concentrations even less than or approximately equal to these ones). After the conditioning of the vessel, the simulated SG was heated to 285 ˚C and 68.94 bar (1000 psig) pressure.

Samples of the vapor and liquid were taken from the vessel. Adsorption of iodine from solution onto the vessel walls was determined by comparing the I^{131} in the liquid samples with that in the feed solution and correcting for the amount in the gas phase. The detailed experimental procedure and the extraction techniques used for iodine speciation were presented in [5].

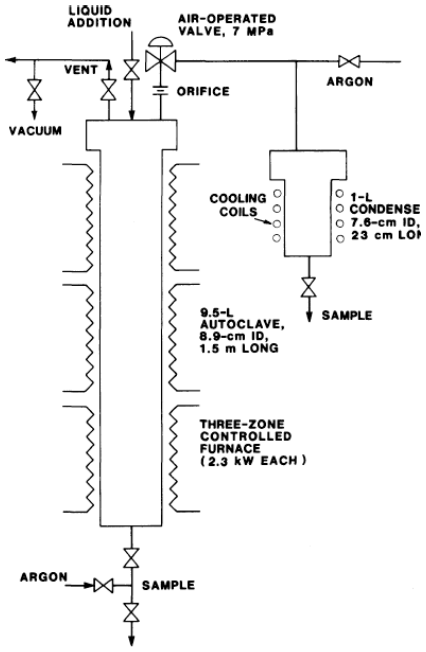

Figure 30. Experimental system for investigating iodine transport from a simulated SG [5].

The PCs were obtained for the tests with a temperature profile such that the top of the pressure vessel near the opening for the steam sample was ≥ 10 °C hotter than the aqueous surface, and there was a smoothly decreasing temperature gradient from the top of the vessel to the aqueous surface. This was done to prevent reflux in the pressure vessel and ensure that the true equilibrium PC was measured [5].

2.4.2. Test matrices

The matrix for the simulated steam generator tests consisted of experiments performed at pH levels of 5, 7, and 9 (measured at 25 ˚C) with an atmosphere of air/steam or argon/steam. In Table 2 the results of the tests in terms of PC and the percentage of iodine in aqueous solution as I_2 and organic iodide are presented.

Atm	pH at 25°C	I_2 in liquid (%)	Organic I in liquid (%)	Partition coefficient, PC
Argon	5	2.04	0.11	6.87E+03
	7	0.44	0.07	5.18E+03
	9	0.02	0.00	4.75E+04
Air	5	22.00	3.95	3.50E+02
	7	1.20	0.15	8.88E+02
	9	0.12	0.01	7.16E+03

Table 15. Summary of results from the SG iodine experiments (285 ˚C, 68.94 bar (1000 psig), 0.2 M borate, 1.10^{-9} M I^-).

2.4.3. Critical assessment of the data

The results show the PC sensitivity to pH, although in all the cases the ratio of aqueous versus gaseous iodine was over 350; i.e., iodine in solution shows little volatility. Specifically, when considering pH in the range of coolant ones (≥ 7), one should expect even less volatility regardless other conditions of the tests.

As for the effect of concentration on PC, the results showed that in aqueous solutions at 285 ˚C and 68.94 bar with concentrations in the range of 10^{-9} M a fraction of I_2 around 2% should be expected. In an SGTR accident if primary and secondary side coolants mix-up more reducing and higher pH conditions should occur, which would result in a fraction even less than such a 2%.

3. Assessment of the FP/aerosol transport models in MELCOR code

3.1. Brief description of the code

MELCOR is a fully integrated, engineering-level computer code whose primary purpose is to model the progression of accidents in light water reactor nuclear power plants. MELCOR is being developed at Sandia National Laboratories for the U.S. Nuclear Regulatory Commission as a second-generation plant risk assessment tool and the successor to the Source Term Code Package. A broad spectrum of severe accident phenomena in both boiling and pressurized water reactors is treated in MELCOR in a unified framework (latest versions are being extended to include phenomena for advanced reactor concepts, like sodium fast reactors, high temperature gas-cooled reactors and others [6]). These include thermal-hydraulic response in the reactor coolant system, reactor cavity, containment, and confinement buildings; core heat up, degradation, and relocation; core-concrete attack; hydrogen production, transport, and combustion; fission product release and transport behaviour. Current uses of MELCOR include estimation of severe accident source terms and their sensitivities and uncertainties in a variety of applications [8].

The MELCOR code consists of an executive driver and a number of major modules, or packages, that together model the major systems of a reactor plant and their coupling. MELCOR modelling makes use of a "control volume" approach in describing the plant system. Reactor-specific geometry is imposed only in modelling the reactor core. Currently, MELCOR often used in uncertainty analyses and sensitivity studies [8].

3.2. Description of the code models for FP/aerosol transport

In MELCOR code the RadioNuclide (RN) package models the behaviour of fission product (FP) aerosols and vapours, from release from fuel and debris to their removal by engineered safety features, going through transport and deposition in the reactor cooling and containment systems. At present, just limited FP chemistry is considered in transport and deposition models (chemistry effects can be simulated in MELCOR just through the class reaction and class transfer models, which are controlled entirely by user-specified parameters).

Rather than tracking all fission product isotopes, the masses of all the isotopes of an element are modelled as a sum; that is, the total element mass, not its individual isotopes, is modelled. Furthermore, elements are combined into material classes, groups of elements with similar chemical behaviour. Fifteen material classes are typically used, thirteen containing fission products, plus water, and concrete oxides. Combination of classes to form new classes upon release, such as Cs + I to CsI, is permitted. The decay heat power per unit initial mass for each class is determined by the Decay Heat (DCH) package based on the class compositions (see Table 3) [8].

Class Name	Representative	Member Elements
1. Noble Gases	Xe	He, Ne, Ar, Kr, Xe, Rn, H, N
2. Alkali Metals	Cs	Li, Na, K, Rb, Cs, Fr, Cu
3. Alkaline Earths	Ba	Be, Mg, Ca, Sr, Ba, Ra, Es, Fm
4. Halogens	I	F, Cl, Br, I, At
5. Chalcogens	Te	O, S, Se, Te, Po
6. Platinoids	Ru	Ru, Rh, Pd, Re, Os, Ir, Pt, Au, Ni
7. Early Transition Elements	Mo	V, Cr, Fe, Co, Mn, Nb, Mo, Tc, Ta, W
8. Tetravalent	Ce	Ti, Zr, Hf, Ce, Th, Pa, Np, Pu, C
9. Trivalents	La	Al, Sc, Y, La, Ac, Pr, Nd, Pm, Sm, Eu, Gd, Tb, Dy, Ho, Er, Tm, Yb, Lu, Am, Cm, Bk, Cf
10. Uranium	U	U
11. More Volatile Main Group	Cd	Cd, Hg, Zn, As, Sb, Pb, Tl, Bi
12. Less Volatile Main Group	Ag	Ga, Ge, In, Sn, Ag
13. Boron	B	B, Si, P
14. Water	H_2O	H_2O
15. Concrete	- -	- -
16. Cesium Iodide	CsI	Classes 2 and 4
17. Cesium Molybdate	CsM	Classed 2 and 7

Table 16. RN Class composition [8].

The calculation of aerosol agglomeration and deposition processes is based on the MAEROS, a multisection, multicomponent aerosol dynamics code that evaluates the size distribution of each type of aerosol mass, or component, as a function of time. This size distribution is described by mass in each size bin or section. Aerosols can deposit directly on surfaces such as heat structures and water pools, or can agglomerate and eventually fall out once they exceed the largest size specified by the user for the aerosol size distribution. Some volatile FP species may revaporize from deposits if the necessary conditions prevail; resuspension can be also modelled, if activated [8].

The condensation and evaporation of FP vapours on pool surfaces, heat structure surfaces and aerosols are evaluated by the rate equations from the TRAP-MELT2 code. The fission product vapour masses in the control volume atmosphere and condensed on the aerosol and heat structure surfaces are determined by rate equations based on the surface areas, mass transfer coefficients, atmosphere concentration, and the saturation concentrations corresponding to the temperatures of the surfaces. Although fission products may condense on pool surfaces, evaporation of fission products residing in control volume pools is not permitted. The fission product vapour location within a phase in a control volume (pool or atmosphere) may change when one phase is no longer present. Any vapour mass associated with a disappearing phase is added to the remaining phase in that control volume [8].

The modeling of the thermal-hydraulic behavior of liquid water, water vapor, and gases in MELCOR is performed by Control Volume Hydrodynamics (CVH) and Flow Path (FL) packages. The control volumes are connected by flow paths through which the hydrodynamic materials may move driven by a separate momentum equation for each field. Most intravolume processes involving radionuclides are calculated first in the RN package, including fission product release, aerosol agglomeration and deposition, fission product condensation and evaporation, distribution of decay heat, and chemical interactions. The effects of these processes are included in the hydrodynamic transport and thermodynamic calculations performed in the CVH package, executed subsequently.

When superheated liquid water enters a control volume at an elevation above the pool surface, some fraction of it will flash to vapor. Another fraction will be dispersed as liquid droplets that are small enough to remain suspended in the atmosphere for a significant time. An optional model is available for flow paths to capture some of these effects. If the water is superheated at the pressure of the receiving volume, the model accounts for stagnation and equilibration at that pressure. Although the model does not explicitly account for heat transfer, at least part of the effect will be captured when the partitioned water vapor, fog, and pool liquid are equilibrated with the previous contents or the volume. The partition between liquid and vapor is calculated from the average enthalpy, and a fraction of the liquid is assigned to the “fog” field. By default, this is taken as the fraction of a Rosin-Rammler distribution that lies below a maximum diameter. If the RN1 package is active, the cut-off diameter is taken as the maximum aerosol size treated by MAEROS, if not active the maximum size is defined by a sensitivity coefficient with the same default value of 50 μm. The user may define the fraction through a sensitivity coefficient. If the MELCOR RN package is active, water droplets in the atmosphere are considered to behave as aerosols [8].

Aerosol and iodine vapour are removed by pool scrubbing. The pool scrubbing model is based on the SPARC-90 code.

Chemistry effects can be simulated in MELCOR through the use of class reactions and class transfers. The class reaction process uses a first-order reaction equation with forward and reverse paths. The class transfer process, which can change the material class or location of a radionuclide mass, can be used to simulate fast chemical reactions. With these two processes, phenomena including adsorption, chemisorption, and chemical reactions can be simulated. Only FP vapours are considered in the chemistry models [8].

A specific model is included in the RN package to model the chemistry of iodine in reactor containments under accident conditions. The model involves four areas of modeling: the transport of iodine species among the walls, the bulk gas, and the pool; the radiolytic formation of acids and the gas-phase destruction and formation of iodine species in the containment atmosphere; the hydrogen ion concentration (i.e., pH), and accounts for the effects of the acids and bases introduced into the pool as well as the removal of iodine due to silver and the aqueous iodine chemistry model where the iodine, hydrogen, oxygen, carbon, iron, and electron balance equations are solved. A detailed description of the models is presented in [8].

3.3. Critical assessment of models applicability

The aqueous chemistry model was designed for volumes where the pressure is less than 10 atm and the liquid temperature is less than 423 K, corresponding to conditions in a commercial reactor containment. If these limits are exceeded, the pool model may become invalid. Thus, the iodine models available in MELCOR could not be applied under the secondary side conditions of a SGTR sequence.

4. Description of the model enhancements

4.1. New considerations in the modelling of the iodine transport

The main radiological concern in the SGTR type sequences is due to the release of the radioactive iodine as a result of the opening of a safety or relief valve on the affected steam generator.

Three distinct mechanisms are considered for transport of the iodine to the environment [13]:

Primary flashing mechanism: as the break flow passes from the high temperature and pressure of the RCS to the lower temperature and pressure of the secondary system, a fraction of the water flashes to steam. The iodine associated with the flashing fraction passes, unmixed with the secondary coolant, to the steam space and is transported through the common steam path to the environment.

Primary bypass mechanism (atomization): small droplets of RCS coolant become entrained with the flashing RCS coolant and pass with the flashing fraction, unmixed with the secondary coolant, out of the steam generator and to the environment.

Partitioning mechanism: most of the RCS break flow (and corresponding iodine) is mixed with the secondary system coolant. As the water continues to boil, because of heat input from the RCS, the iodine partitions between liquid and vapor states and is transported, with the steam, out of the steam generator and ultimately to the environment. This mechanism is characterized by the partition coefficient.

Figure 5 illustrates the mechanisms involved in the modelling of the iodine mass transfer during an SGTR.

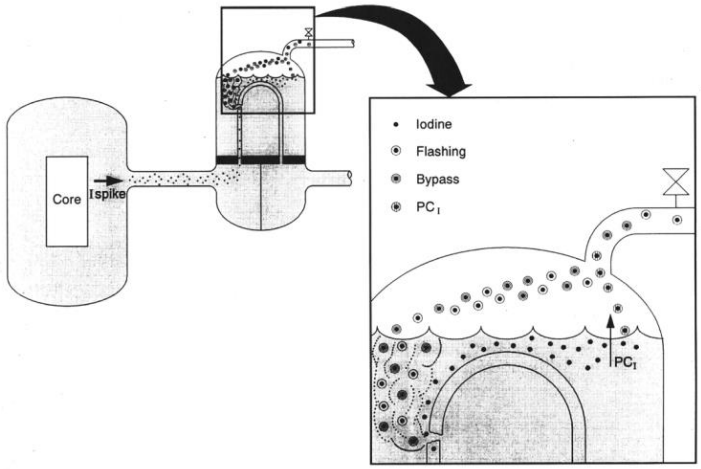

Figure 31. Model for iodine mass transfer during and SGTR [13].

To consider the above mechanisms in the transport and behavior of the iodine during SGTR sequences in DBA and DEC-A conditions a model, based on the MELCOR flashing model, was implemented using external control functions.

4.2. Iodine transport modelling in MELCOR.

If superheated liquid water enters a control volume at an elevation above the pool surface, some fraction of it flashes to vapor. Another fraction is dispersed as liquid droplets that are small enough to remain suspended in the atmosphere for a significant time. This effect is captured by the MELCOR flashing model. If the water is superheated at the pressure of the receiving volume, the model accounts for stagnation and equilibration at that pressure. Although the model does not explicitly account for heat transfer, at least part of the effect is captured

when the partitioned water vapor, fog, and pool liquid are equilibrated with the previous contents or the volume [7,8].

The partition between liquid and vapor is calculated from the average enthalpy, and a fraction of the liquid is assigned to the "fog" field. By default, this is taken as the fraction of a Rosin-Rammler distribution that lies below a maximum diameter. If the Radionuclide package (RN1) is active, the cut-off diameter is taken as the maximum aerosol size treated with a default value of 50 μm. The user may also specify the fraction directly through a sensitivity coefficient [7,8].

The flashing model is selected in the flow path package (FL) and the process is modelled as a transformation that takes place "within" a flow path. The transformed flow, in general, contains both liquid water and water vapor. The vapor is added to the atmosphere, and some portion of the liquid is retained in the atmosphere as fog. The details of the model are controlled in MELCOR by sensitivity coefficient.

Figure 6 shows a schematic representation of the model to describe the transport of iodine released from the RCS to the secondary part of the SG and to the environment.

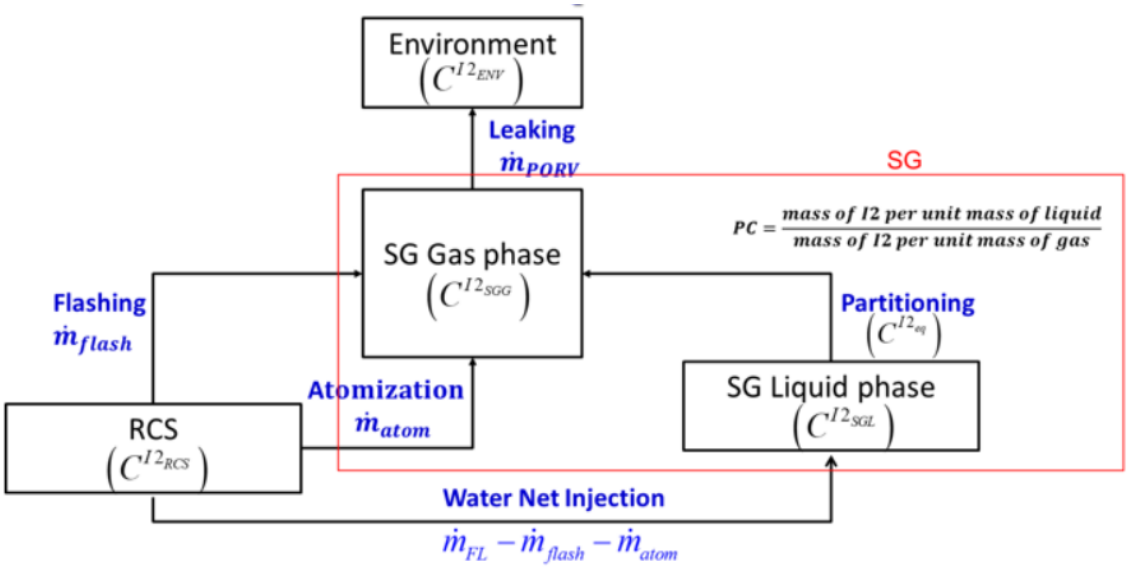

Figure 32. Schematic representation of the iodine transport model.

Considering the application of the flashing and fog formation model in the case of pool entering a volume through a flow path, the calculation of the contribution of the three mechanisms explained above is implemented with the use of MELCOR control functions (CF) as follows:

Flashing

The iodine mass flow rate due flashing is calculated as the multiplication of the mass flow rate of vapor through the flow path that model the tube rupture by the concentration of iodine in the RCS (concentration in the control volume from which the liquid fluid comes):

$$\dot{m}_{I2}\ \left(\frac{kg}{s}\right) = \dot{m}_{breakSteam} * C_{I2}^{RCS} \quad (1)$$

where:

$\dot{m}_{breakSteam}$: mass flow rate of vapor throughout the flow path that model the steam generator tube rupture (MELCOR variable "FL-MFLOW-TR (sgtr-c, H2O-VAP)"

C_{I2}^{RCS} (kgI_2/kgwater): iodine concentration in RCS.

Atomization

Similarly, the iodine mass flow rate due atomization is calculated as the multiplication of the mass flow rate of "fog" through the flow path that model the tube rupture ($\dot{m}_{breakFog}$) by the concentration of iodine in the RCS (in equation (1) the value $\dot{m}_{breakSteam}$ is substituted by $\dot{m}_{breakFog}$).

Partitioning

The partitioning is defined as a rate of mass concentration of iodine in the liquid and the mass concentration of iodine in the gas. That's mean, knowing the partitioning coefficient (PC) and the mass concentration of iodine in the liquid we can calculate the concentration of iodine in the gas phase:

$$PC = \frac{mass\ of\ I2\ per\ unit\ mass\ of\ liquid}{mass\ of\ I2\ per\ unit\ mass\ of\ gas} \quad (2)$$

In this case, the mass of iodine in the pool calculated by MELCOR is corrected considering the flashing and atomization contributions. This correction needs to be made as the MELCOR I2 (class 4) is retained in the SG pool due no applicability of the MELCOR iodine model in the SGTR conditions. The concentration of iodine in the SG pool is calculated as the rate between the mass of iodine in the pool and the mass of liquid and then is calculated the concentration of iodine in the SG atmosphere considering the PC = 100 (NRC recommended value established in [14]).

The total iodine released to the environment is calculated knowing the mass of the steam released throughout the SG relief valve and the total concentration of iodine in the atmosphere of the SG (considering the flashing, atomization and partitioning contributions).

It is important to point out that the model, with minor modifications is also applied in the sequences where the first release is through the breaking steam line (e.g. DEC-A SGTR sequences).

A sensitivity analysis of the MELCOR modelling of the water drops size in the flashing model has been conducted for the SGTR DBA sequence with a double-ended break located in the apex of the longest U-tube of one of the three SGs. In this scenario, the radioactivity release is maximised as the break remains uncovered for a longer period of time with respect to the lower part of the U-tubes. As shown in Figure 7, the droplet size affects drastically the relative importance of each phenomenon. If a droplet size between 35 and 50 μm is assumed, atomization became in the main mechanism of iodine release as is expected in this kind of sequences.

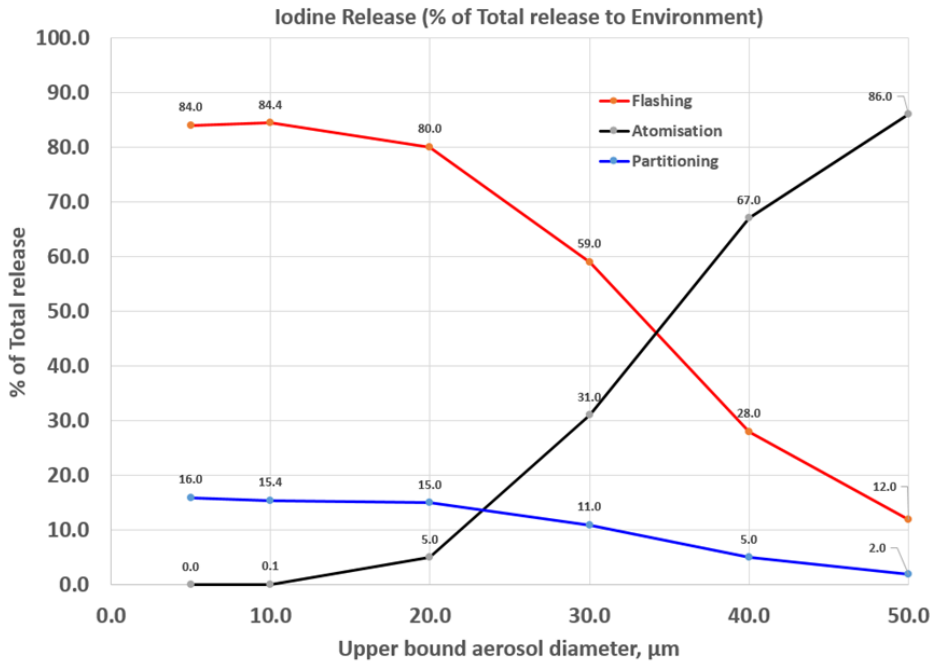

Figure 33. Impact of the droplet sizes on the total released activity to the environment.

5. Conclusions and remarks

An assessment of the experimental data that could be applicable to the transport processes that are postulated to dominate FP transport in the primary circuit and transfer to the secondary one during SGTR sequences, has been performed. Particular attention has been paid to the representativeness of the initial and boundary conditions, the reliability of the experimental techniques used and the experimental protocol adopted. The analyzed data could be of interest for the validation of code models.

At the same time, the implemented FP transport models in MELCOR have been examined paying more attention to the models concerning the iodine transport and chemistry. Taking into account the non-application of this model for the conditions of the secondary side during SGTR sequences, a model approach based on the MELCOR flashing model have been implemented in MELCOR to consider the mechanism involved in the release and transport of iodine from fuel to the environment. From the results of the modeled sequence presented above and the sensitivity analysis, it can be concluded that the droplet size affects drastically the relative importance of each released mechanisms.

References

10. Zoltán Hózer, et.al: Report on SGTR and LOCA available experimental data. T2.1.3. Review of experimental database, R2CA project, August, 2020.

11. F. Funke, G. Langrock, S. Gupta, B. von Laufenberg, E. Schmidt, M. Freitag, A. Kühnel: Iodine release from a flashing jet. (Test ID: Iod-29) Technical Report. OECD NEA THAI-2 Project, June 2014.

12. T. Lind, A. Dehbi, S. Guentay: Aerosol retention in the flooded steam generator bundle during SGTR, Nucl. Eng. Des. 241, 357-365, 2011.

13. R. Kapulla, S. Danner, S. Guentay: Droplet retention and velocity field in a steam generator. Proceedings of the 2008 Annual Meeting of the American Nuclear Society in Anaheim, CA, American Nuclear Society, La Grange Park, IL, 2008.

14. E. C. Beahm, S. R. Daish, J. Hopenfeld, W. E. Shockley, P. Voilleque. Iodine speciation and partitioning in PWR Steam Generator Accidents, NUREG/CR-5365, October 1989.

15. MELCOR Code Change History: Revision 14959 to 18019 SAND2020-14302, October 2020.

16. MELCOR Computer Code Manuals Vol. 1: Primer and Users' Guide Version 2.2.14959, SAND2019-12536 O, October 2019.

17. MELCOR Computer Code Manuals Vol. 2: Reference Manual Version 2.2.14959, SAND2019-12537 O, October 2019.

18. MELCOR Computer Code Manuals Vol. 3: MELCOR Assessment Problems Version 2.1.7347 2015, SAND2015-6693 R, August 2015.

19. D. A. Powers, J. L. Sprung, and C. D. Leigh, Fission Product Behavior During Severe LWR Accidents: Recommendations for the MELCOR Code System, Sandia National Laboratories, SAND2020-1030 (Unpublished January 2020).

20. M. R. Kuhlman, D. J. Lehmicke, and R. O. Meyer, CORSOR User's Manual, BMI-2122, NUREG/CR-4173 (March 1985).

21. MELCOR Best Practices as Applied in the State-of-the-Art Reactor Consequence Analyses (SOARCA) Project, NUREG/CR-7008, August 2014.

22. James P. Adams. Iodine release during a steam generator tube rupture. Nuclear Technology, August 1994.

23. U.S. Nuclear Regulatory Commission, Office of Nuclear Research, Regulatory Guide 1.183, Alternative Radiological Source Terms for Evaluating Design Basis Accidents at Nuclear Power Reactors, July 2000.

Appendix F- SSTC NRS Report

Contents

Abbreviations

BRU-A	Steam Dump Valve to Atmosphere
DG	Diesel Generator
ECCS	Emergency Core Cooling System
ENV	Environment
FP	Fission Product
FW	Feed Water
HA	Hydroaccumulator
HPSI	High Pressure Safety Injection
IE	Initiating Event
LPSI	Low Pressure Safety Injection
MSIV	Main Steam Isolation Valve
RCS	Reactor Coolant System
SG	Steam Generator
SV	Safety Valve
SGTR	Steam Generator Tube Rupture
SI	Safety Injection
SSTC NRS	State Scientific Technical Centre on Nuclear and Radiation Safety
TH	Thermalhydraulic

1. Modelling approach

1.2. General remarks

This report estimates the activity release in SGTR event accounting for the RCS coolant dilution (by ECCS water) in the primary and secondary side. As the basic analysis for the comparison the DBA case from T2.3 task is taken. The estimation of the dilution is performed by the same TH model for RELAP5 code that is used for T2.3 task. The estimation of the release is performed by external calculations as it is described later in the report.

1.3. Modelling approach

The following text describes the modelling approach to the RCS coolant dilution and FP transport analysis.

In such calculations it was assumed the activity is transported with primary coolant and total activity in the RCS coolant water is A=1. The activity is distributed uniformly in liquid phase of the reactor coolant over all RCScomponents, including pressurizer. Initial RCS water mass is M_{ini}=250t. During the break from RCS to the secondary side of SG-1 the part of the activity transits from the liquid phase to the vapour with transfer coefficient K_g. The activity that remains in the liquid phase is calculated as K_f=1-K_g.

The overall approach to activity transport is based on tracing the RCS activity dimensionless concentration with application of RELAP5 code boron tracing model with boron playing the role of the tracer. This allows to account for the dilution of radioactive coolant content by injected non-radioactive ECCS water (with tracer concentration of 0) and mixing in RCS and SG secondary side.

The following figure presents the simplified layout of the RELAP5 RCS to SG-1 break model and specifies the points of tracing the activity content concentration.

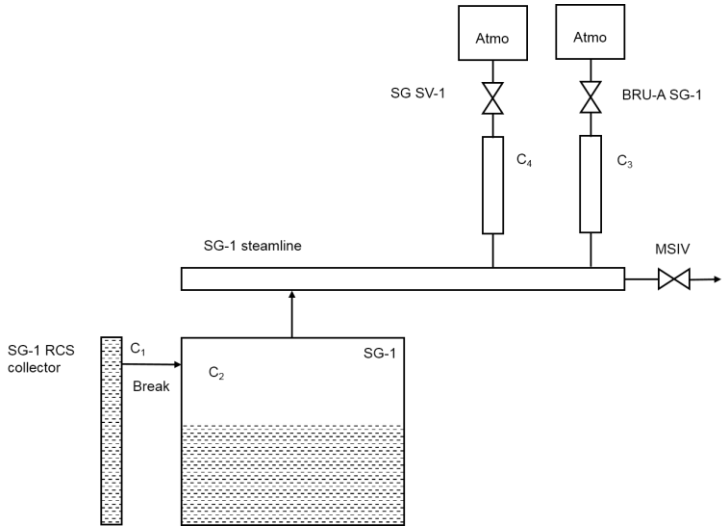

Figure 1-1. SGTR break simplified nodalization with target points for the analysis.

The RELAP5 code simulates boron propagation in liquid phase only, and dimensionless concentrations (in mass parts of tracer per mass part of liquid phase) are obtained as follows:

- C_1 concentration of tracer in the control volume upstream the break, initial concentration is 1;
- C_2 –concentration of tracer in the liquid phase of SG control volume downstream the break, initial concentration is equal to 0;
- C_3 –concentration of tracer in the liquid phase of the SG steam line control volume upstream the steam dump valve to atmosphere (BRU-A), initial concentration is equal to 0;
- C_4 – concentration of tracer in the liquid phase of the SG steam line control volume upstream SG safety relief valve SV-1, initial concentration is equal to 0.

It is assumed that in the gas phase the activity concentration is uniformly distributed in SG free volume V_{free}, thus the volumetric concentration in SG free volume can be calculated as

$$C_{atm}(t) = \frac{A_{atm}(t)}{V_{free}(t)},$$

where $A_{atm}(t)$ is the activity content in SG steam volume.
Total activity transported from RCS to SG-1 via the break is

$$A_{tot}(t) = \frac{1}{M_{ini}} \int_0^t G_1(t) C_1(t) dt,$$

where $G_1(t)$ is the mass flowrate of the break (kg/s).

The balance of the activity in the SG atmosphere can be formulated in terms of incoming activity and activity release through the steam dump valves (BRU-A) and SG SV:

$$\frac{dA_{atm}(t)}{dt} = K_g \frac{G_1(t)}{M_{ini}} C_1(t) - \sum_{j=3}^{4} C_{atm}(t) v_j \cdot void_j \cdot \frac{\rho_j}{\rho_{sg}} S_j,$$

where

v_j –the gas velocity at BRU-A (j=3) or SG SV (j=4) junction;
$void_j$ - the gas void fraction at BRU-A (j=3) or SG SV (j=4) junction;
ρ_j –the gas density at the BRU-A (j=3) or SG SV (j=4) junction;
ρ_{sg} –the gas density in the SG steam volume (kg/m^3);
S_j –flow area of BRU-A (j=3) or SG SV (j=4) junction.

The equation for $A_{atm}(t)$ is solved at each timestep of RELAP calculation by first order integration that gives the $A_{atm}(t)$ value at every given time of the accident.

After that the total release of activity to environment with gas and liquid phases can be calculated using the formulas below. In calculation the integration is performed via control variables.

$$A_{env\_atm}(t) = \int_0^t \sum_{j=3}^{4} C_{atm}(t) \cdot v_j \cdot void_j \frac{\rho_j}{\rho_{sg}} S_j \, dt + \frac{K_g^*}{M_{ini}} \sum_{j=3}^{4} \int_0^t G_j(t) C_j(t) dt,$$

where $C_3(t)$ and $C_4(t)$ are the tracer concentrations of activity in the liquid phase upstream the steam dump and relief valves;

K^*_g –the gas transfer coefficient, is equal to K_g after the free SG volume becomes 0, and equal to 0 prior that time. Thus, the second term is not equal to 0 when the SG is completely filled. This allows to account the release of gas activity to environment even after SG is totally filled and the vapour phase is no longer discharg. Before that time point the gas activity is released only with gas phase at steam dump junction.

Release with the liquid phase:

$$A_{env\_liq}(t) = \frac{K_f}{M_{ini}} \int_0^t \sum_{j=3}^{4} C_j(t) \cdot vf_j \cdot voidf_j \cdot \rho f_j \cdot S_j \, dt,$$

where

vf_j –the liquid velocity at BRU-A (j=3) or SG SV (j=4) junction;
$voidf_j$ - the liquid volumetric fraction at BRU-A (j=3) or SG SV (j=4) junction;
ρf_j –the liquid density at the BRU-A (j=3) or SG SV (j=4) junction (kg/m^3).

Total activity released to environment in both gas and liquid phases is

$$A_{tot\_env}(t) = A_{env\_atm}(t) + A_{env\_liq}(t).$$

As a reference initial activity of RCS coolant the steady state activity plus DBA iodine spike values are used.

2. Results and discussion

2.1 Steady-state calculation results

The analysis uses the same initial conditions for the model as for T2.3 report. The model is initiated at steady state with shifted power 104%. The initial conditions are presented in the following table.

Table 2-1. RELAP model steady state values for SGTR DBA case

#	Description	Units	RELAP model steady state
1	Reactor thermal power	MWt (%)	3120 (104)
2	Reactor flow	m^3/h	80000
3	Reactor outlet pressure	Kgf/cm^2	157.0
4	Reactor inlet temperature	°C	290.1
5	Reactor outlet temperature	°C	323.0
6	Pressurizer water level	m	9.0
7	Pressure in SG	Kgf/cm^2	63.1-63.2
9	Steam flow from SG	Kg/s	425-426
10	Feedwater temperature	°C	225
11	SG water level (collapsed)	m	2.25
12	HA water temperature	°C	55.0
13	HPSI tanks water temperature	°C	55.0
14	SI water temperature from the sump	°C	70.0

2.2. SGTR event results

The TH behaviour of the accident follows the previous calculations for T2.3 report. The general information and the unit data are also provided in T2.3 report. The information on analysis results is provided in this section with additional figures and explanations. RELAP5 Mod 3.2 is used for the simulations.

The provided results in this section correspond to gas transfer coefficient K_g=0.01 that is close to the iodine transfer from liquid phase to the gas phase. The calculation is repeated for several K_g values from 0 to 1.

2.2.1. IE and Boundary conditions

As the initiating event the SG-1 cold collector cover lift-up is assumed. This results in the primary to secondary circuit break of 100 mm diameter.

Following system failures/assumptions are considered in the analysis:

- Loss of normal power supply is assumed at 0 s;
- DG-3 is failed to start thus leaving 2/3 HPSI and 2/3 LPSI available for the safety injection;
- All 4 HAs are available.

Following operator actions/assumptions are considered:

- 15 min after SCRAM operator closes BRU-A on SG-1 and terminates all FW supply to SG-1;
- 30 min after IE the operator stops all HPSIs;
- 30 min after IE the operator closes MSIV at SG-1 steam line;
- 30 min after IE the operator closes MSIVs at SG-2,3,4 steam lines and starts cooldown via intact SGs with 60°C/h rate until pressure of 35 kgf/cm^2 is reached;
- No additional SG feeding is assumed.

2.2.2. TH model specific changes

According to the approach the tracing of the RCS activity dilution and transport is modelled via RELAP5 boron tracking model. By this the RELAP5 model is initiated with boron “tracer” concentration equal to 1g/kg at each RCS control volume with liquid. It is assumed that ECCS coolant activity is equal to 0 thus tracer concentration is set to 0 g/kg. By this the mixing and transport of the RCS coolant activity is automatically calculated by RELAP5. SG secondary model is quasy-3D and can simulate the mixing of coolant. Other model features correspond to T2.3 report values and DBA approach.

The reactivity effect of the boron is corrected to avoid the re-criticality in the scenario.

2.2.3. Fuel mechanic analysis model

No fuel mechanical analysis is performed in this analysis. The fuel pins overheating is not expected.

2.2.4. Main events

The SG-1 cold collector cover lift-up which initiates primary to secondary circuit break of Dn100 mm is analysed (DBA case).

Table 2-2. Event table

Time, s	Description	Comment
0	SG-1 cold collector cover lift-up	Primary to secondary break initiated
0	Loss of power, reactor shutdown, stop of FW, RCPs runout start	
0	DG-3 failure to start	Scenario assumption, leads to failure of spray, HPSI-3, LPSI-3
2	BRU-A of SG-1-4 are open	SG pressure >73 kgf/cm^2
2	SG-1-4 control SVs are open	SG pressure >84 kgf/cm^2
32	Loop subcooling less than 10°C	SI signal
40	HPSI-1,2 injection start (TQ13,23 trains)	With transport delay
350	SG-1 level is 4m	SG-1 is completely filled
900	BRU-A SG-1 is closed FW to SG-1 is closed	Operator action
1350	SG-1 control SVs start to open periodically	SG pressure >84 kgf/cm^2
1800	HPSI injection stop	Operator action
1800	SG-1 MSIV is closed	Operator action
1800	SG-2,3,4 MSIVs are closed	Operator action
1800	SG-2,3,4 cooldown via BRU-As is initiated with rate 60°C/h	Operator action, SG target pressure is 35kgf/cm^2
2500	Last SG-1 SV cycle to decrease pressure	Primary pressure is equalized with SG-1 pressure with no tendency to increase Break flow is “0”
4500	SG-2,3,4 pressure equal to 35kgf/cm^2	Target pressure for intact SGs achieved
10000	End of calculation	

2.2.5. Thermal-hydraulic analysis

SG-1 cold collector cover lift-up break results in a leak from the primary circuit to SG-1 with equivalent break diameter of 100 mm. The break mass flow rate at the very beginning of the accident reaches its maximum value. Loss of coolant causes sharp decrease in primary pressure and coolant boiling in the reactor core.

The loss of offsite power is postulated at the beginning of IE and leads to DG startup. After closure of turbine steam supply the steam dump to atmosphere valves BRU-As open at 2 s on all SGs. SI signal is activated by loop subcooling less than 10°C at 35 s followed by HPSI-1,2 trains injection.

Because of the leak to SG-1 it’s secondary side is completely filled by 350s and water release to environment begins. At 900s by operator actions the BRU-A-1 is closed and afterwards the release occurs through the SG-1 SV periodical operation.

At 1800 s the HPSI is fully stopped by operator, all MSIVs are closed and cooling of RCS through SG-2,3,4 is initiated to the target SG pressure of 35 kgf/cm^2. By 2500 s the last opening cycle of SG-1 SV occurs, and the break flow decreases to 0. From that time the break is isolated.

The maximum value of fuel cladding temperature of 351 °C is reached at the beginning of the IE. No challenge to cladding cooling is foreseen in the transient. The simulation is stopped at 10000 s when all the RCS and SG parameters are stabilized.

The plots of the calculation results are provided below according to following list:

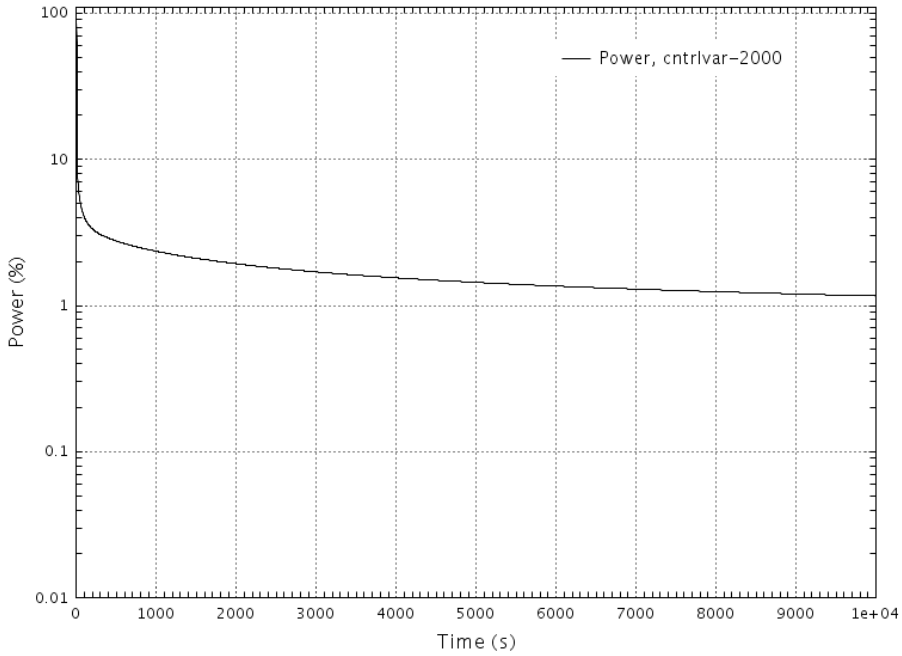

Figure 2-1 Reactor power.

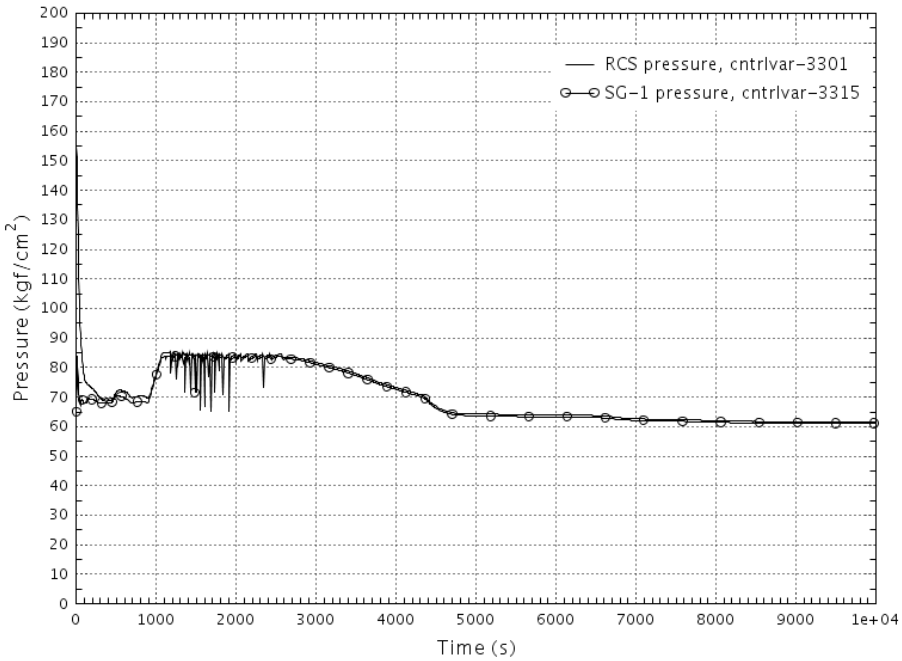

Figure 2-2 Primary and affected SG pressure.

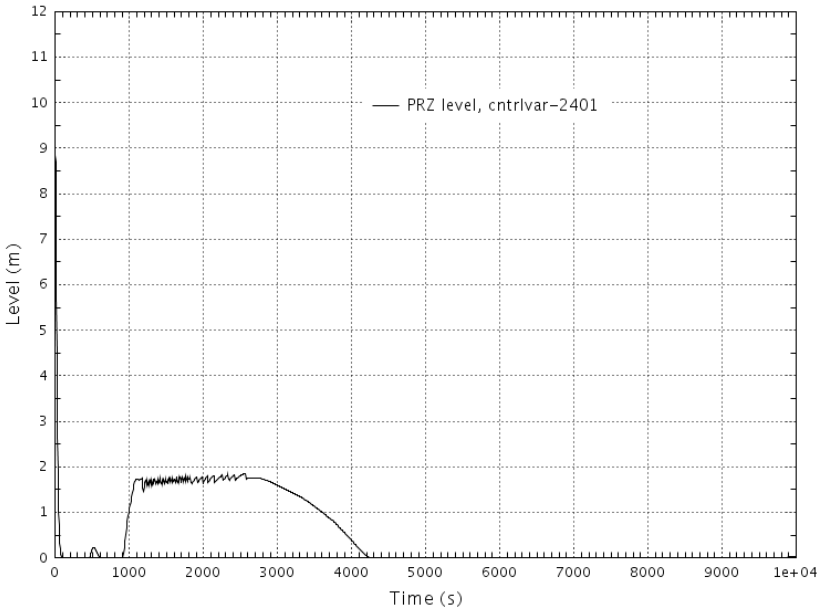

Figure 2-3 Pressurizer level.

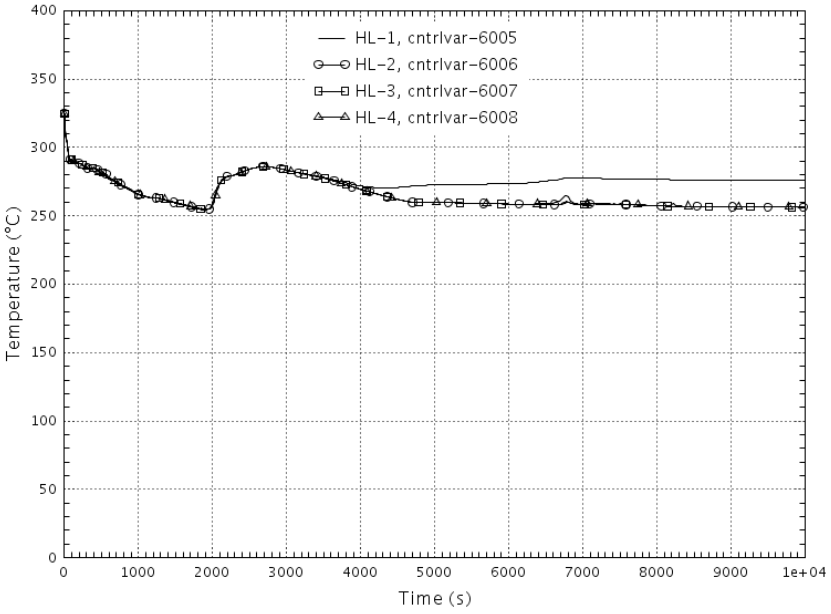

Figure 2-4 Hot leg temperatures.

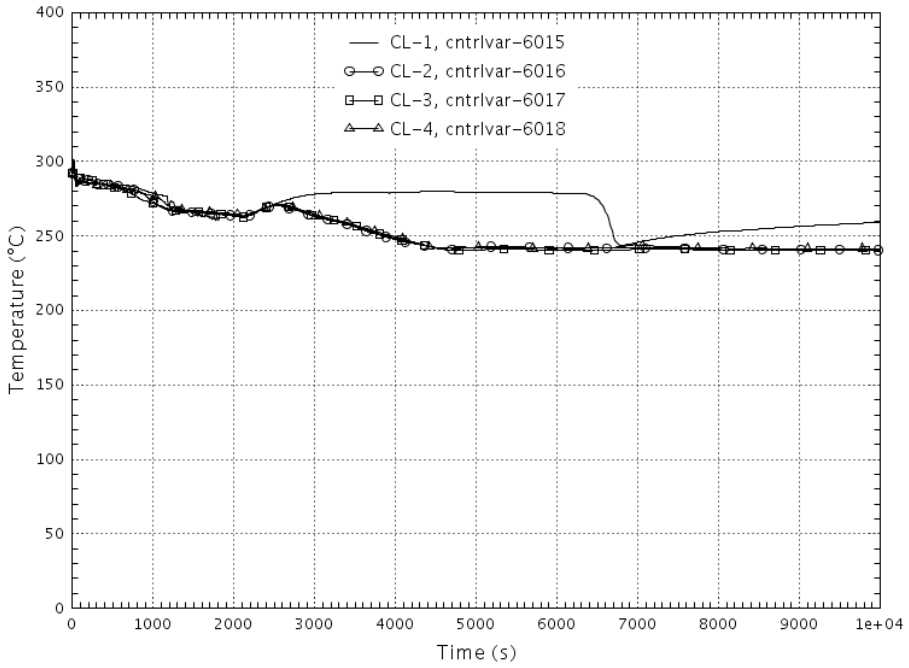

Figure 2-5 Cold leg temperatures.

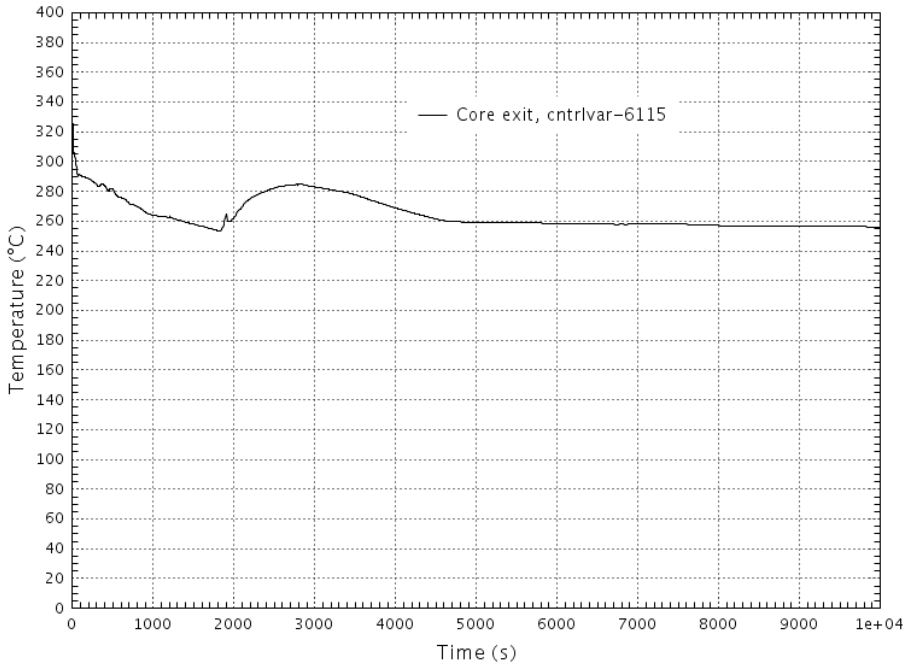

Figure 2-6 Core exit temperature.

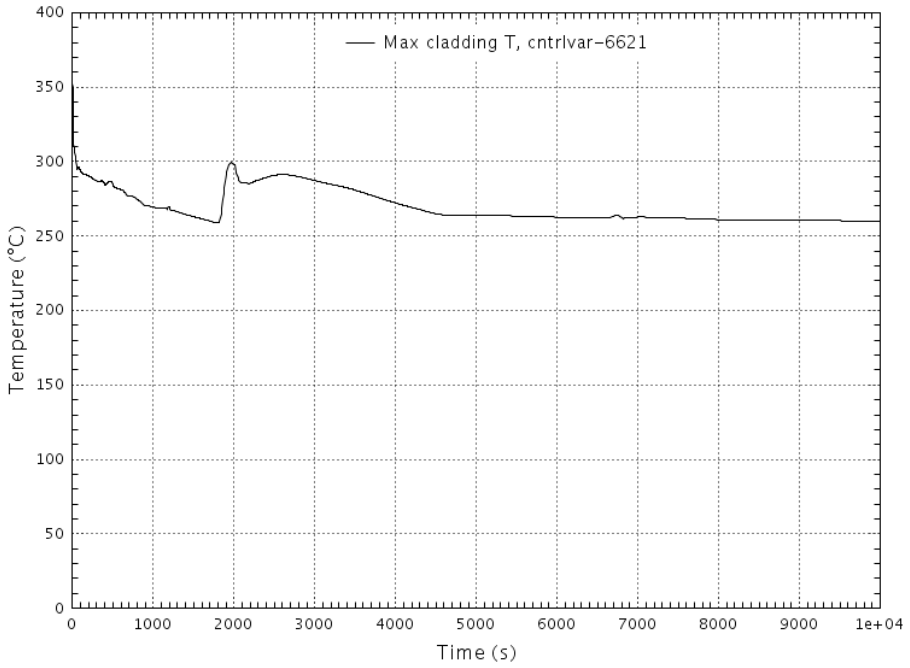

Figure 2-7 Maximal cladding temperature.

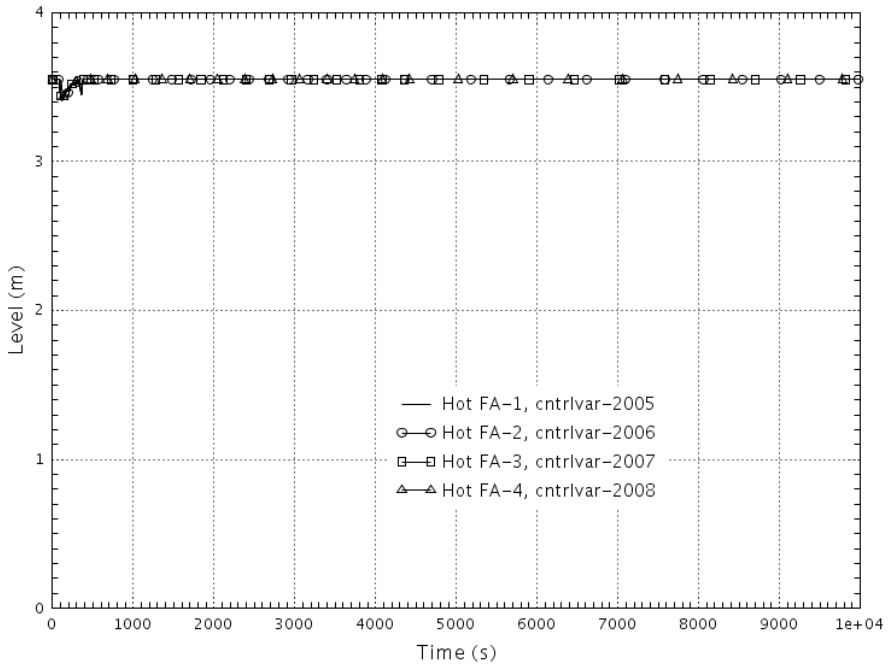

Figure 2-8 Core collapsed level.

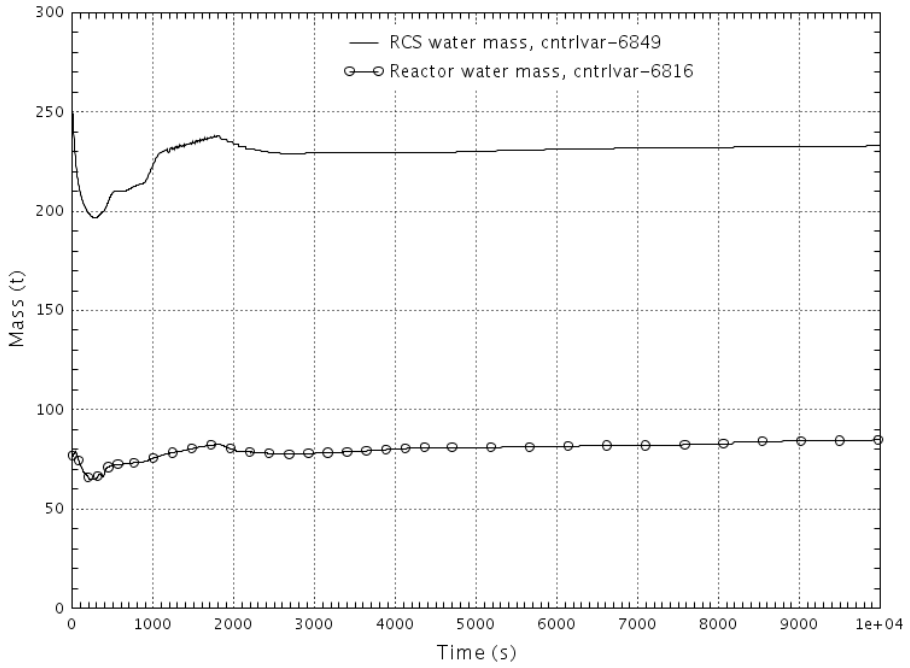

Figure 2-9 RCS and reactor coolant mass.

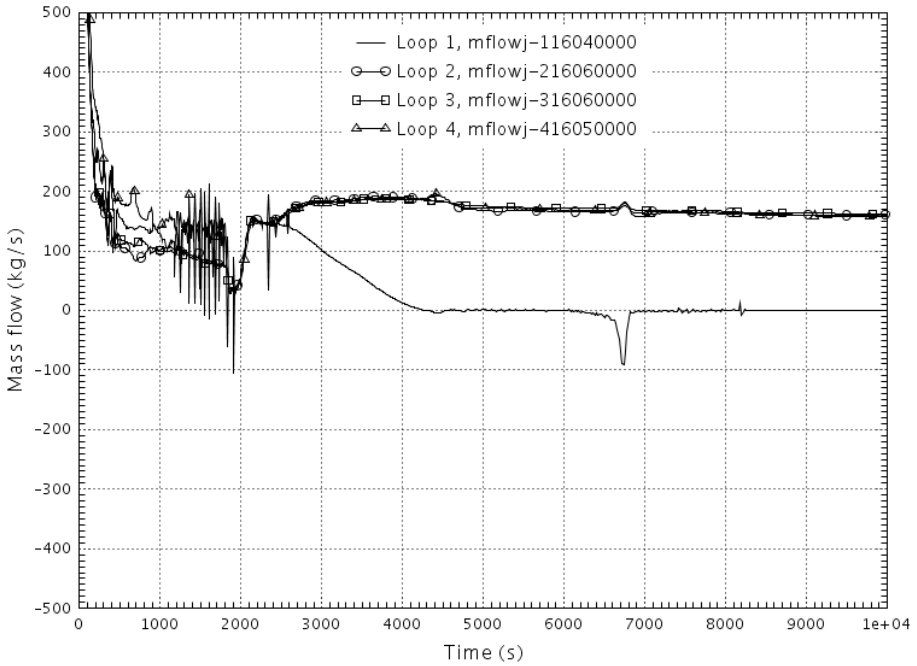

Figure 2-10 Loops flow.

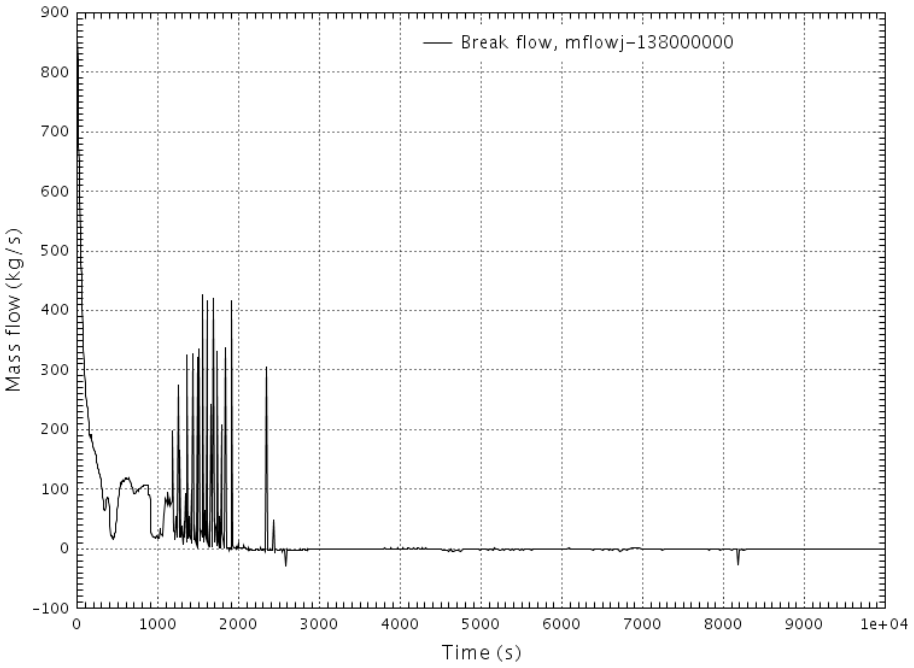

Figure 2-11 Break mass flow.

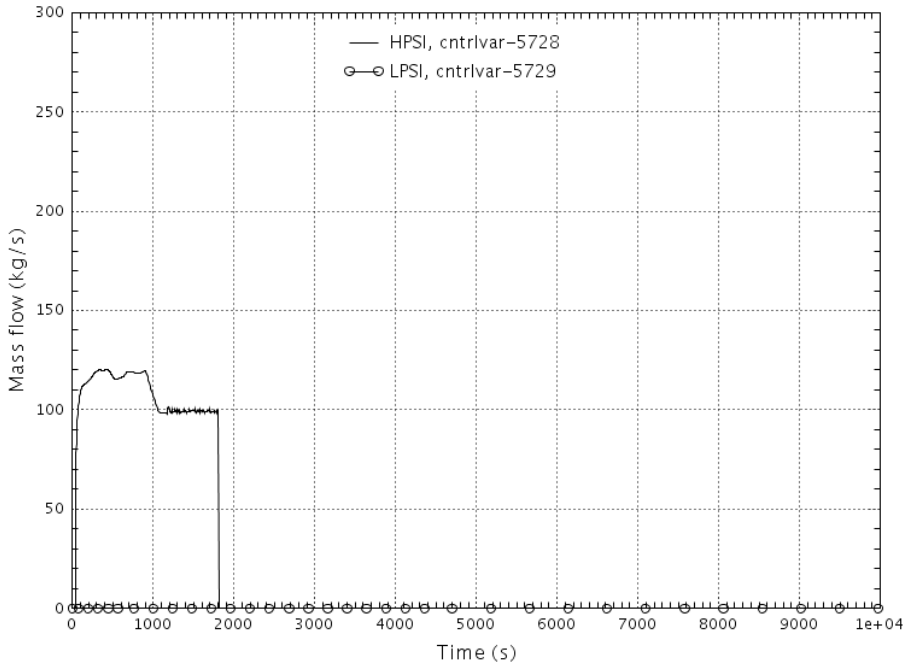

Figure 2-12 HPSI and LPSI flow.

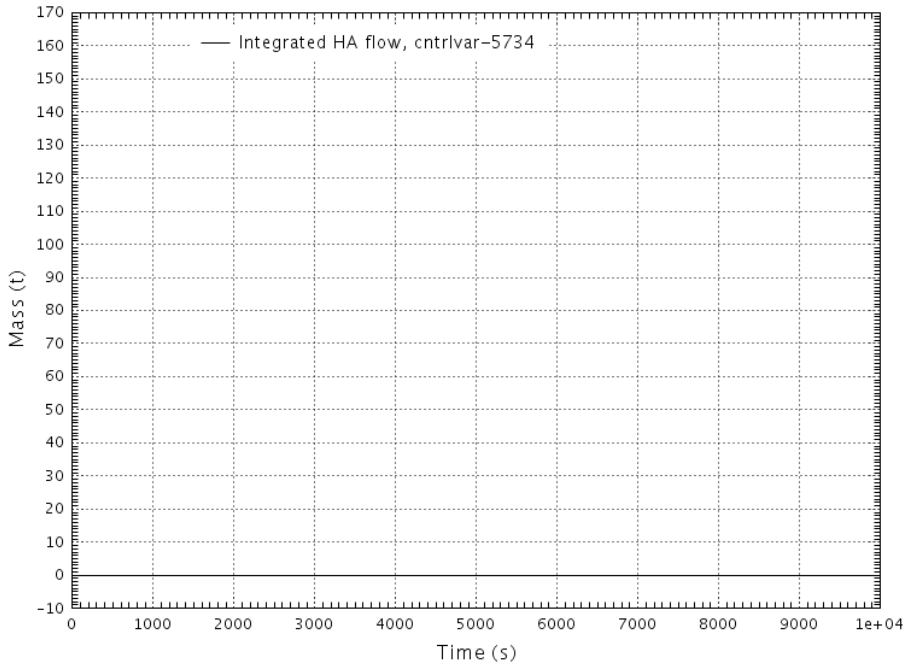

Figure 2-13 Integrated HA flow.

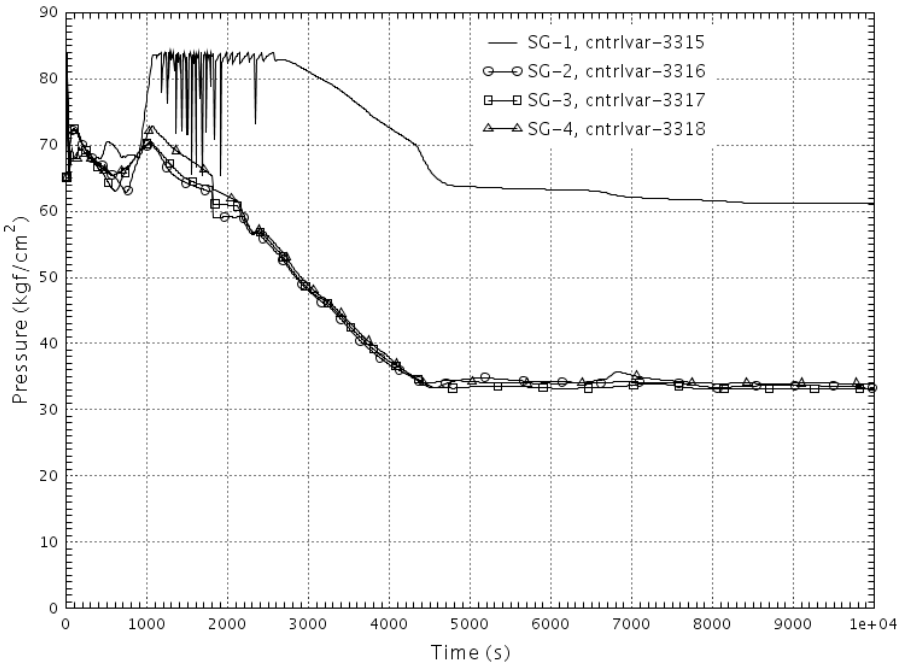

Figure 2-14 SG pressure.

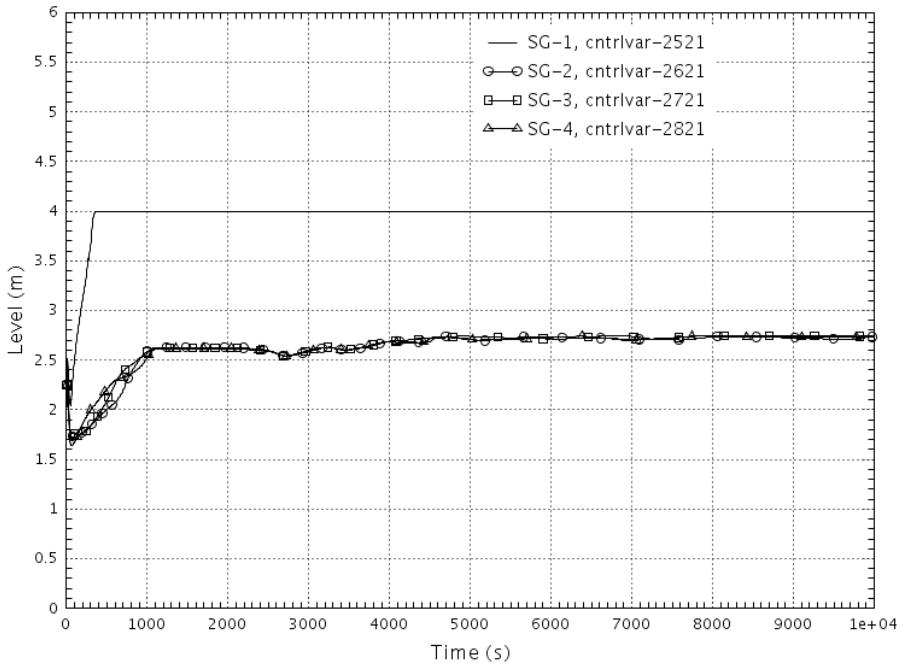

Figure 2-15 SG level.

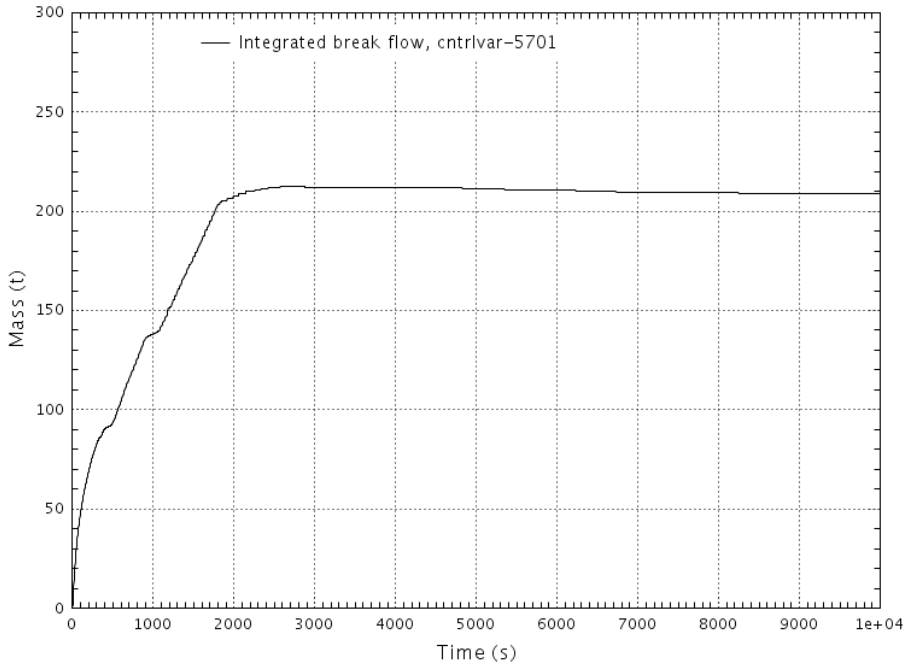

Figure 2-16 Integrated break mass flow.

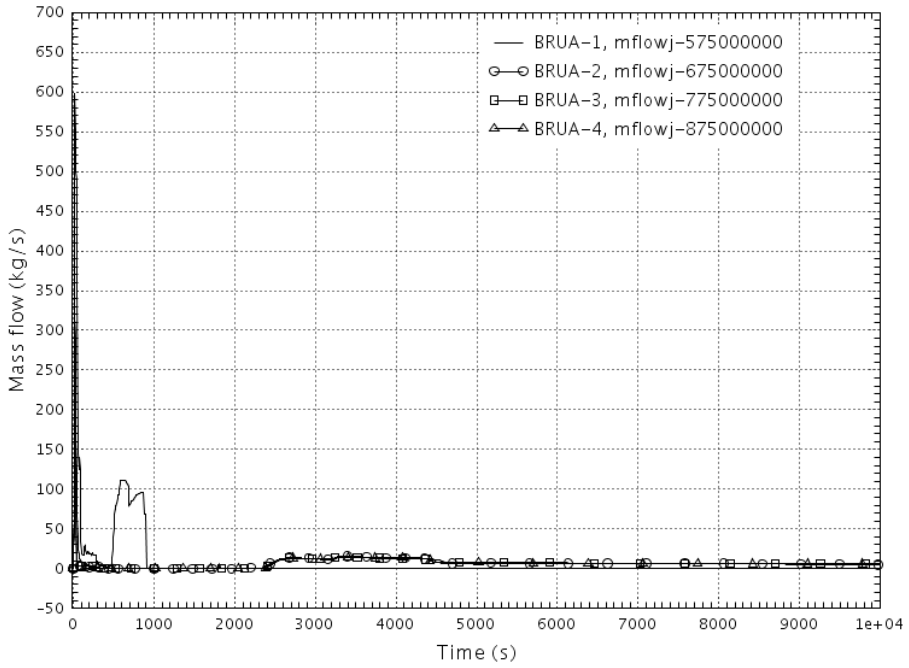

Figure 2-17 BRU-A flow.

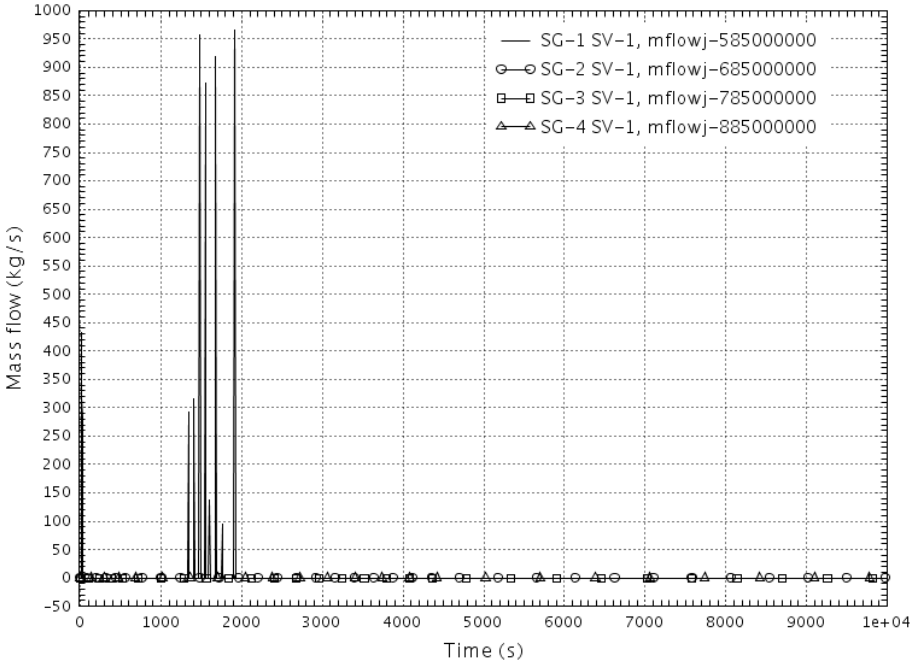

Figure 2-18 Control SG SV flow.

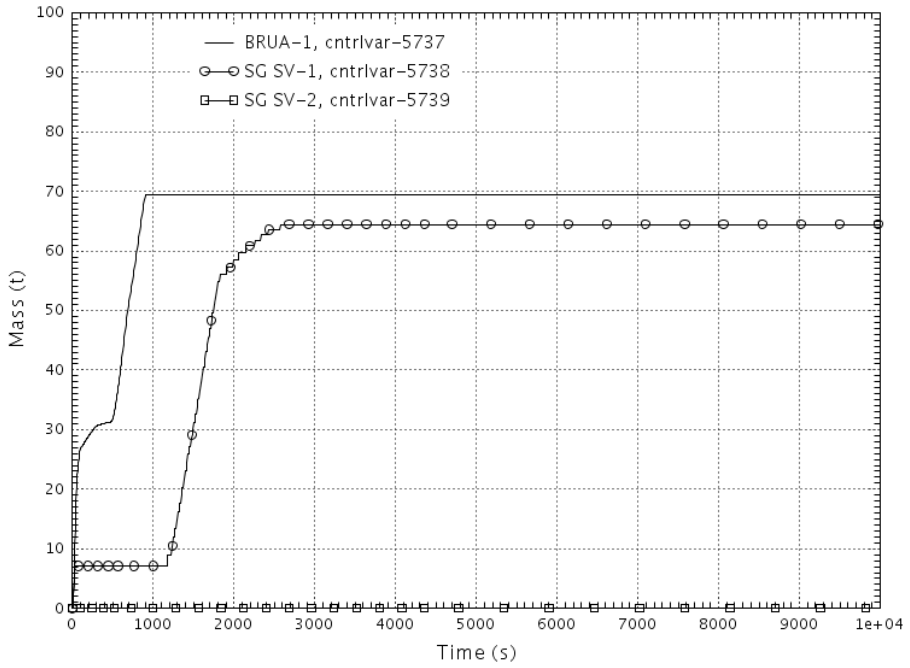

Figure 2-19 Integrated BRU-A and SG SV flows for SG-1.

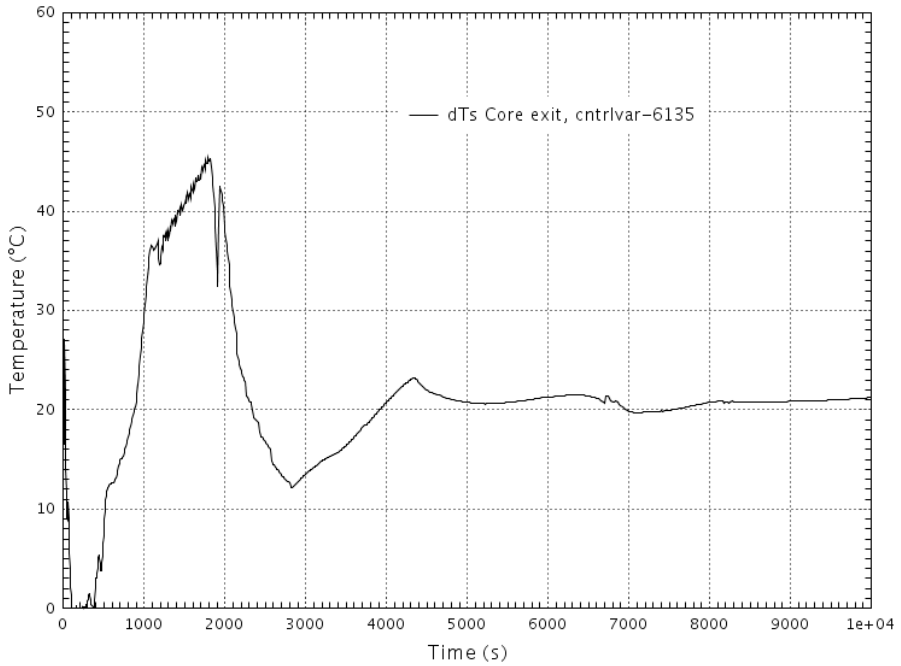

Figure 2-20 Subcooling at core exit.

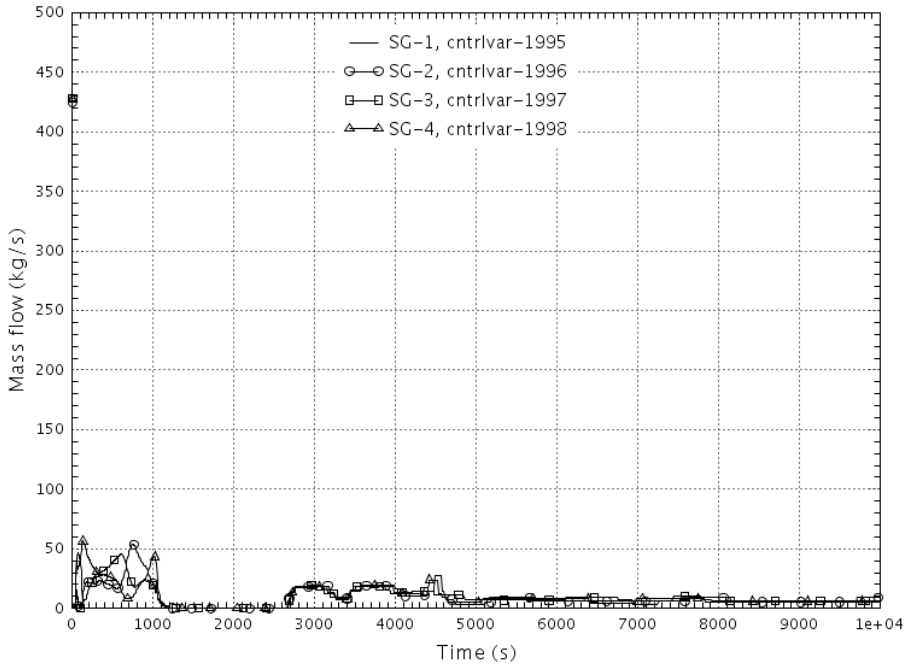

Figure 2-21 Feed water flow to SGs.

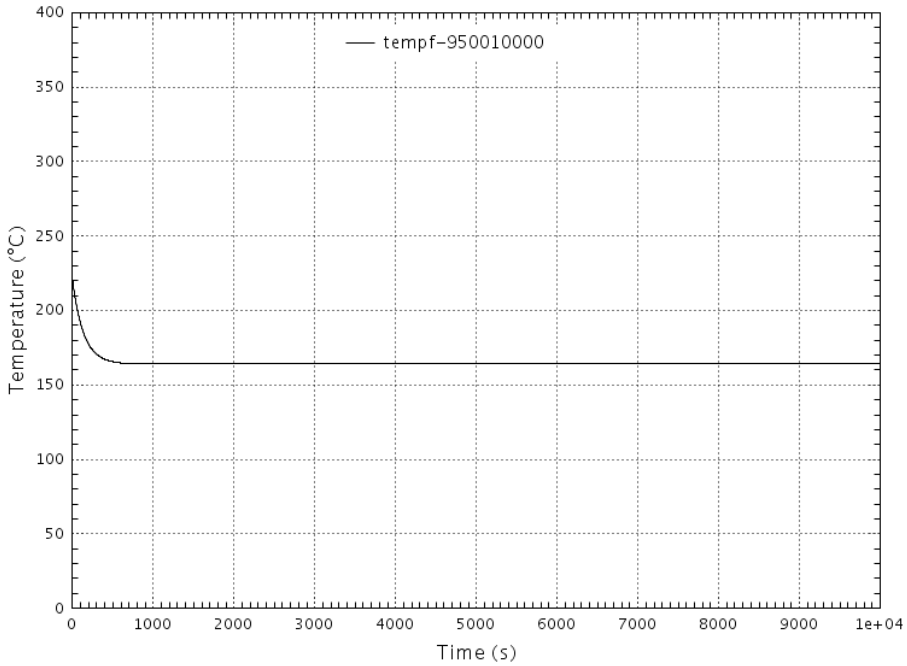

Figure 2-22 Feed water temperature.

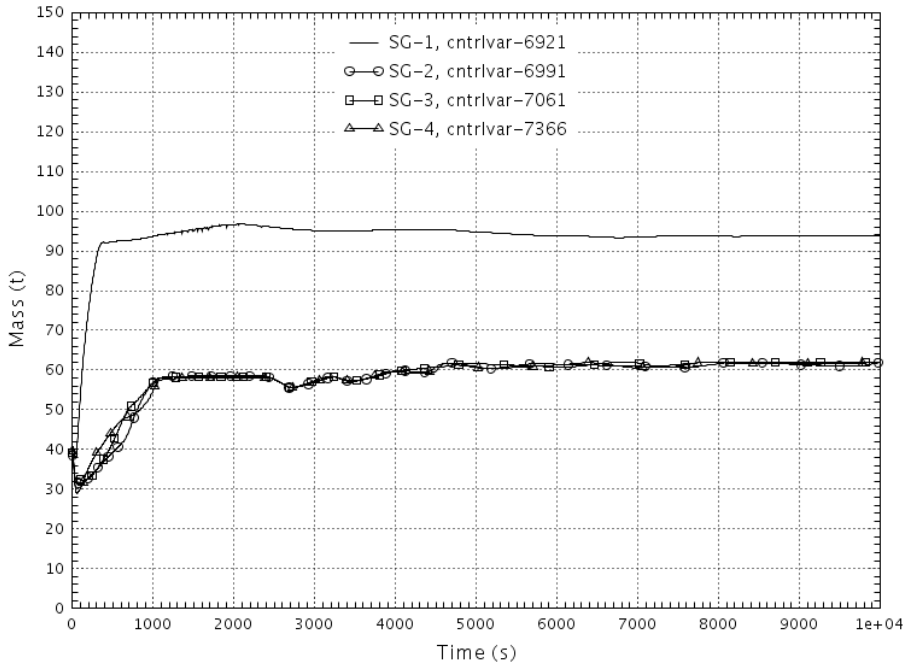

Figure 2-23 SG water mass.

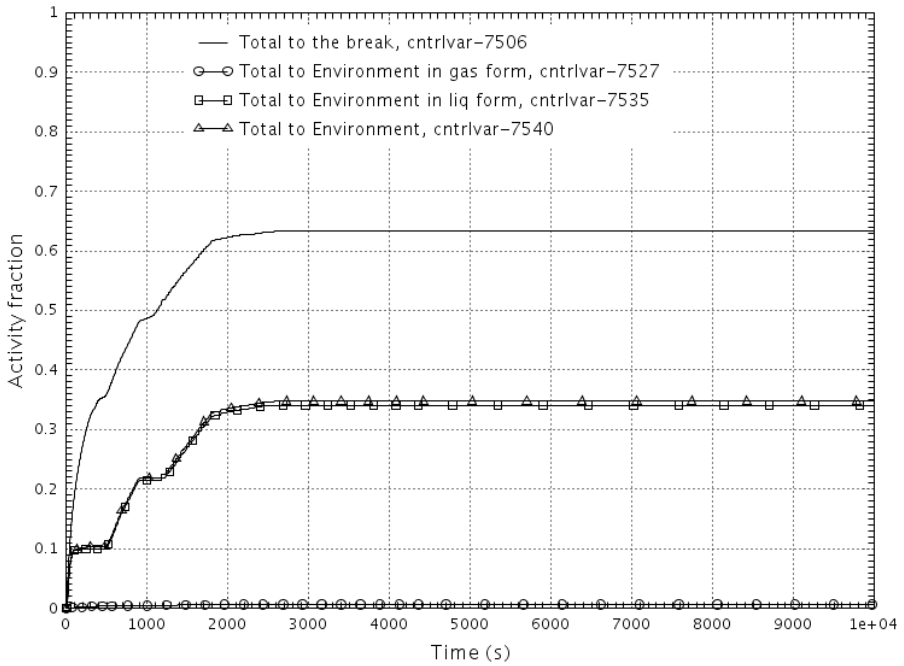

Figure 2-24 Activity fraction transported to SG and environment.

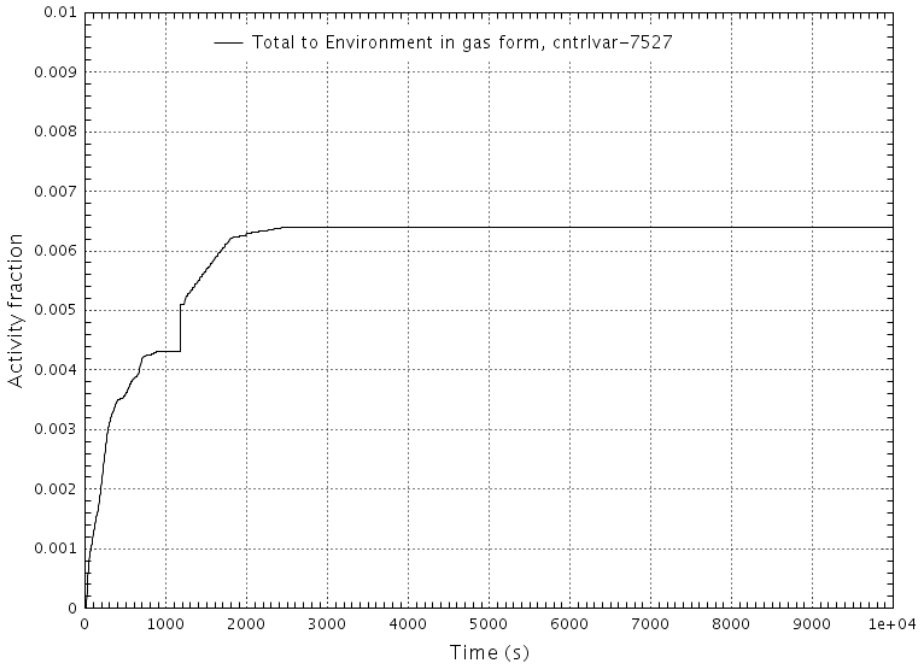

Figure 2-25 Activity fraction transported to environment in gas form.

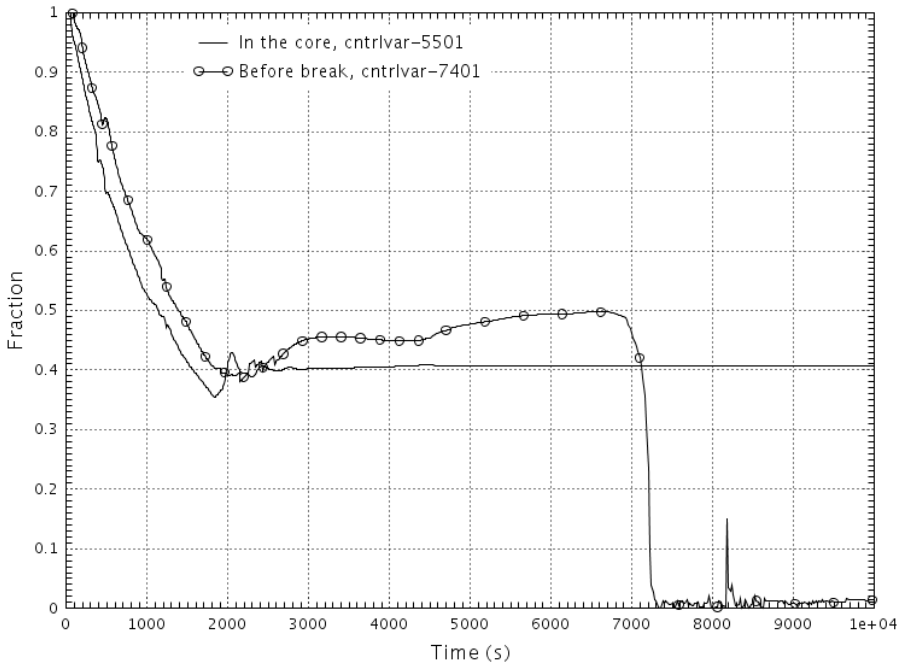

Figure 2-26 RCS coolant fraction in the core and at the break after ECCS dilution.

2.2.6. Thermal-mechanical analysis

The thermal-mechanical analysis is not applied to the scenario. TH results show no challenge to cladding cooling thus keeping the cladding integrity.

2.2.7. FP behaviour

The results of the analysis of FP release distribution for different gas transfer coefficients K_g is presented in the following table.

Table 2-3. Fraction of RCS primary activity transferred to SG and Environment for SGTR DBA case.

#	K_g	Total activity transferred to SG cv7506	Total activity release in gas form to ENV cv7527	Total activity release in liquid form to ENV cv7535	Total activity release in liquid+gas form to ENV cv7540
1	0	0.6400	0	0.345	0.345
2	0.00638	0.6400	0.00409	0.3423	0.3464
3	0.01	0.6400	0.0063	0.341	0.3474
4	0.1	0.6400	0.064	0.31	0.374
5	0.5	0.6400	0.3201	0.1722	0.4923
6	1	0.6400	0.6400	0	0.6400

The following figure represents the fraction of RCS initial activity release to SG and environment in both gas and liquid phase for different gas transfer coefficients K_g.

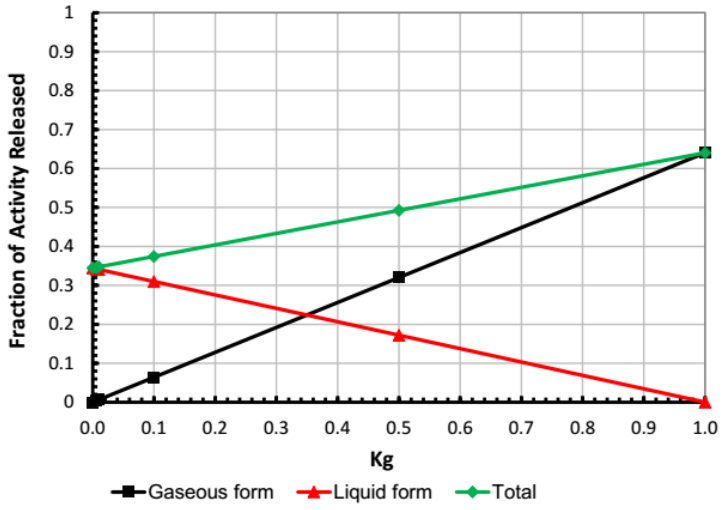

Figure 2-27 Activity fraction transported to SG and environment for different K_g.

It can be seen that the fraction of RCS activity transferred to SG in case of such break is about 0.64 and depends on the timing of operator actions on break isolation and ECCS termination/throttling (prescribed by emergency operating procedures). The total amount of activity released to environment (gas + liquid) depends on the transfer coefficient from liquid to gas phase and corresponds to the value 0.345 for Kg = 0 and to 0.64 for Kg = 1 (as for non-condensable gases).

The collector cover lift-up is the most limiting (bounding) case of the primary-to-secondary breaks for the release because the mixing with water in SG lower levels is minimal. In case of SG tube break (when the break is located below SG water level) the influence of SG water dilution and release decrease would be more substantial.

Table 2-4. Fraction of RCS primary activity transferred to SG and Environment for SGTR DBA case.

#	Isotope	Primary activity (with iodine spike), Bq	Released to environment (gas phase), Bq **DBA**	Primary activity (with iodine spike) released to SG, Bq **Dilution accounted**	Released to environment (gas phase), Bq **Dilution accounted**
1	Kr-85	5.08E+09	5.08E+09	3.25E+09	3.25E+09
2	Kr-85m	7.59E+12	7.59E+12	4.86E+12	4.86E+12
3	Kr-87	2.12E+13	2.12E+13	1.36E+13	1.36E+13
4	Kr-88	1.99E+10	1.99E+10	1.27E+10	1.27E+10
5	Xe-133	2.51E+13	2.51E+13	1.61E+13	1.61E+13
6	Xe-135	9.42E+12	9.42E+12	6.03E+12	6.03E+12
7	Xe-135m	5.57E+12	5.57E+12	3.56E+12	3.56E+12
8	I-131	1.60E+13	1.09E+12	1.02E+13	1.12E+11
9	I-132	4.26E+13	2.39E+12	2.73E+13	2.98E+11
10	I-133	3.56E+13	2.00E+12	2.28E+13	2.49E+11
11	I-134	3.35E+13	1.88E+12	2.14E+13	2.34E+11
12	I-135	2.68E+13	1.69E+12	1.72E+13	1.87E+11
13	Ru-103	1.72E+07	1.09E+05	1.10E+07	7.02E+04
14	Ru-106	9.06E+05	5.78E+03	5.80E+05	3.70E+03
15	Cs-134	1.69E+11	1.08E+09	1.08E+11	6.90E+08
16	Cs-137	2.49E+11	1.59E+09	1.59E+11	1.02E+09
17	Ce-141	1.21E+08	7.74E+05	7.74E+07	4.94E+05
18	Ce-144	7.46E+06	4.76E+04	4.77E+06	3.05E+04
19	La-140	1.37E+09	1.37E+07	8.77E+08	5.59E+06
20	Sr-90	9.68E+06	1.34E+05	6.20E+06	8.55E+04
21	**Total**	**2.24E+14**	**7.79E+13**	**1.43E+14**	**4.52E+13**

3. Radiological consequences evaluations

According to the analysis the accounting for the RCS coolant dilution and some activity absorption in SG water volume the SGTR FP release can be decreased by the factor from 0.345 for K_g=0 to 0.64 for K_g=1 (as for non-condensable gases).

The total amount of activity, released to SG during the SGTR DBA case decreased from 2.24E+14Bq to 1.43E+14Bq. The released activity to the environment in gas phase is decreased from 7.79E+13Bq to 4.52E+13Bq. This fact gives substantial decrease of the dose estimates on human body outside the plant.

According to the T2.2 report the doses are calculated for the environment release for DBA SGTR case. The results are presented in the following table.

Table 3-1. Doses in environment for SGTR DBA case with accounting for the RCS coolant dilution

#	Name	0-1 y.o.	1-2y.o.	2-7y.o.	7-12 y.o.	Teenagers	Adults
1	Event thyroid equivalent dose (mSv)	0.957	1.654	1.521	1.444	1.148	0.787
2	Event effective dose from external exposure (mSv)	0.0254	0.0239	0.0231	0.0220	0.0213	0.0205
3	Event effective dose from inhalation (mSv)	0.0497	0.0846	0.0769	0.0748	0.0600	0.0421
4	Total effective dose (mSv)	**0.0752**	**0.1085**	**0.1000**	**0.0968**	**0.0813**	**0.0626**

The DBA SGTR case doses without accounting for the RCS coolant dilution are about 8-10 times higher and are given below.

Table 3-2. Doses in environment for SGTR DBA case without accounting for the RCS coolant dilution (Task 2.3 release)

#	Name	0-1 y.o.	1-2y.o.	2-7y.o.	7-12 y.o.	Teenagers	Adults
1	Event thyroid equivalent dose (mSv)	8.684	15.059	13.926	13.267	10.561	7.242
2	Event effective dose from external exposure (mSv)	0.0578	0.0546	0.0528	0.0502	0.0489	0.0470
3	Event effective dose from inhalation (mSv)	0.4496	0.7657	0.6993	0.6819	0.5450	0.3817
4	Total effective dose (mSv)	**0.5075**	**0.8204**	**0.7521**	**0.7322**	**0.5939**	**0.4287**

4. Main final remarks

The Ukrainian DBA traditional approach to the estimation of FP release in SGTR assumes all RCS coolant activity plus iodine spike transferring to the environment via steam dumps. The more correct analysis could use the water dilution assumption to evaluate more precisely the FP activity release to SG and environment.

The estimations in this report show that only 0.345 of initial RCS activity is released to environment if it's not transferred to gas form (K_g=0). In case of non-condensable gases with full transfer from RCS liquid to gas form (K_g=1) the activity release to environment is estimated as about 0.64 of initial RCS activity.

This approach is rather simple in realistic estimations of the doses as a result of SGTR events and might be used for operator and automatics actions optimization.